Accumulation of microplastic in fjord sediments – the Bunnefjord, inner Oslofjord, Norway

Cecilie Singdahl-Larsen

Thesis submitted for degree of

Master of Science in Environmental Geoscience

60 credits

Department of Geosciences

FACULTY OF MATHEMATICS AND NATURAL SCIENCES

UNIVERSITY OF OSLO

October / 2019

Accumulation of microplastic in fjord sediments – the Bunnefjord, inner Oslofjord, Norway

Cecilie Singdahl-Larsen

Photo by Silvia Hess, May 2018.

Accumulation of microplastic in fjord sediments – the Bunnefjord, inner Oslofjord, Norway

http://www.duo.uio.no/

Printed: Reprosentralen, University of Oslo

ABSTRACT

Plastic in the marine environment is of increasing concern because of their persistence and the not so well-known effects on wildlife and humans. A lot of plastic waste ends up in the ocean every year and it is expected to increase over time. High-density plastic will sink to the bottom of the ocean, and low-density plastic will float in the water surface and the water column, and the plastic can be fragmented to smaller particles called microplastic (and nanoplastic). A high percentage of the plastic sinks to the bottom of the ocean where it can be accumulated in the sediment. Sediment is therefore considered a major sink. Two sediment cores were collected to look at the accumulation of microplastic over time, and they were collected from different locations: one outside the shoreline of Langøyene, and the other was collected close to the outlets of Bekkelaget sewage treatment plant. Plastic waste in the ocean often origin from land, so sediment samples were collected from different water depths and they form a transect from outside the coastline of Langøyene to the deeper parts of the Oslofjord to see if the island constitutes a source of microplastic contamination. To analyse microplastic in the sediment samples, the microplastic particles were separated from the sediment by performing a density separation with the high-density solution $ZnCl_2$-$CaCl_2$. The separated microplastic was analysed visually with an optical microscope, and then analysed with FT-IR. The analysis of the sediment cores showed that the microplastic concentration seemed to decrease upwards in the two sediment cores. The sediment core close to Langøyene had a minimum concentration of 2 015 particles/kg dry sediment, and a maximum concentration of 106 745 particles/kg dry sediment. The sediment core close to Bekkelaget sewage treatment plant had a minimum concentration of 1 738 particles/kg dry sediment, and a maximum concentration of 57 088 particles/kg dry sediment. The analysis of the sediment samples from the transect showed that the microplastic concentration decreased with water depth, with increasing distance from Langøyene. The sediment from the transect had a minimum concentration of 4 030 particles/kg dry sediment, and a maximum of 66 890 particles/kg dry sediment. The decreasing concentration of microplastic in the sediment cores could be explained by the increased focus on plastic waste, coastal clean-ups, and the improvement of waste management that has resulted in a higher amount of plastic that is being recycled. The decreasing concentration of microplastic with increasing water depth, in the sediment samples from the transect, confirms that a lot of the plastic waste that ends up in the ocean is transported from land.

ABSTRAKT

Plast i det marine miljøet er av økende bekymring på grunn av dets persistente egenskaper og ukjente effekter på dyreliv og mennesker. Mye plastavfall havner i havet hvert år, og det er forventet at denne mengden skal øke. Plast med høy tetthet synker til bunn i havet, og plast med lav tetthet vil flyte i overflaten av vannet, og andre deler av vannsøylen, og det kan bli fragmentert i mindre biter kalt mikroplast (og nanoplast). En stor andel av plasten synker til bunnen av havet hvor det kan akkumuleres i sedimentet. Sedimentet er derfor ansett som en «sink» der plasten samles. To sedimentkjerner ble undersøkt for å se på akkumulasjon av mikroplast over tid, og de ble samlet inn fra ulike lokaliteter: en utenfor strandlinjen til Langøyene, og den andre ble samlet inn i nærheten av utslippsrørene til Bekkelaget renseanlegg. Plastavfall i havet kan ofte stamme fra land, så sedimentprøver ble samlet inn fra ulike vanndybder og de dannet et transekt fra strandlinjen til Langøyene til dypere deler av Oslofjorden for å se om øya utgjør en kilde til mikroplast kontaminering. For å analysere mikroplast i sedimentprøvene, ble mikroplast separert fra sedimentet ved å utføre en tetthetsseparasjon med den høy-tetthetsløsningen $ZnCl_2$-$CaCl_2$. Den separerte mikroplasten ble undersøkt visuelt med lysmikroskop, og så analysert med FT-IR. Analysen av sedimentkjernene viste at konsentrasjonen av mikroplast så ut til å minke oppover i de to sedimentkjernene. Sedimentkjernen nærme Langøyene hadde en minimum konsentrasjon på 2 015 partikler/kg tørr sediment, og en maksimum konsentrasjon på 106 745 partikler/kg tørr sediment. Sedimentkjernen nærme Bekkelaget renseanlegg hadde en minimum konsentrasjon på 1 738 partikler/kg tørr sediment, og en maksimum konsentrasjon på 57 088 partikler/kg tørr sediment. Analysen av sedimentprøvene fra transektet viste at mikroplast konsentrasjonen minket med vanndybden, og med økende avstand fra Langøyene. Sedimentet fra transektet hadde en minimum konsentrasjon på 4 030 partikler/kg tørr sediment, og en maksimum konsentrasjon på 66 890 partikler/kg tørr sediment. Den minkende konsentrasjonen av mikroplast i sedimentkjernene kan forklares av det økende fokuset på plastavfall, strandrydding, og forbedringen av avfallshåndteringen som har ført til at en større andel av plast blir resirkulert. Den minkende konsentrasjonen av mikroplast med økende vanndybde, i sedimentprøvene fra transektet, bekrefter at mye av plastavfallet som ender opp i havet transporteres fra land.

ACKNOWLEDGEMENT

I would like to dedicate this thesis to my dad. He has been supporting me my whole life, and he was always proud of my achievements. He was with me the day it all started – at "Åpen Dag" at the University of Oslo. This day, I got to learn about the bachelor programme in Geosciences and I thought that this was the right study for me. The time passed by and I finished my bachelor's degree and it was time to start on my master's degree. My dad became ill shortly after the start of my master, and it ended the worst way, so he did not get to see the final result of my work during my master. That is why my thesis is dedicated to him. I would also like to thank my family for always supporting me. A special thanks goes to my soon-to-be husband, Kevin Nguyen for all the love and support during the last two years that have been challenging.

I would like to thank my supervisors Helge Hellevang (professor at UiO), Elisabeth Alve (professor at UiO) and Hans Peter Arp (Senior specialist at NGI, and professor at NTNU) for giving me very helpful tips and comments on my thesis. I would also thank the Environmental Department at NGI for making me feel welcome and included, and Heidi Knutsen for giving me answers whenever I had any questions about the lab work.

I am also thankful for Lars Bjørneby for the good discussions about Langøyene and Bekkelaget sewage treatment plant, and for sharing his results with me, and Jakob Cyvin for the helpful discussions about microplastic, and last but not least, Sindre Holm and the crew on board RV Trygve Braarud for the help in collecting the sediment samples that were to be analysed in this thesis.

TABLE OF CONTENT

TABLE OF FIGURES

LIST OF TABLES

1 INTRODUCTION

The term “plastic” appeared for the first time in the 1630s and it was used to describe substances that could be moulded or shaped. “Plastic” is used for a lot of different polymers, and each polymer has its own history of when they were successfully synthesised and used in commercial products (Crawford and Quinn, 2017, page 2).

1.1 THE HISTORY OF PLASTIC

1.1.1 Global history

In 1899, the German scientist Adolf Spitteler noticed a formation of a solid substance after his cat spilled a bottle of formaldehyde into its saucer of milk. Before this incident, the German inventor Wilhelm Krische had been experimenting with casein and observed the development of casein plastic, and they established patents in Germany and the United States in 1899. Casein is a protein in milk, so casein plastic is a semi-synthetic polymer, and it has often been used to produce buttons. The modern use of “plastic” was first coined by the Belgian chemist Leo Hendrick Baekeland in 1909, who successfully managed to fully synthesize the polymeric compound Bakelite in 1907. By the end of the 1930s, more than 200,000 tons of Bakelite had been made into a vast array of household items (Crawford and Quinn, 2017, page 2-9). The plastic polymer polyvinyl chloride (PVC) was successfully synthesised in 1926 by the American inventor Waldo Lonsbury Semon while he was working for the B.F. Goodrich Company in the United States. Though, the polymer was an unworkable substance. Semon did some more experiments and managed to make it more flexible, and a large-scale production of this polymer started in Germany and the United States in 1928. Two years later, in 1930, polystyrene (PS) was commercially manufactured by the German company IG Farben (Crawford and Quinn, 2017, page 11-12). The British organic chemist Eric Fawcett and the British physical chemist Reginald Gibson started working for Imperial Chemical Industries (ICI) in 1932. Their experimentation lead to the discovery of polyethylene (PE) but they experienced a lot of problems. Fawcett moved to the United States, but Gibson continued the experimenting. It was not until four years after, in

1936, that Gibson and ICI succeeded at synthesising polyethylene and the polymer product was sold under the trade name Polythene. In 1937, while working for IG Farben, the German chemist Otto Bayer and his colleagues synthesised polyurethane (PUR). This polymer is used in a lot of types of products today. A year later, in 1938, the first full-scale production of Nylon (Polyamide) began and the toothbrushes were made with bristles made of Nylon instead of hair from horse or boar (Crawford and Quinn, 2017, page 13-16). Many of the popular plastic that are in use today had their beginning in the early 1930s and 1940s, and the ones that are mentioned are only some of them. Food containers made of polyethylene were introduced by inventor Earl Silas Tupper in 1946 under the trade name Tupperware, and plastic started competing with glass as packaging for foods and drinks (Crawford and Quinn, 2017, page 19). The development of new plastic polymers and improvement of already discovered polymers continued with time. Two of the most popular polymers today, polypropylene (PP) and high-density polyethylene (HDPE), were discovered and synthesised in the 1950s (Crawford and Quinn, 2017, page 20-21).

1.1.2 Production in Norway

The very first product of plastic in Norway was a socket cover made of Bakelite, and it was produced by "Norsk Teknisk Porselesnfabrik" in Fredrikstad in 1929 (Nickelsen, 2015). From that time, porcelain in electrical components was replaced with Bakelite. Ten companies made products of plastic already before the start of the second World War. Most of them made products of Bakelite, and they made, among other things, ashtrays, buttons, and doorknobs. The company "Norsk Extruding" in Notodden was established in 1948 by Johan Aasheim after he travelled to England and brought polyethylene back to Norway. The company became a major producer of plastic bottles. A few years later, in 1950, "Tomte Småvareindustri" started making dolls of PVC. Around 10 years later, there were at least 200 different companies that produced products of plastic, and almost 40 % of them was already established before 1952. Most of the companies that made products of plastic, were located in Moss (Nickelsen, 2015).

1.2 PLASTIC TODAY

Plastic is a popular material because of its many qualities. It can be shaped by using heat and pressure, and it can be made into a great variety of products (Møskeland et al, 2018). It is also possible to make it inert to oxidation by use of additive chemicals (kilde?). Plastic is divided into many types based on properties, and a lot of the plastic types have already been mentioned. In addition to PE, PP, PS, PVC, PUR and nylon (polyamide, PA), there are other types like polyethylene terephthalate (Polyester, PET, PES), acrylic (AC), polyoxymethylene (POM), polyvinyl alcohol (PVA), poly methyl acrylate (PMA), alkyd (AKD). The usage of all these types is illustrated in Figure 1.2. The global production has increased to meet the growing demand of plastic as a material. The mass production started in 1950, and the amount of produced plastic has increased almost exponentially since that time. In the 1950s, the amount of globally produced plastic was 1.5 million tons/year (Van Cauwenberghe et al., 2015), and the amount increased to as much as 250 million tons/year in 2009, and 311 million tons/year was produced in 2014 (Crawford and Quinn, 2017, page 31).

Figure 1.2 *– Common plastic types and examples of products that are made of the different types (Thompson, 2018).*

1.3 INTRODUCTION OF THE PROBLEM

1.3.1 Plastic in the marine environment

When different plastic products have fulfilled their purpose, the plastic waste may be recycled, burned in combustion facilities or buried in a landfill (Barnes et al., 2009). Burning of plastic releases highly toxic chemicals, such as furans and dioxins which should be filtered, and recycling of plastic waste is not required in many countries. They often choose a cheap solution, which is dumping the plastic waste in an open landfill (Crawford and Quinn, 2017, page 40). Plastic waste can easily end up in the environment if it is not managed correctly. It can be transported to the ocean through rivers, wastewater, by wind and tides, and as litter from land and marine vessels (Ziccardi et al., 2016). It is assumed that there is around 150 million tons of plastic in the ocean, and as much as 8 million tons of plastic find its way to the ocean each year. It is estimated that 16 million tons of plastic will enter the ocean in 2030, and 32 million tons in 2050 (Crawford and Quinn, 2017, page 37). The density of seawater depends on temperature and salinity, but it is usually 1.02 g/cm^3 (Van Cauwenberghe et al., 2015). Plastic particles with a smaller density will float in the water surface and in the water column, where it can be consumed by pelagic organisms such as fish. Particles with a low density can also be transported by the oceanic circulation pattern and by wind if they are not consumed. Plastic can therefore be found in all parts of the marine environment all over the world. Particles with a higher density than seawater will sink to the bottom where they can either accumulate in the sediments or be consumed by and accumulate within benthic organisms. Fouling by bacteria and algae can alter the density of plastic particles and make the plastic sink (Barnes et al., 2009). Weathering is another factor that can alter the density, and low-density particles can sink because of these two factors. As much as 94 % of the plastic waste (Miljødirektoratet, 2019b) that enters the marine environment sinks to the bottom, and the sediment is therefor considered a major sink (Jambeck et al., 2015; Van Cauwenberghe et al., 2015; Ziccardi et al., 2016). Plastics in the marine environment are of increasing concern because of their persistence and the not so well-known effects on mostly wildlife but also humans (Jambeck et al. 2015).

1.3.2 Degradation and fragmentation of plastic

Plastic can be degraded by abiotic factors such as UV-light, oxygen, temperature (Crawford and Quinn, 2017, page 78; Ivar do Sul & Costa, 2013), or it can be fragmented from bigger particles. The level of degradation is dependent on the physiochemical properties of the different plastic types. Strong plastic types are highly persistent in the aquatic environment and it may take thousands of years for these plastic types to degrade. Soft and brittle plastic types break apart easily, and some types are designed to biodegrade. The types that are biodegradable can be degraded by microbes. For this to happen, the plastic must first be degraded by abiotic factors until the plastic is small enough to go through microbial cell walls (Crawford and Quinn, 2017, page 78-79). Studies have shown that some species of microorganisms and fungi have the ability to degrade some of the common types of plastic, such as PET, PE, PUR, PVC, PP and PMMA. Though, the plastic material must be degraded by abiotic factors before microorganisms and fungi can continue the degradation (Crawford and Quinn, 2017, page 85-87). Because of degradation and fragmentation, plastic is present in the environment in a variety of sizes, from metres to micrometres, and even nanometres.

1.3.3 Microplastic

Microplastic is divided into two categories: primary and secondary. Primary microplastic is for example plastic resin pellets and microbeads, while secondary microplastic is fragmented or degraded from larger pieces of plastic. The particles are categorised in different classes based on their overall appearance using simple features such as shape, colour etc. They are often described as pellets, fragments, granules, fibres, and films (Van Cauwenberghe et al., 2015; Ziccardi et al., 2016). Microplastic in the marine environment was first reported in the early 1970s. Some years later, in the late 1970s, microplastic in sediments was reported. Industrial resin pellets with a size of 2-5 mm in diameter were observed in samples from beach sediments in New Zealand, Canada, Bermuda, Lebanon, and Spain (Van Cauwenberghe et al., 2015). Plastic particles with a size of less than 1 mm in diameter were first reported in 2004 by Thompson et al. (2004). They studied sediment samples from different locations in the UK. A study of sediment cores from the Belgian coast showed that the plastic deposition had tripled over the last 20 years (Claessens et al., 2011).

1.4 AREA OF INTEREST

The inner Oslofjord is delimited from the North Sea by a narrow strait and shallow sill located at the Drøbak Sound. The sill is 20 m deep and restricts deep water circulation in the Oslofjord. The fjord is divided into two main basins, the Vestfjord and Bunnefjord basin (Figure 1.4a). They both have a maximum depth of 160 m. The Bunnefjord basin is the innermost of the Oslofjord with Oslo, Oppegård and Ås to the East, and Nesodden and Frogn to the West. Vertical mixing of water is weak in the basin as a result of being far away from the Drøbak Sound, and the water renewal occurs every 3-4 years (Arp et al., 2011; Dolven et al., 2013; Staalstrøm & Røed, 2016).

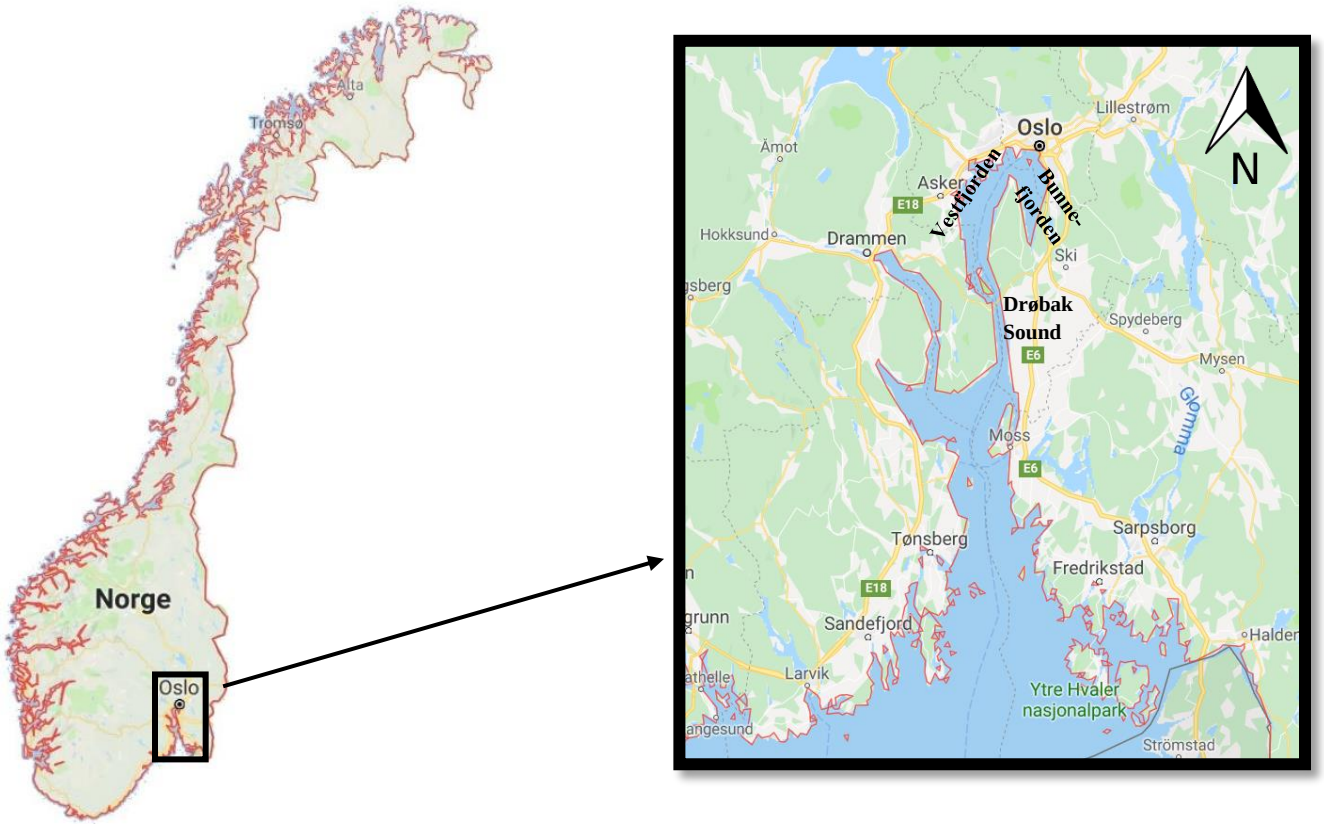

Figure 1.4a *– Maps of Norway that show the area of interest. The maps are taken and modified from Google Maps. The one to the left shows Norway, and the one to the right is zoomed in on the Oslofjord.*

1.4.1 Bekkelaget basin

Bekkelaget basin is located northeast of the Bunnefjord. The basin is 72 m at its deepest, and the outlets of Bekkelaget sewage treatment plant direct water into the basin at a water depth of ~50 m (Figure 1.4b). The Midgardsormen is a new network of waterpipes, and it was finished June 2014. The purpose of the waterpipes is to direct runoff water, sewage and rain away from Oslo city centre. The aim of Midgardsormen is to improve the water quality in Aker river and Bjørvika by leading the contaminated surface water away from the city centre, through tunnels and pipes. A new pumping station and a new shaking facility were built at Bekkelaget sewage treatment plant, and they help with directing the water into the fjord at a depth of 50 m, outside Ormøya. If the sewage is flooded, it will be discharged through the same network of waterpipes (Bekkelagetvel, 2011).

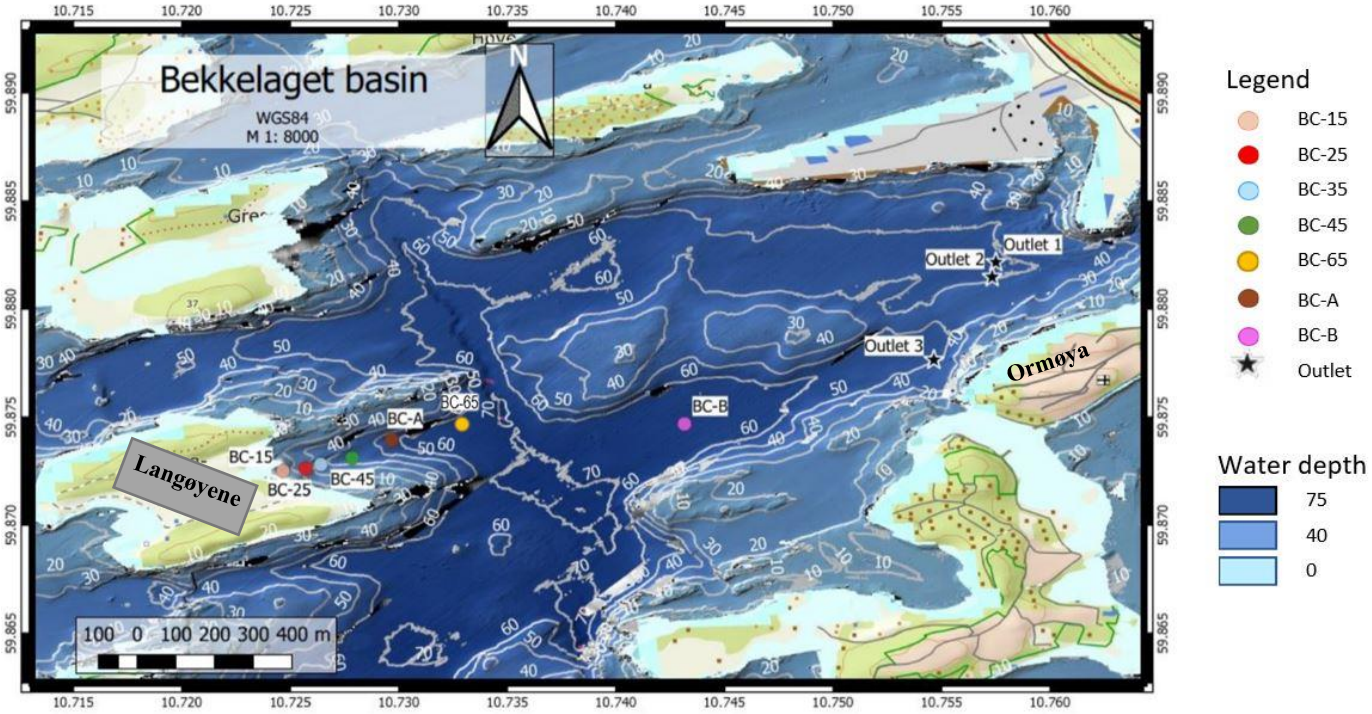

Figure 1.4b *– The map shows the sampling locations with Langøyene to the west, and the outlets of Bekkelaget sewerage treatment plant to the east. The map was made by fellow master student Lars Bjørneby, and the map data was retrieved from NGU.*

1.4.2 Langøyene

Langøyene is an island in Bekkelaget basin. Today, the island serves as a recreation area and a swimming spot, and the ferry quay is located on the north-east side. The island was originally two islands, Nordre Langøy and Søndre Langøy, and between them was a strait with a depth of 8 to 25 m. The municipality of Oslo used the strait as a landfill in the period 1908-1949 and filled it with household waste and industrial waste. In the start of the filling period, the waste was dumped right into the water and a containment boom was used to prevent the waste from drifting away. Then, several vessels were lowered at each end of the strait, and the two islands became one as the waste started to reach the water surface (Figure 1.4c). Despite the methods that were used to keep the waste at the landfill site, it managed to escape the strait and drifted to the shore of the mainland. In 1911, when the waste reached the water surface, the filling was sprayed with borax and pesticides, such as DDT, to get rid of flies. People that lived on the island were forced to move in the 1950's, and the island got status as a recreation area for the population of Oslo (Multiconsult, 2013: Multiconsult, 2014: Oslo kommune, n.d.).

Figure 1.4c *– Picture of the landfill when it was active, in 1930. The waste was floating in the water between the islands (Oslobilder, 2010).*

It is assumed that the total volume of waste at Langøyene is at least 1 million m^3, and 85 % of this waste is underneath the water surface. Today, the area between the two islands, where the waste was dumped, is covered with grass. Waste started to appear on this grass area in 2013, and environmental surveys were conducted. Sediment samples were collected from both land and from the sea bottom outside the coastline of the landfill. The survey detected high concentrations of environmental toxins. Based on this, the municipality of Oslo applied for permission from Miljødirektoratet to implement remediation measures of contaminated sediment at the island and the area around the island. The measures involve covering contaminated sediment on land, and the seabed down to a depth of 30 m (Miljødirektoratet, 2019a).

1.5 AIMS OF THE STUDY

The main of the study is to examine the amount and type of plastic in two sediment cores and sediment from different water depths, in Bekkelaget basin, in the Bunnefjord, inner Oslofjord. The analysis of microplastics in the sediment cores will show distribution of microplastic through time, and the amount of microplastic in the sediment surface sample will show how the plastic particles accumulate at different water depths. Plastic waste can end up in the marine environment by being transported from land, so Langøyene was the focus in this study. A sediment core was collected close to Langøyene, and samples from different depths were collected in a transect from the island. The other core was collected further away from the island, and closer to Bekkelaget sewage treatment plant. The two core sampling locations may have different sedimentation rates, nutrient access, and they may have different sources of plastic pollution. The following hypotheses were tested in this study:

I. The amount of microplastic will increase with time, so it would be expected to see an increasing amount of microplastic upward in the sediment cores.
II. There will be no microplastic in the sediment representing the time before the start of the mass production of plastic.
III. The concentration of microplastic is higher in the sediment closest to Langøyene than Bekkelaget sewage treatment plant.

To validate the aims, the microplastic concentrations in number of particles per kg dry sediment and mg per kg dry sediment were quantified using density separation, chemical digestion, visual analysis with microscope, and FT-IR analysis. A fellow student of mine, Lars Bjørneby, participated on the cruise and collected sediment samples from the same sampling stations. Some of his results were used to aid interpretation of my data and to test the hypotheses.

2 METHODS AND MATERIALS

2.1 SAMPLING AND SAMPLING LOCATION

The sediment samples that have been analysed and studied in this thesis were collected May 2018 on a cruise using the research vessel Trygve Braarud. The sediment samples were collected outside the north-eastern coastline of Langøyene, and Bekkelaget basin. Both sediment cores and surface samples were collected and analysed. A Gemini corer was used to collect the sediment cores, and this sampling device can collect two sediment cores at the same time (Figure 2.1a). The corer tubes were made of plexiglas, and they had an inner diameter of 8 cm. The surface samples were collected by using a Van Veen grab sampler. Salinity, temperature and dissolved oxygen were measured with a CTD before the sampling. The sampling stations and the equipment used to collect the different samples are listed in Table 2.1. All the samples were stored in pre-weighed plastic containers and put in a freezer on board the boat. The plastic containers that were used for the sampling were made of polypropylene (PP).

Table 2.1 *– Overview of sample stations.*

Station	Latitude (N)	Longitude (E)	Water depth (m)	Equipment	Sample interval
BC-15	59.872505	10.724657	15	Van Veen grab	0-2 cm
BC-25	59.872616	10.725700	25	Van Veen grab	0-2 cm
BC-35	59.872810	10.726392	35	Van Veen grab	0-2 cm
BC-45	59.873108	10.727848	45	Van Veen grab	0-2 cm
BC-65	59.874332	10.732978	65	CTD + Van Veen grab	0-2 cm
BC-A	59.873955	10.729670	55	Gemini corer	Core: 0-15 cm with 1 cm interval
BC-B	59.874683	10.743150	65	CTD + Van Veen grab + Gemini corer	Grab: 0-2 cm Core: 0-27 cm with various intervals

2.1.1 Sediment core samples

Sediment core BC-A was collected outside the north-eastern coastline of Langøyene from a water depth of 55 m. The other core, BC-B was collected closer to the outlets of Bekkelaget sewage treatment plant and the outlet of Midgardsormen, and from a water depth of 65 m (Figure 1.4b). Before core BC-A and BC-B was collected, sediment cores from the same locations as these two cores, were studied. The sediment cores were collected, pushed out of the tubes, placed on deck and sliced vertically with metal plates made of aluminium. The stratigraphy of the cores was examined to make sure that the sediment was undisturbed and deposited evenly over time, and to look for bioturbation as this can lead to disturbance of the sediment layers. The core was logged when it seemed to have undisturbed layers of sediment, and the next step of the sediment sampling was different for core BC-A and BC-B.

Figure 2.1a *– A Gemini corer ready to collect sediment.*

BC-A:

Four new cores (two sets of pseudo-replicates) were collected with the Gemini corer (Figure 2.1a). Each of the corer tubes was placed on a device that would slowly push the sediment from the bottom of the tubes. The sediment cores were sliced horizontally in intervals of one cm with aluminium metal plates. A round transparent measuring device and the aluminium metal plates were used to collect and transfer the sediment to the plastic containers. The device was washed between the slicing to get rid of residual sediment and prevent smearing of sediment from upper layers. The four cores were merged by placing sediment from the same core depth interval in the same plastic container. This was done to get enough sediment material for the microplastic analysis. Sediment from core depth 0 to 15 cm was collected as it was assumed that 15 cm represents a time before the mass production of plastic started. The rest of the core was flushed out in the seawater.

BC-B:

Two cores (one set of pseudo-replicates) were placed on deck and logged (Figure 2.1b). And the same two cores were sliced and put in plastic containers. After being sliced vertically and logged, the cores were sliced horizontally. These cores were sliced horizontally by the layering, and the same depth intervals from the two cores were put together in the same container to get enough sediment material. The core sampling interval varied because of the varying thickness of the sediment layers. The core from this location seemed to have a higher sedimentation rate based on the stratigraphy, so sediment from a bigger depth interval, 0 to 27 cm, was collected.

Figure 2.1b *– One set of pseudo-replicates (BC-B) that have been sliced vertically and logged.*

2.1.2 Surface samples

The surface samples were collected from water depths of 15 m, 25 m, 35 m, 45 m, and 65 m. Sediment from the uppermost layer (0-2 cm) of each grab was collected with a spoon, and put in a plastic container with a volume of 1 L (Figure 2.1c). The sampling stations of the grab samples form a transect that starts at 15 m depth at the north-eastern coastline of Langøyene, and in the direction of core BC-B (Figure 1.4b). The sampling station of core BC-A is on the transect, and the uppermost layer (0-2 cm) of this core represents the water depth of 55 m in the transect. A grab sample was also collected from the same sampling station as core BC-B at 65 m water depth.

Figure 2.1c *– Collecting sediment sample from the Van Veen grab.*

2.2 FREEZE DRYING

The frozen samples were freeze dried to remove the water content, and this method is based on the phase diagram of water. The solid state of water is removed from the sediment through sublimation under vacuum and temperature colder than -10 °C. The two freeze dryers *Christ Alpha 1-4LD pluss* and *Christ Alpha 1-4* were used. One round of freeze drying lasted four days and could remove the water content from 35 plastic containers with sediment sample (Figure 2.2). The pressure was set to 0.040 mbar, and the temperature was set to -50 °C. The lids of the plastic containers were changed to lids with holes so that the water vapor could escape from the sediment samples. The vapor settled on the bottom, inside of the freeze dryer in solid state, and this needed to be melted and removed through an outlet on the bottom of the freeze dryer before the next round of freeze drying. If the samples were not completely frozen during the process, the sediment particles would behave like popcorn that is being popped, and the sediment could end up outside the container.

Figure 2.2 *– Freeze dryer with 35 samples inside, ready to be dried.*

The sediment samples were expected to have a high content of water as they were collected from the seabed of a fjord, and the sediment seemed to have a high content of clay. By freeze drying the samples, the porosity of the sediment remained intact and the structure of the material would not collapse. Later, in the method, dry sediment is used for the density separation to avoid dilution of the density solution that is used for the separation (See section 2.7 Density separation), and the risk of damaging and generating more microplastic particles is smaller when homogenizing freeze dried sediment. The salinity from the CTD profiles (See section 3.1 CTD profiles) was used to correct the weight of dry sediment (Equation 2.2a).

$$m_{dry,corr} = \left(m_{dry} - \left(m_{wet} - m_{dry}\right)\right) * salinity \qquad \textit{Equation 2.2a}$$

Where $m_{dry,corr}$ is the salt corrected dry sample weight (g), m_{dry} is the dry sample weight (g), m_{wet} is the wet sample weight (g).

The water content was calculated with the corrected dry sample weight (Equation 2.2b). The weight of the samples from core BC-A, BC-B, and the surface samples are listed in Appendix B.

$$\textit{Water content (\%)} = \left(\frac{m_{wet} - m_{dry,corr}}{m_{wet}}\right) * 100\% \qquad \textit{Equation 2.2b}$$

2.3 TOTAL ORGANIC CARBON (TOC)

The sediment samples that were used for the analysis of total organic carbon (TOC) were prepared by Lars Bjørneby. He used between 0.7 and 1.4 g of dry sediment from the core - and surface samples that he collected at the cruise, and the sediment were prepared and delivered to the Department of Biosciences, University of Oslo for TOC analysis with the instrument *FlashEA 1112*. The preparation and analysis are explained in more detail in the master thesis by Bjørneby (2019, page 15-16).

2.4 GRAIN SIZE DISTRIBUTION

The grain size distribution analysis was carried out by Lars Bjørneby at the Department of Geosciences, University of Oslo. He analysed the grain size distribution of his own sediment samples. The instrument *Beckman Coulter LS13 320* was used for the analysis, and the instrument can measure particles with a size from 0.39 to 1909.00 µm. The preparation and analysis are explained in more detail in the thesis by Bjørneby (2019, page 15).

2.5 SEDIMENT CORE DATING

The sediment core dating was carried out by the Environmental Radioactivity Research Centre at the University of Liverpool, in England. The sediment samples were prepared by Lars Bjørneby at the Department of Geosciences, University of Oslo, and he sent ~7 g of dry sediment from each core interval of the core named LØ55 (Bjørneby, 2019, page 14-15 and 60-63). This core was collected from the same location as BC-A. The dating was based on the half-life of the ^{210}Pb- and ^{137}Cs-isotopes, and the activity of the isotope ^{226}Ra and ^{137}Cs. See Appendix B for the full report from the University of Liverpool.

2.6 HEAVY METALS

The preparation of sediment samples that were used for the heavy metal analysis was carried out by Lars Bjørneby (2019). The content of the heavy metals chromium (Cr), nickel (Ni), copper (Cu), zinc (Zn), arsenic (As), cadmium (Cd), lead (Pb) and mercury (Hg) was analysed. Around 1 g of dry sediment from the core – and surface samples that he collected, was used for the analysis and prepared so that it could be analysed with the mass spectrometer *Inductively Coupled Plasma Mass-Spectrometry (ICP-MS)* at the Department of Geosciences, University of Oslo.

2.7 DENSITY SEPARATION

2.7.1 The Bauta Microplastic-Sediment Separator (BMSS)

A Bauta Microplastic-Sediment separator (BMSS) was used to separate microplastics from benthic sediments. The concept is based on the same idea as the Munich Plastic Sediment Separator by Imhof et al. (2012). The BMSS uses density separation to separate microplastics from sediments, and the design was developed by Norwegian Geotechnical Institute (NGI) in Oslo. The protocol of separating microplastic from sediment was optimized by Mahat (2017), and the method is also described in Møskeland et al. (2018). The high-density solution $ZnCl_2$-$CaCl_2$ with a density between 1.53 g/cm^3 and 1.57 g/cm^3 was used for the microplastic-sediment separation. Particles with a higher density than the $ZnCl_2$-$CaCl_2$ solution, such as small rocks, sand and clay will sink to the bottom of the solution, while particles with a lower density, such as organic material and plastic, will float on the top. The BMSS consists of four separable components: the base unit, sediment chamber, a glass column and a separation chamber (Figure 2.7a).

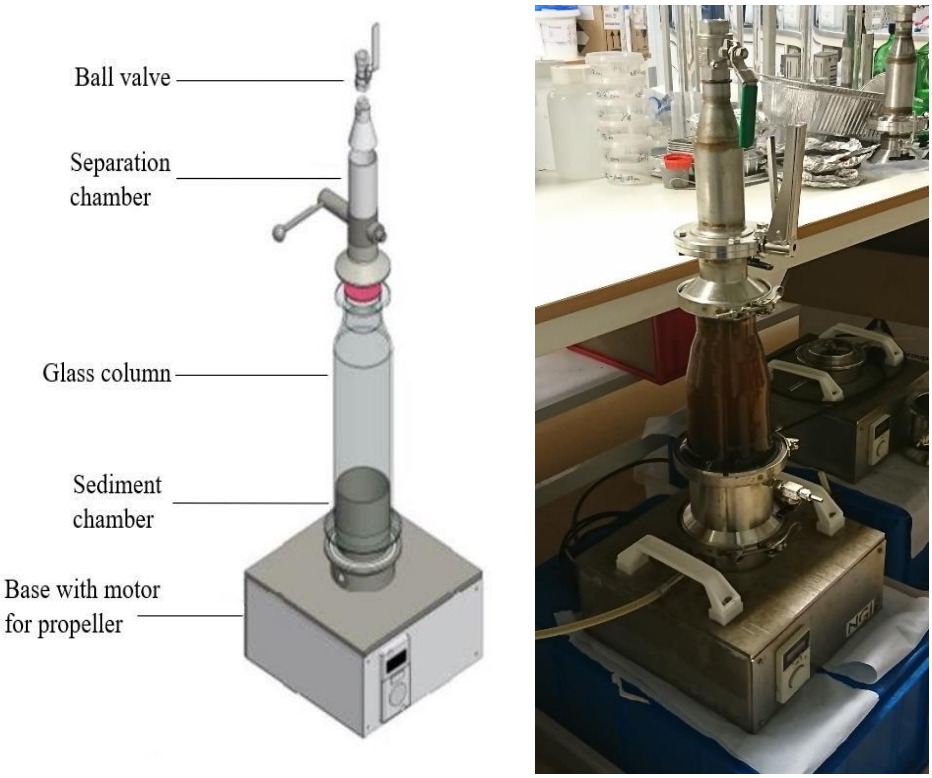

Figure 2.7a *– Left: illustration of the BMSS and the different units. Borrowed and modified from Møskeland et al. (2018). Right: setup of the BMSS. The density solution is visible through the glass column.*

2.7.2 The different units of the BMSS

The *base unit* is the bottom part of the BMSS. It is stationary and it is made of stainless-steel. There is a frequency-controlled propeller in the base unit which has a maximum speed of 400 rounds per minute, though the propeller was not used for the separation of the sediment samples in this thesis. There is also an inlet and an outlet valve. The density solution comes in through the inlet valve, and when the separation is complete, the density solution is drained through the outlet valve. The *sediment chamber* is a 12.6 cm tall cylinder made of stainless-steel, and it fits on top of the base. There is also an outlet valve for draining the $ZnCl_2$-$CaCl_2$ solution at this unit which can be used if the outlet valve of the base unit was clogged with sediment. This valve is located at the top of the sediment chamber, above the level of the sediments. The *glass column* is a transparent glass cylinder with a height of 25.0 cm. The bottom of the glass cylinder has an inner diameter of 10.5 cm, but the top has an inner diameter of 6.5 cm to fit the separation chamber. The *separation chamber* is also made of stainless-steel, and it is used to collect the particles with a low density from the glass column by raising the level of the solution. There is a ball valve at the top of the unit, and a shut-off valve at the bottom. It is also equipped with a depressurizing valve below the shut-off valve to lower the solution level when both the ball valve and the shut-off valve are shut. Each component is fitted with an O-ring between each joint to prevent leakage and loss of solution, and clamps are used to fasten the units.

2.7.3 Assembly of BMSS

All units were washed thoroughly with distilled water and dried before assembly and between each microplastic-sediment separation. The BMSS was assembled in the same order for each separation, and the O-rings were controlled before assemblage. First, the sediment chamber was fastened to the base unit with adjustable clamps. Then, the glass column was placed and fastened on top of the sediment chamber. All the valves were shut, the BMSS was filled with $ZnCl_2$-$CaCl_2$ solution to just below the narrowed neck of the glass column before the introduction of sediment.

2.7.4 Introduction of sediment sample to BMSS

All the collected sediment from each core interval of core BC-A and BC-B was used for the density separation. The surface samples had a lot of sample material so only a specific weight amount of homogenized material was used for the separation. The dry sediment sample was transferred to a pre-weighed aluminium tray, and the weight of the sediment was noted. The amount of sediment varied between the core intervals, and it is listed as mean and standard deviation in Table 2.7. The weight of sediment that was introduced to the BMSS, from each sediment sample is listed in Appendix C.

Table 2.7 *– Weight of dry sediment (g) that was introduced to the BMSS.*

Sediment sample	Equipment	No. of samples	Mean	Standard deviation
Surface sample	Van Veen Grab	6	42.26	3.40
Core BC-A	Gemini corer	15	68.59	21.32
Core BC-B	Gemini corer	9	54.55	20.73

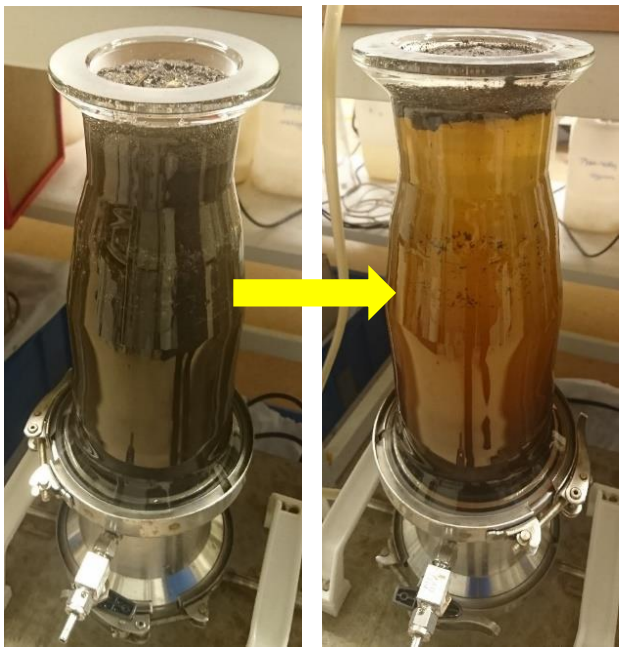

Figure 2.7b *– Left: Same day as sediment was introduced to the BMSS. Right: The day after sediment was introduced to the BMSS.*

Before introducing the sediment to the BMSS, a slurry was made by adding 100 mL $ZnCl_2$-$CaCl_2$ to the sediment. Introducing the sediment as a slurry reduced surface tension between the sediment and the $ZnCl_2$-$CaCl_2$ and to prevent particles from sticking to the inside of the glass column (Mahat, 2017). The aluminium tray with the slurry was put in a sonic bath for 10 minutes to make an even mixture of the sediment and the $ZnCl_2$-$CaCl_2$, and to loosen lumps of particles. After sonic bath, the slurry was introduced to the BMSS by using a metal spoon. A wash bottle with $ZnCl_2$-$CaCl_2$ was used to wash out remaining material from the

aluminium tray. The sample material was separated the day after the sediment sample was introduced to the BMSS, when the density solution was clearer, and particles had settled on top of the solution (Figure 2.7b).

Figure 2.7c *– The filtration setup. Sample material was collected onto a steel mesh filter by using a vacuum filtration system.*

2.7.5 Sample extraction and filtration

The separation chamber was placed on top of the glass column and the level of $ZnCl_2$-$CaCl_2$ solution was slowly raised from the bottom and up, until it was above the shut-off valve. Both the ball-valve and the shut-off valve were closed and the level of the $ZnCl_2$-$CaCl_2$ in the glass column was lowered by opening the depressurizing valve, and the solution was drained by opening the outlet valve on the base unit or the sediment chamber. Once the level of the solution was below the neck of the glass column, the valves were shut, and the separation chamber was removed and placed onto a rack in an inverted position. A vacuum filtration system (Figure 2.7c) and a pre-weighed and pre-washed steel mesh filter (pore size: 26 µm) was used to collect the sample material. This filter size was used because a smaller size would have made it difficult to analyse the particles with the FT-IR instrument as it uses transmission when the particles are scanned (the use of the FT-IR instrument is explained in section 2.11 FT-IR analysis). The steel mesh filters used for the microplastic-sediment separation were pre-washed with sodium dodecyl sulphate soap and put in ultra-sonic bath for 20-30 minutes and rinsed with distilled water. The separation chamber was placed in an inverted position and flushed with $ZnCl_2$-$CaCl_2$ solution by using a wash bottle. Sample material that was stuck on the inside of the glass column, was washed and separated. At the end of the

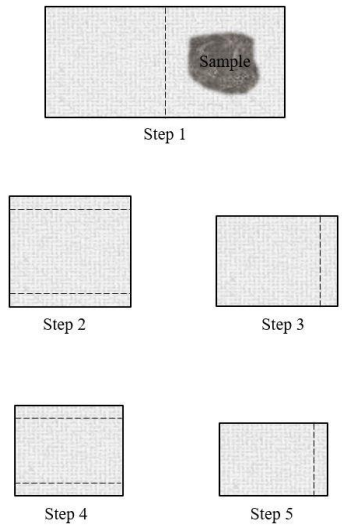

Figure 2.7d *– Illustration of the folding technique. The dotted lines represent the folding line. The top, bottom and the right side of the steel mesh filter were folded twice.*

separation, the separation chamber was flushed with milli-Q water to get any remaining particles. After separation and filtration, the steel mesh filter with sample material was folded like an envelope (Figure 2.7d) and secured with a pre-weighed steel wire, and dried over-night in an oven at 60 °C. A higher temperature than 60 °C could potentially damage the plastic particles. Sediment samples with a high content of material were filtered onto more than one steel mesh filter.

2.7.6 Preparation and recycling of $ZnCl_2$-$CaCl_2$ solution

The density solution, $ZnCl_2$-$CaCl_2$ is highly corrosive, and safety equipment such as eyewear, lab coat, and nitrile gloves were used when handling the solution. It is also considered hazardous to aquatic environments. In addition, the process of separating microplastic from sediment requires a lot of $ZnCl_2$-$CaCl_2$, and the preparation of the solution takes 2 days and it is a time-consuming and expensive procedure. Recycling of used $ZnCl_2$-$CaCl_2$ solution is a preferable option. Though, the solution would slowly decrease after every microplastic-sediment separation as it was difficult to drain all the solution through the outlet valve and a lot of solution often remained in the sediment chamber with the sediment. Therefore, it was also necessary to prepare a new density solution in addition to recycling. Prepared density solution was made and stored in a carboy container made of high-density polyethylene (HDPE), and the container has a volume of 10 L. $ZnCl_2$ salt was mixed with $CaCl_2$ and milli-Q water in the ratio by weight 4.4:2:3.6 (H_2O:$ZnCl_2$:$CaCl_2$) (Hudgins, 1964). Information of the chemicals used for the density separation is listed in Table 2.8 in the next section. The preparation of $ZnCl_2$-$CaCl_2$ was made the same way as it is described in Imhof et al. (2012). The chemical reaction between $ZnCl_2$, $CaCl_2$ and milli-Q water is exothermic, so the carboy container was placed in ice bath under a fume hood until the reaction reached equilibrium, when the temperature had decreased to room temperature. The carboy container with the prepared solution was placed on a mechanical shaker over-night for the salts to be evenly mixed. Salt crystals and impurities were removed by filtration through a Whatman GF/D glass fibre filter using a high-pressure filtration system with N_2 gas. The filter has a 2.7 µm pore size, and a diameter of 150 mm. The density of the solution was tested after filtration of used and new solution, and it was calculated by using following equation:

$$Density\ (\rho) = \frac{g}{cm^3} = \frac{(m_{V.f.} + m_{ZnCl_2-CaCl_2}) - m_{V.f.}}{V_{V.f.}}$$ *Equation 2.7*

Where $m_{V.f.}$ is the weight (g) of the volumetric flask, $m_{ZnCl_2-CaCl_2}$ is the weight (g) of the solution, and $V_{V.f.}$ is the volume (cm^3) of the volumetric flask.

2.8 CHEMICAL DIGESTION

The sediment samples could contain organic material, such as leaves, twigs and detritus, and not only sediment and microplastic. Organic material can obstruct the visual analysis and disturb signals transmitted by the Fourier-transform infrared (FT-IR) instrument when identifying different plastic particles. Chemical digestion removes the organic material by dissolution. The intention is to remove organic material in a way that does not damage the plastic particles. The method of dissolution is based on the work and results by Olsen et al. (in preparation), and the process is also described in Mahat (2017) and Lilleeng (2018). It is a two-step process and it takes at least five days to complete one round. All the equipment that was used in this process was washed with a wash bottle containing methanol.

The first step involves dissolving organic compounds using a solution made of sodium hydroxide (NaOH), urea ($CO[NH_2]_2$), and thiourea (CH_4N_2S). Preparation of this solution is described in the next section (2.8.2 Preparation of urea-solution). Each sample was put in a glass jar with a magnetic stir bar. Then, 80 mL of $NaOH:CO(NH_2)_2:CH_4N_2S$ per 2 g dried sample material was added to the glass jars. The glass jars were put in a freezer at -20 ° C for 45 minutes with a lid made of aluminium foil, and they were stirred every 15 minutes to prevent freezing of the solution. After 45 minutes, they were placed on a magnetic stirrer (Figure 2.8a) until they reached room temperature, which usually took 1 to 1.5 hours.

Figure 2.8a *– Step 1 of chemical digestion. The wrapped steel mesh filters with low-density material were placed in glass jars, and urea-solution was added.*

The last part of this step was to rinse the samples 15 times with milli-Q water. They were left submerged in milli-Q water for 15 minutes every fifth wash.

The second step involves oxidizing the samples by using 30% hydrogen peroxide (H_2O_2). The same glass jars from the first step were also used for this part of the process, and 60 mL of H_2O_2 per 2 g dry sample material was added to the glass jars. In addition, as a catalyst, a few droplets (3-4) of 10 M NaOH were added to the glass jars. The reaction between H_2O_2 and NaOH is exothermic so all the glass jars with samples were put in tall plastic containers (made of PP) to control the boil-up from the reaction. Aluminium foil was used to make a lid on the glass jars, and every part of this step was carried out in a fume hood. The plastic containers with the glass jars were placed on a magnetic stirrer for at least 2-3 hours, and they were left standing in the fume hood for three days (Figure 2.8b). After three days, the samples were rinsed 10 times with milli-Q water and left submerged in milli-Q water for 15 minutes every fifth wash. Lastly, they were dried at 60 °C and weighed the next day.

Figure 2.8b *– Step 2 of chemical digestion. The samples in the glass jars have been placed in tall plastic (PP) containers.*

The weight of separated sample was calculated by following equation:

$$w_{calc.sample\ weight\ for\ digestion} = m_{total\ sample} - \left(m_{filter} + m_{wire}\right) \qquad \textit{Equation 2.8}$$

Where $w_{calc.\ sample\ weight\ for\ digestion}$ is the weight (g) of the sample material, $m_{total\ sample}$ is the total weight (g) of the sample including sample material, steel mesh filter and steel wire.

The separated material from some of the sediment samples had a high material weight. Chemical digestion is a time-consuming process, and ideally, the whole process should be repeated until the reduction is ≤ 4%, or if the weight of the sample material is ≤ 0.005 g because with these values, it was assumed that digestion is no longer effective and the would be a minimal loss of organic material. To save time, around 0.2 g material was extracted from the separated material. All the samples, from core BC-A, BC-B and the surface samples, went through at least two rounds of chemical digestion. One of the surface samples was only digested one round and opened to look at the amount of organic material. Another surface sample was digested two rounds, and the rest of the samples were digested three rounds. The recovery blanks were digested two rounds, but the method blanks were digested one round because of the low material weight.

After chemical digestion, the steel mesh filters with samples were wrapped in aluminium foil and put in a desiccator (Figure 2.8c) to avoid formation of rust by reaction between water and remaining $ZnCl_2$-$CaCl_2$. They were kept in the desiccator, with silica gel in the bottom, until they were analysed further with microscope and the FT-IR instrument.

Figure 2.8c *– Desiccator with a few samples that have been through chemical digestion.*

2.8.1 Preparation of urea-solution

The chemical reaction when preparing the urea-solution is exothermic so the preparation was done under a fume hood. A glass bottle was used to mix the chemicals, and the solution was placed on a magnetic stirrer as the chemicals were added to the bottle. First, around 387.5 g of milli-Q water was added to the glass bottle, then 40 g urea, 32.5 g thiourea, and lastly, 40 g NaOH. The bottle containing the urea-solution was left on stirring until all chemicals had dissolved in the water. All the chemicals that were used for the density separation and chemical digestion are listed in Table 2.8.

Table 2.8 *– Chemicals used for the microplastic-sediment separation, chemical digestion and cleaning.*

Chemical	Molecular formula	Manufacturer/distributor	Purity (%)
Microplastic-sediment separation			
Zinc chloride	$ZnCl_2$	VWR International	97
Calcium chloride	$CaCl_2$	VWR International	90-98
Chemical digestion			
Urea	$CO(NH_2)_2$	Sigma Aldrich	≥ 98
Thiourea	CH_4N_2S	Merck KGaA	≥ 98
Sodium hydroxide	NaOH	Merck KGaA	99-100
Hydrogen peroxide	30% H_2O_2	VWR International	Analytical grade
Cleaning of steel mesh filters			
Sodium dodecyl sulphate	$CH_3(CH_2)_{11}OSO_3Na$	Sigma Aldrich	≥ 99 (Chromatography)
Cleaning of equipment			
Methanol	CH_3OH	Merck KGaA	99-100

2.9 QUALITY CONTROL

The method of quantifying and qualifying microplastics consists of a lot of steps and there is a risk of contamination whenever handling the sample in the lab. It is therefore important to follow the protocol carefully, though it is impossible to avoid any contamination of the samples as the samples can be contaminated by microplastics in the chemicals that were used, in the water and even air. Possible impurities and contamination were corrected for by preparing and separating method blanks, and the precision of the method was expressed through recovery blanks.

2.9.1 Method blanks

The procedure of method blanks is identical to microplastic-sediment separation protocol, but it involves no sediment sample. The BMSS was filled with $ZnCl_2$-$CaCl_2$ solution, and 100 mL of the density solution was added to an aluminium tray, and the density solution was introduced to the BMSS. The method blanks give an indication of the purity of the method. They reflect laboratory conditions, cleaning of the equipment and the quality of the chemicals that were used, including the recycled $ZnCl_2$-$CaCl_2$ solution. A total of nine method blanks were separated, and the data from the method blanks were reported by weight, microscopy and by FT-IR analysis. The mass of impurities was calculated by following equation:

$$m_{impurities} = m_{method\ blank} - (m_{filter} - m_{wire}) \qquad \textit{Equation 2.9a}$$

Where $m_{impurities}$ is the weight (g) of the material of the method blank, and $m_{method\ blank}$ is the total weight (g) of the method blank including sample material, steel mesh filter and steel wire.

2.9.2 Recovery blanks

Recovery blanks were performed by using sediment from sediment samples that had already been through microplastic-sediment separation. The recovery blanks were carried out by draining $ZnCl_2$-$CaCl_2$ solution from the outlet valve of the sediment chamber. A metal spoon was used to transfer some of the sediment to a pre-weighed aluminium tray by best effort. The sediment samples in this study had a high content of clay, so the extracted sediment was a mix of sediment and $ZnCl_2$-$CaCl_2$, and the rest of the sediment was left in the sediment chamber. The glass column was washed, placed on top of the sediment chamber, and it was filled with $ZnCl_2$-$CaCl_2$ solution. No visible particles were observed in the surface of the density solution. The extracted mixture of sediment and $ZnCl_2$-$CaCl_2$ solution was spiked with plastic particles, and the total amount of spiked material ranged from 0.12 to 0.16 g. Then, the spiked sediment was re-introduced to the BMSS and filtered following the microplastic-sediment separation protocol. The sediment samples were spiked with either powder or five granulates and fibre. All three types of spiking material are white in colour, and their specifications are listed in Table 2.9.

Table 2.9a *– Specifications of the spiking material.*

Shape	Polymer type	Density (g/cm^3)	Manufacturer/distributor	Size
Powder	Polyethylene terephthalate (Polyester, PET)	1.40	Goodfellow Cambridge Ltd. (UK) Catalogue no. ES306030	Diameter: < 300 µm
Fibre			Goodfellow Cambridge Ltd. (UK) Catalogue no. ES305720/1	Diameter: 17 µm Length: 2-3 cm
Granulate			Goodfellow Cambridge Ltd. (UK) Catalogue no. ES306312	Diameter: 3-5 mm

A total of six recovery blanks were prepared and separated to determine the accuracy of the microplastic-sediment separation. Three of them were prepared by using the sediment from core BC-A, and the other three were prepared by using sediment from core BC-B. Three sediment samples were spiked with powder, and three samples were spiked with granulates and fibre. The samples and the type and weight of spiking material are listed in Table 2.9b.

Table 2.9b *– Sediment samples, type and weight of spiking material.*

Sample name	Weight of spiking material (g)			Total weight (g)
	Powder	Fibre	Granulates (5 pcs)	
Spiked BC-A 1-2cm	0.16250	-	-	0.16250
Spiked BC-A 6-7cm	-	0.02940	0.09783	0.12723
Spiked BC-A 12-13cm	0.15580	-	-	0.15580
Spiked BC-B 5-8cm	-	0.03650	0.08770	0.12420
Spiked BC-B 15-18cm	0.11610	-	-	0.11610
Spiked BC-B 25-27cm	-	0.03555	0.09158	0.12713

There was often some organic material left in the sediment that had already been through separation, and this organic material was separated and filtrated onto a steel mesh filter together with the spiked material. Therefore, the recovery blanks would also have to go through digestion. The recovery rate (%) is the percent amount that was recovered and separated, and it was calculated by using the following equation:

$$Recovery\ rate\ (\%) = \frac{m_{recovery\ blank} - (m_{filter} + m_{wire})}{m_{spiking\ material}} * 100\% \qquad \textit{Equation 2.9b}$$

Where $m_{recovery\ blank}$ is the total weight (g) of the recovery blank including material, steel mesh filter and steel wire. $m_{spiking\ material}$ is the weight (g) of the added plastic. The recovery rate was calculated by using the total weight of the recovery blank after the final chemical digestion.

2.10 VISUAL ANALYSIS

2.10.1 Visual inspection by microscope

After chemical digestion, 0.0008 ± 0.0008 g of the separated and digested material was transferred to two pre-punched and pre-weighed clean steel mesh filters with pore size 26 µm and diameter of 13 mm. These circular filters were obtained by punching holes in a pre-washed steel mesh filter. The filters were placed on a steel-grey platform slide (Figure 2.10), and sample material was carefully scattered over the filters with a tweezer.

Figure 2.10 *– Two sub-samples with material from the core interval 8-9 cm of core BC-A.*

The weight of the extracted material was noted, and the samples were analysed by using the optical microscope *Nikon Eclipse E400*. The oculars had a magnification of x10, and optics with magnification x4 and x10 were used. Particles that stood out with an unnatural colour, special shape or size were categorized based on shape (fibre, film and granule), colour, and size. The size was divided in A, B, C and D. A is the smallest size fraction from 45 to 100 µm, B represents particles from 100 to 300 µm, C represents particles from 300 to 1000 µm, and D is the biggest fraction from 1 to 5 mm. A template (Table 2.10) was used to fill in the information on size, shape and colour.

Table 2.10 *– Template for categorization of particles with a distinct shape or/and colour. They were categorized by shape, size, and colour.*

Colour	**Fibre 1D**				**Film 2D**				**Granule 3D**			
	A	**B**	**C**	**D**	**A**	**B**	**C**	**D**	**A**	**B**	**C**	**D**
Clear/white	≥45 to <100 µm	100-300 µm	300-1000 µm	1-5 mm								
Light brown												
Dark brown												
Black												
Blue												
Red												
Green												
Orange												
Yellow												

2.11 FT-IR ANALYSIS

The samples were analysed with the FT-IR (Fourier-Transform Infrared spectroscopy) in addition to visual analysis. The FT-IR detects functional groups of polymers using infrared spectroscopy which results in fast and precise identification. Visual analysis with microscope is based on the shape, size and colour of the particles, and it may give an underestimation or overestimation of the number of microplastic particles (Song et al., 2015). The benefit of FT-IR is that the instrument can provide information about whether it is plastic or not, and what type. However, the FT-IR analysis is in 2D so it is difficult to see fibres and it was important that the 13 mm steel-mesh filters were as flat as possible. IT was also difficult to see the colour of the particles.

The FT-IR analysis were divided in two parts: microFT-IR analysis and macroFT-IR analysis. In the microFT-IR analysis, the steel-grey platform slide with the same two sub-samples from the visual analysis were analysed with the *FT-IR Microscope Spotlight 200i* instrument. In the macroFT-IR analysis, macroparticles (> 5 mm) were extracted from the rest of the sample material that was left in the wrapped steel mesh. The particles were extracted by using a tweezer and analysed with the *FT-IR spectrometer* instrument (Figure 2.11a).

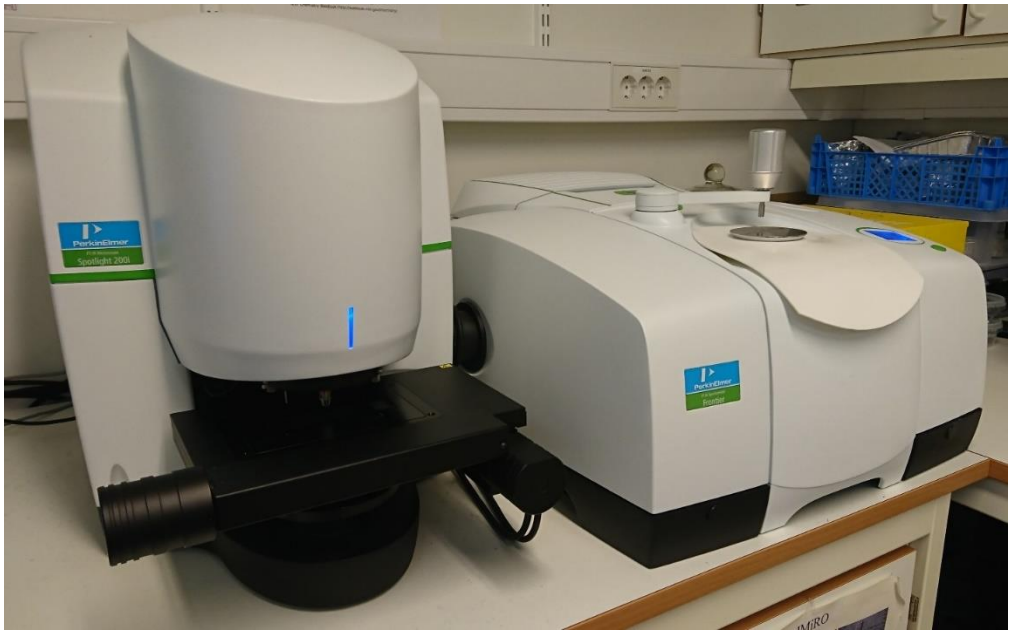

Figure 2.11a – *Left: FT-IR Microscope Spotlight 200i for the microFT-IR analysis. Right: FT-IR Spectrometer Frontier for the macroFT-IR analysis.*

2.11.1 microFT-IR analysis

Before the FT-IR Microscope Spotlight 200i could be used, it had to be filled with liquid nitrogen (Figure 2.11b). The instrument was ready to be used after ~30 minutes, the steel-grey platform slide with the two sub-samples were placed on the motorized stage. A joystick, connected to the instrument, was used to control the stage. The program *PerkinElmer Spectrum IR* was used to analyse the samples and to adjust the settings. The aperture was set to a 10 000x10 000 µm survey image, and the wavenumber of the transmittance beam was set to 4000-650 cm^{-1}. Particles were marked manually, and after placing a marker on a particle, the markers were visible in the survey image. All particles ≥ 45 µm on the filter were marked, and all markers were scanned and compared with the library provided by PerkinElmer (Spectrum IR). The best hit was set to represent the identified markers. Each identified marker was saved with score and identification. The scanned results of the sub-samples were exported, merged and sorted in Excel. The identified markers with a search score ≥ 0.7 were categorized as either mineral, organic, oxy-resin, petro-pyro, plastic or rubber. Petro-pyro includes all petroleum-based particles other than plastic, such as coal, tars etc. The identified markers with a search score < 0.7 were categorized as unknown (Table 2.11a).

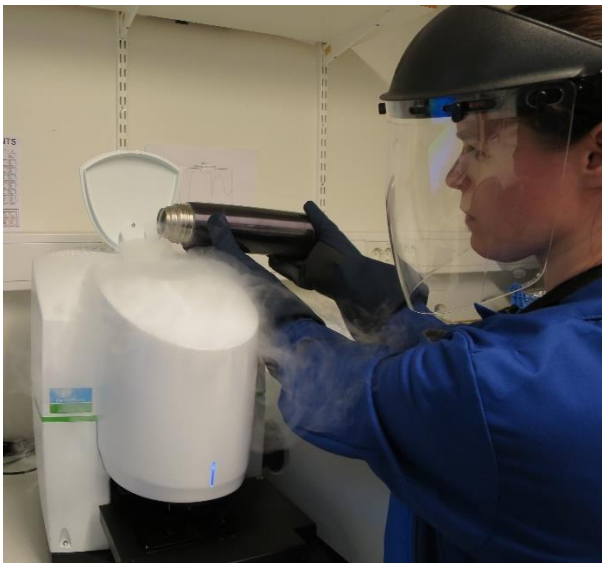

Figure 2.11b *– The FT-IR Microscope Spotlight 200i had to be filled with liquid nitrogen before use.*

Studies have proven that plastic increases drastically in number as the particles fragment into smaller particles, and the smaller the cut-off of the particle size in the study, the higher the concentration in number of particles (Bergmann et al. 2017). Steel mesh filter with a pore size 45 µm has been used for the filtration of the separated material from sediment samples in previous studies (Mahat, 2017; Lilleeng, 2018; Møskeland et al., 2018). The filters used for the microplastic-sediment separation in this study were assumed to be 45 µm, but it was quickly discovered that the filters had a pore size of 26 µm during the FT-IR analysis as there was a measuring scale in the same window as the survey image. By marking particles with a size ≥ 45 µm, it will be easier to compare the results with other studies where a steel-mesh filter with pore size 45 µm has been used.

Table 2.11a – *Categorization of the identified particle.*

Unknown	Particles identified by FT-IR with a search score < 0.7.
Mineral	Particles with no organic chemical bond visible in the IR spectrum, such as inorganic salts, glass, etc.
Organic	Particles identified as organic macromolecules like cellulose, rayon, chitin, proteins, or in general particles containing organic carbon molecular bonds that do not fit into any of the other categories.
Oxy-resins	Particles identified to be composed of oxy-resins, such as ethoxy resin, epoxy resin, phenoxy resin, or bisphenol-a containing particles.
Petro-pyro	Typical petroleum substances, such as hydrocarbon resins, petroleum products, etc.
Plastic	Commercial synthetic polymers, or a weathered derivative thereof, such as oxygenated polymers; semi-synthetics derived from biopolymers like cellulose, such as rayon, viscose etc. are not included.
Rubber	Particles identified as rubbers, polymers used as rubbers (e.g. SBR, silicon rubber), or resins containing rubber compounding products.

The particles identified as plastic were further subdivided into the plastic categories listed in Table 2.11b. The main composition of blends was chosen.

Table 2.11b *– Categories of plastic types, abbreviations and densities.*

Plastic category	Description	Density* (g/cm^3)
PE	Polyethylene (LDPE, HDPE, LLDPE etc.)	0.92-0.95
PE-chlorinated	Chlorinated polyethylene	1.10-1.25
PE-chlorosulfonated	Chlorosulfonated polyethylene	1.28
PE-oxidized	Oxidized polyethylene	-
PP	Polypropylene	0.87-0.90
PP-chlorinated	Chlorinated polypropylene	0.93
PET	Polyester, polyethylene terephthalate	1.40
PS	Polystyrene	1.05
Polyacrylamide	Polyacrylamide	1.30
PMMA	Poly(methyl methacrylate) and other polyacrylates	1.20
PU	Polyurethane	1.05
PVC	Polyvinyl chloride	1.40
PVF	Polyvinyl fluoride	1.38
PE:PP	Blends of polyethylene and polypropylene	0.86
Melamine	Melamine (all resin blends)	1.48
Nylon	Nylon (polyamide)	1.01-1.12
EVA	Ethylene-vinyl acetate	0.93-1.06
Unresolved	Plastic additives and other synthetic polymers	-

* The densities listed are the same as those presented in Scientific Polymer Products, Inc. (2013).

2.11.2 macroFT-IR analysis

FT-IR Spectrometer Frontier was used for analysing the macroplastic. The macroparticles was extracted from the sub-samples with a tweezer, and it was placed directly on an ATR crystal. The crystal was cleaned with methanol, and the background information was collected before placing the unknown macroparticle on it. Search score and identification was noted, and additional information about the particle was also noted. The template in Table 2.11c was used to collect the information of the macroparticles. Shape was divided into fibre, film and granule.

Table 2.11c *– Template for macroFT-IR analysis.*

Sample ID	Colour	Shape *(fibre, film, granule)*	Length/width (mm)	Comments	Oxy-resin, Petro-Pyro, Plastic, Rubber	Type

2.12 CORRECTION OF DATA

2.12.1 Method blanks

The weight of the method blanks was used to correct the separated sample material. The mean weight of the method blanks (n=9) was used for the correction (Equation 2.12a).

$$m_{corrected\ (MB)} = m_{separated\ material} - \frac{\sum m_{method\ blanks}}{n} \qquad \textit{Equation 2.12a}$$

Where $m_{corrected\ (MB)}$ is the corrected weight (g) of the separated material from the sediment sample, $m_{separated\ material}$ is the weight (g) of the separated material from the sediment sample, and $\Sigma m_{method\ blanks}$ is the total weight (g) of all nine method blanks, and n is the number of method blanks.

2.12.2 Recovery blanks

The recovery rate (%) achieved from the recovery blanks was used to correct the weight of separated material from the sediment samples (Equation 2.12b).

$$m_{corrected\ (MB,RB)} = \frac{m_{corrected\ (MB)}}{recovery\ (\%)} \qquad \textit{Equation 2.12b}$$

Where $m_{corrected\ (MB,\ RB)}$ is the weight (g) of the separated material from the sediment sample after being method and recovery blank corrected, $m_{corrected\ (MB)}$ is the weight (g) of separated material after being method blank corrected. Recovery (%) is the mean recovery rate based on six recovery blanks spiked with plastic powder, granulates and fibres.

2.12.3 Chemical digestion

The weight of the low-density material that was separated from the sediment was high (≥ 0.5 g) in some of the samples. Around 0.2 g was transferred to a new, pre-weighed steel-mesh filter and used for the chemical digestion. The reduction of this material was used to calculate the theoretical reduction if all the separated material was digested. The ratio between the material that was used for digestion, and the total separated material was used to calculate the corrected weight of the total separated material after digestion (Equation 2.12c).

$$m_{total\ correction} = m_{corrected\ (MB,RB)} * \frac{m_{separated\ material\ (total)}}{m_{digestion}} \qquad \textit{Equation 2.12c}$$

Where $m_{total\ correction}$ is the corrected weight (g) of the separated material after the final round of chemical digestion if all the separated material was digested. This is the weight that is used for the concentration of microplastic particles. $m_{corrected\ (MB,\ RB)}$ is the corrected weight (g) of the separated material that was used for the chemical digestion, $m_{separated\ material\ (total)}$ is the total weight (g) of the separated material, and $m_{digestion}$ is the weight of the separated material used for the chemical digestion.

2.13 QUALITY CONTROL

2.13.1 Method blanks

The weight of all nine method blanks, before chemical digestion, showed that there was some background contamination from the method. The weight of the method blanks varied, and the weight was 0.0072±0.0050 g before chemical digestion, and 0.0001±0.0002 g after chemical digestion. The weight of the method blanks is listed in Table 2.13a.

Table 2.13a *– List of the method blank weights with mean and standard deviation (SD).*

Method blank-ID	**Density of $ZnCl_2$-$CaCl_2$ (g/cm^3)**	**Weight (g) before chemical digestion**	**Weight (g) after chemical digestion**	**Reduction (%)**
Blank 1	1.53	0.0029	0.0000	100.0
Blank 2	1.53	0.0034	0.0000	100.0
Blank 3	1.54	0.0062	0.0000	100.0
Blank 4	1.53	0.0057	0.0000	100.0
Blank 5	1.53	0.0102	0.0000	100.0
Blank 6	1.53	0.0149	0.0003	98.0
Blank 7	1.53	0.0020	0.0002	90.0
Blank 8	1.54	0.0043	0.0000	100.0
Blank 9	1.55	0.0150	0.0004	97.3
MEAN ± SD	1.53±0.01	0.0072±0.0050	0.0001±0.0002	98.4±3.3

The measuring weight that was used (*Mettler AE 240*) had two options. The weight could be shown with four or five decimals, but the weight was unstable with five decimals so the option with four decimals was used. The accuracy of the measuring weight was regularly tested with a 1.0004 g weight in the period of September 2018 to August 2019. The minimum of 42 measurements was 1.000 g, the maximum was 1.0005 g, the mean was 1.0003 g and the standard deviation was 0.0001 g. The last digit in the weights has an uncertainty and there could be a

significant difference between the method blank weights that are listed as 0.0000 g in Table 3.5a. The visual analysis showed that there were particles in the method blanks with 0.0000 g as final weight, after chemical digestion. The particles were small and few in number and the weight would therefore be shown as 0.0000 g. There may have been a more significant difference between the method blanks with five decimals.

The first method blank (Blank 1) was not analysed visually with microscope or with FT-IR as the 13 mm filter with sample material was lost. The mean weight of the rest of the method blanks, 0.0001 g (after chemical digestion), was used to correct the weight of the separated sample material from the sediment samples.

2.13.2 Recovery blanks

In total six recovery blanks were separated by spiking sediment from sediment samples from core BC-A and BC-B. The core sample intervals 1-2 cm, 6-7 cm and 12-13 cm from core BC-A were spiked, and the intervals 5-8 cm, 15-18 cm and 25-27 cm from core BC-B were spiked with plastic fibres, granulates and powder. The specifications of the plastic used as spiking material are listed in Table 2.9a and the amount of added plastic is listed in Table 2.9b, under section 2.9.2 Recovery blanks. The recovery rates of the spiking material are listed in Table 2.13b.

Table 2.13b *– List of recovery rates (%) of powder, fibre and granulates.*

Recovery blank - ID	Density of $ZnCl_2$-$CaCl_2$ (g/cm^3)	Recovery rate after digestion (%)		
		Powder	Fibre	Granulates
Spiked BC-A 1-2cm	1.55	85.0	-	-
Spiked BC-A 6-7cm	1.55	-	3.0	100.0
Spiked BC-A 12-13cm	1.53	90.0	-	-
Spiked BC-B 5-8cm	1.53	-	23.0	100.0
Spiked BC-B 15-18cm	1.53	91.0	-	-
Spiked BC-B 25-27cm	1.54	-	-5.0	100.0
MEAN ± SD	1.54±0.01	88.7±3.2	7.0±14.4	100.0±0.0

All the added granulates were separated so particles with a size of 3 mm seem to be easily separated by density separation. Powder has a smaller size and it has a smaller recovery rate with 91% as the highest recovery. Lumps of fibres were observed in the sediment (in the sediment chamber) after draining the $ZnCl_2$-$CaCl_2$ after separating Spiked BC-B 25-27cm, and a lump of fibres were observed in the lower part of the glass column after preparing and introducing Spiked BC-A 6-7cm to the BMSS. This could explain the very low recovery rate of these recovery blanks. The recovery rate of fibres in Spiked BC-B 5-8 cm is also very low compared to powder and granulates, so the amount of fibres was analysed semi-quantitative. The recovery rates give an indication of the amount of microplastic particles that were separated and the amount that could be left in the density solution and the sediment. The mean recovery rate of powder, 88 % was used to correct the microplastic concentration and this concentration is the maximum amount of microplastic in the sediment samples.

Sediment sample BC-A 6-7cm was spiked with PET fibres. Sample BC-A 5-6cm was separated after the spiked sample, and white fibres were visible in this sample. They were analysed with FT-IR and appeared to be PET fibres with high scores. The samples seemed to have been contaminated by the previous spiked sample, and PET results were categorized as “unknown” and not presented as plastic in the results.

2.13.3 Density separation and extraction recoveries

There was a lot of material left after all the separated samples had been through at least two rounds of chemical digestion, except one of the surface samples. An amount of the separated material was therefore extracted and extrapolated, and the results after the extrapolation were supposed to represent the whole sample material after separation and digestion. The percentages of the sample weights after digestion from core BC-A, BC-B and the surface samples are given in Table 2.13c, Table 2.13d and Table 2.13e.

Table 2.13c *– Material weight and percentage of the weight after digestion (core BC-A). The weights are method blank and recovery blank corrected.*

Sample ID	Total weight of separated material (g)	Weight (g) after digestion	Amount (g) analysed with FT-IR	Percentage of weight after digestion (%)
BC-A 0-1	1.1828	0.0497	0.0003	0.60
BC-A 1-2	0.5080	0.0715	0.0005	0.70
BC-A 2-3	0.3119	0.0263	0.0009	3.42
BC-A 3-4	0.3838	0.0313	0.0016	5.11
BC-A 4-5	0.2286	0.0283	0.0008	2.83
BC-A 5-6	0.1173	0.0126	0.0006	4.76
BC-A 6-7	0.0804	0.0141	0.0008	5.67
BC-A 7-8	0.2981	0.0418	0.0005	1.20
BC-A 8-9	0.2435	0.0256	0.0006	2.34
BC-A 9-10	0.3101	0.0602	0.0003	0.50
BC-A 10-11	0.1486	0.0508	0.0003	0.59
BC-A 11-12	0.2298	0.0380	0.0004	1.05
BC-A 12-13	0.5049	0.2031	0.0007	0.34
BC-A 13-14	3.5602	1.1797	0.0012	0.10
BC-A 14-15	11.0432	4.7860	0.0014	0.03
MEAN±SD	1.2767±2.8376	0.4413±1.2375	0.0007±0.0004	2.09±1.95

Table 2.13d *– Material weight and percentage of the weight after digestion (core BC-B). The weights are method blank and recovery blank corrected.*

Sample ID	Separated material (g)	Weight (g) after digestion	Amount (g) analysed with FT-IR	Percentage of weight after digestion (%)
BC-B 0-5	0.0366	0.0055	0.0001	1.82
BC-B 5-8	0.0347	0.0016	0.0003	18.75
BC-B 8-11	0.0640	0.0051	0.0006	11.76
BC-B 11-15	0.0528	0.0041	0.0007	17.07
BC-B 15-18	0.1424	0.0078	0.0002	2.56
BC-B 18-20	0.9363	0.0102	0.0004	3.92
BC-B 20-22	0.1670	0.0169	0.0014	8.28
BC-B 22-25	0.1773	0.0132	0.0005	3.79
BC-B 25-27	0.8091	0.1289	0.0008	0.62
MEAN±SD	0.2689±0.3481	0.0215±0.0406	0.0006±0.0004	7.62±6.78

Table 2.13e *– Material weight and percentage of the weight after digestion (surface samples). The weights are method blank and recovery blank corrected.*

Sample ID	Separated material (g)	Weight (g) after digestion	Amount (g) analysed with FT-IR	Percentage of weight after digestion (%)
BC-15	1.9445	0.2437	0.0002	0.08
BC-25	0.7328	0.1397	0.0003	0.21
BC-35	0.7838	0.2069	0.0012	0.58
BC-45	0.5353	0.0476	0.0006	1.26
BC-65	0.2018	0.0171	0.0005	2.92
BC-B	0.2508	0.0576	0.0013	2.26
MEAN ± SD	0.7415±0.6362	0.1188±0.0927	0.0007±0.0005	1.22±1.16

3 RESULTS

3.1 CTD PROFILES

The CTD profiles from station BC-65 (closest to Langøyene) and BC-B (closest to Bekkelaget sewage treatment plant) show similar profiles of salinity and temperature. Oxygen was also similar in the profiles from both stations, but it was different from 10 m water depth to the water surface. The three parameters seemed to be stable and had the same value below 30 m water depth (Figure 3.1a, Figure 3.1b). The salinity from the bottom of the profiles to 30 m depth was 32-33, the temperature was 8-8.5 °C, and the oxygen was 4 mg/L. From 24-30 m and upwards to the water surface, salinity decreased from 32-33 to 21. The temperature decreased from 8-8.3 °C at 24 m depth to 5.3-5.5 °C at 16 m depth, and then it increased to 9.3 °C in the water surface. The oxygen increased from 4 mg/L at 26-30 m depth to 11.4-11.6 mg/L at 16-18 m, and the values from this depth and upwards to the water surface is different for the two stations. At BC-65, the oxygen decreased to 7.4 mg/L in the water surface, while it decreased to 10.2 mg/L in the water surface at station BC-B.

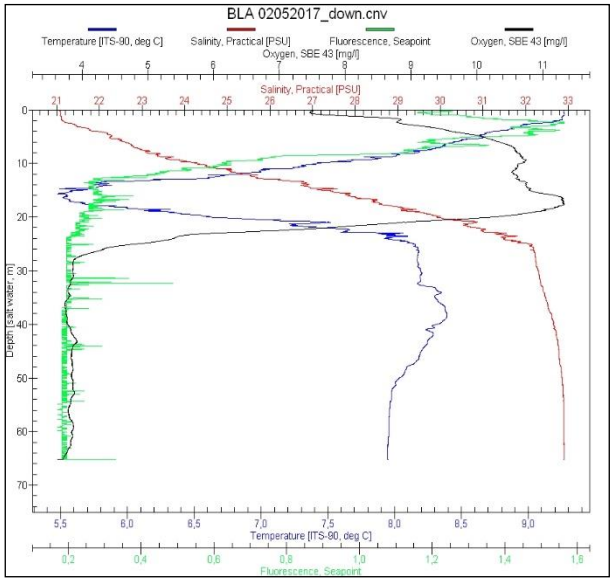

Figure 3.1a *– CTD profile from station BC-65. Provided by Sindre Holm, captain of RV Trygve Braarud.*

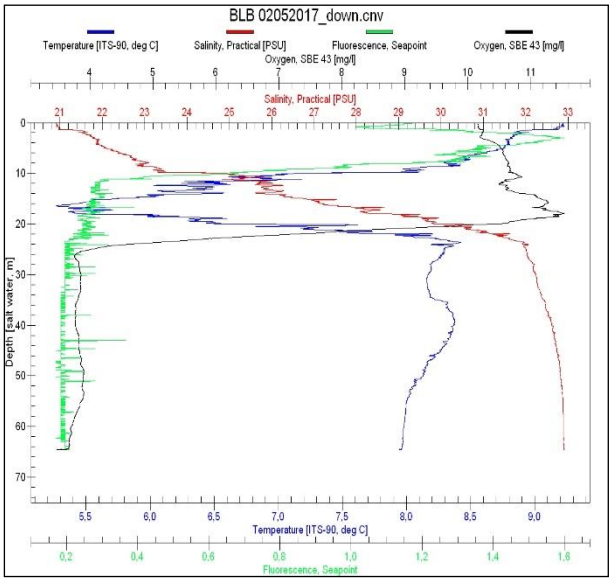

Figure 3.1b *– CTD profile from station BC-B. Provided by Sindre Holm, captain of RV Trygve Braarud.*

3.2 CORE BC-A

The interval from 0-15 cm from BC-A was used for the microplastic analysis, and BC-A is a different core than the one that was described. The data of grain size, TOC and heavy metals are from another core. There are three cores that have been analysed but they are all from the same sampling station.

3.2.1 Core description

The core is 54 cm long, and shell fragments were observed in the deepest part to 40 cm. The sediment is grey, firm and seemed to have a high content of clay. The colour changes to black around 34 cm, and the sediment is gradually darker from 34 to 20 cm. There is a black horizon at 19-20 cm with very coarse material and big fragments of rock. There seems to be traces of oil in the dark sediment from 20 to 10 cm. From 10 to 6 cm, the sediment is grey and firm, and the sediment from 6 to 0 cm is brown. The sediment in the upper part of the core was loose, and it seemed to have a high content of water (Figure 3.2a).

Figure 3.2a *– The core labelled "BL-A-A" is from the same station as BC-A.*

3.2.2 Water content

The water content is varying from 0 to 15 cm. It is starts with 60 % at the depth of 14.5 cm, and it increase upwards to 9.5 cm where the water content is 80 %. Then, it starts to decrease, and it goes from 80 % at 9.5 cm to 68 % at 4.5 cm. From this depth and upwards, it starts to increase again, and it reaches 80 % at the core surface (Figure 3.2b). The values of water content, and wet and dry weight of the sediment samples are listed in Appendix A.

3.2.3 Total organic carbon and C/N

The TOC starts with a high value of 114 mg/g at a depth of 12.5 cm. The value decreases towards the core surface and ends up with a value of 50 mg/g (Figure 3.2b). There are no values of TOC between core depth 13 and 15 cm because the sediment was too coarse to be analysed. The ratio of carbon and nitrogen seems to show the same trend as the TOC. The highest value of carbon and nitrogen is 15.2 at the depth of 12.5 cm (Figure 3.2b).

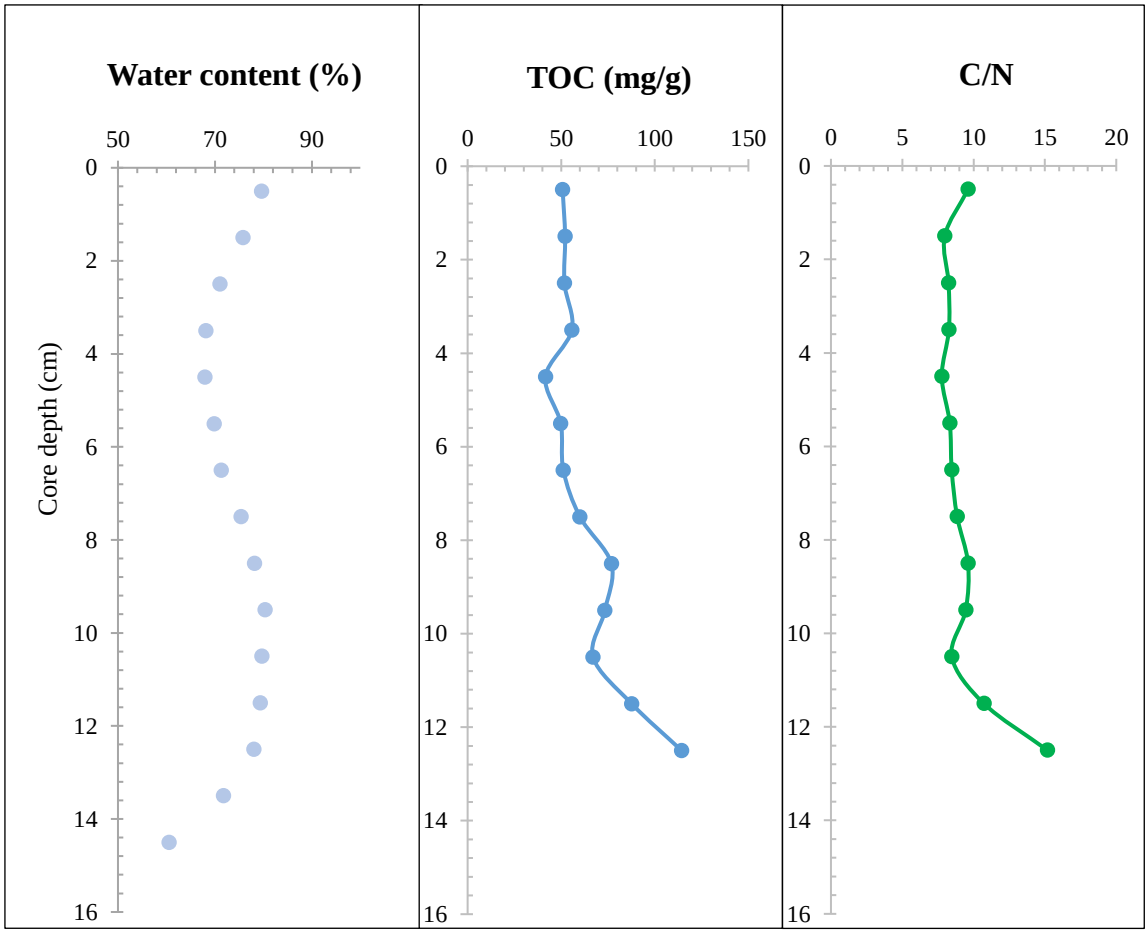

Figure 3.2b – *Left: water content in core BC-A. Middle: TOC (the values are retrieved from Bjørneby (2019)). Right: C/N (the values are retrieved from Bjørneby (2019)).*

3.2.4 Grain size distribution

The full analysis of grain size distribution shows that the samples from 12-13 cm, 13-14 cm and 14-15 cm core depth have a distribution of grain size that differs from the rest of the samples. They seem to have a much higher proportion of particles with a larger diameter (Figure 3.2c). Plot of the sand content (Figure 3.2c) shows a high amount of sand in the lower part of the core. It decreases upwards and seems to be stable from 7.5 cm core depth to the core surface.

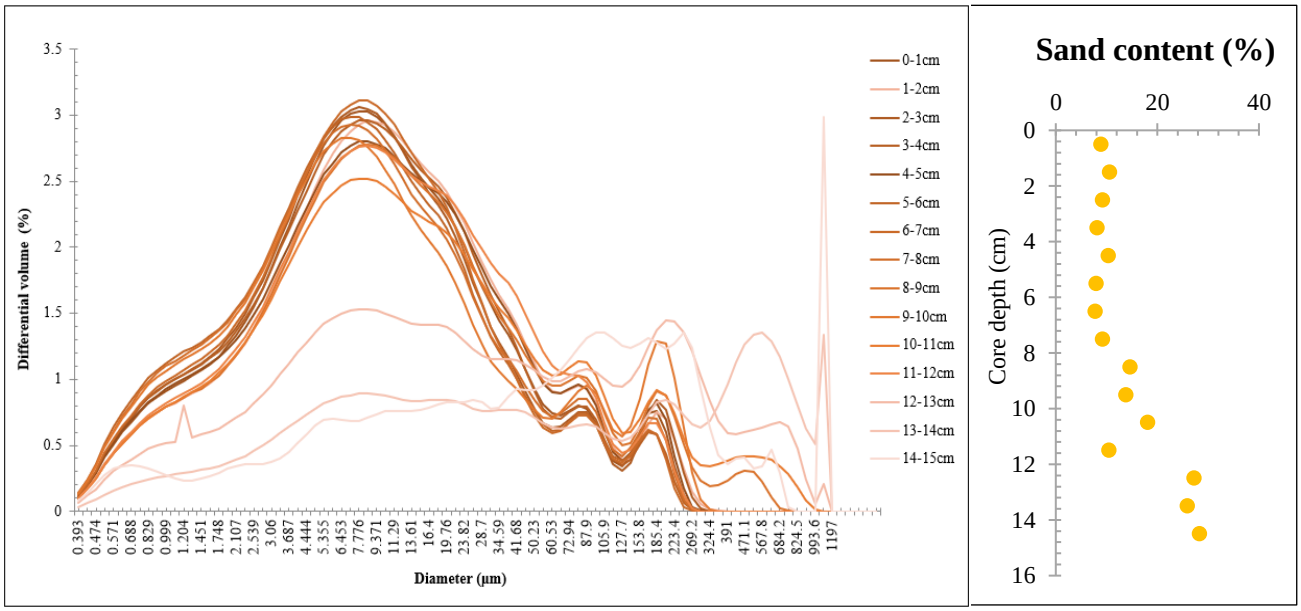

Figure 3.2c *– <u>Left</u>: distribution of grains with diameter from 0.393 to 1197 µm. <u>Right</u>: sand content (the values are retrieved from Bjørneby (2019)).*

3.2.5 Dating

The report from the University of Liverpool (Appendix B) said that the analysis showed variations of ^{210}Pb activity in the core samples from a depth under 12 cm. The activity of ^{226}Ra was analysed together with ^{210}Pb activity to look at the relation between these two. The lowest value was found in the 14-15 cm core sample, and the highest value was found in the 13-13 cm core sample. A possible explanation of these variations is deposition at this location of allochthonous material from two different sources, one ^{226}Ra poor and one that is ^{226}Ra rich. ^{137}Cs concentrations showed a well-defined peak in the 5-6 cm sample which could possibly be a record of fallout from the 1986 Chernobyl accident. There were two smaller peaks at 9-10 cm and 14-15 cm which could also be records of atmospheric fallout, though it is not certain. The CRS model that was used to calculate the ^{210}Pb dates, states that the 6.5 cm core depth represents 1986 and 10 cm core depth represents 1963. This may support the ^{137}Cs peaks at 5.5 and 9.5 cm, which could be associated with fallout events from 1986 and 1963. The calculations suggest that the high values of ^{210}Pb between 12 and 17 cm could be explained by a rapid sedimentation in the 1940s. The sedimentation rates were relatively constant from the late 1950s through the end of the 20th century with a mean sedimentation rate of 0.056 g cm^{-2} y^{-1}, and there may have been a small increase in the sedimentation rate in the recent years. Dates for the sediments below 12 cm are highly uncertain because of the very low ^{210}Pb concentrations. The report states that the sediment deeper than 13 cm was deposited in the 1940s.

3.2.6 Heavy metals

All the plots seem to have the same overall pattern with a maximum concentration in the core depth interval 11.5-13.5 cm which represents the 1940s and 1950s. The concentration increases from this depth and towards the core surface. It seems to stabilize in the upper part of the core in all the plots, except arsenic (Figure 3.2d). Cd was under the detection limit in the sediment samples from the core depth intervals 0-2 cm and 14-15 cm, and Hg was analysed semi-quantitative.

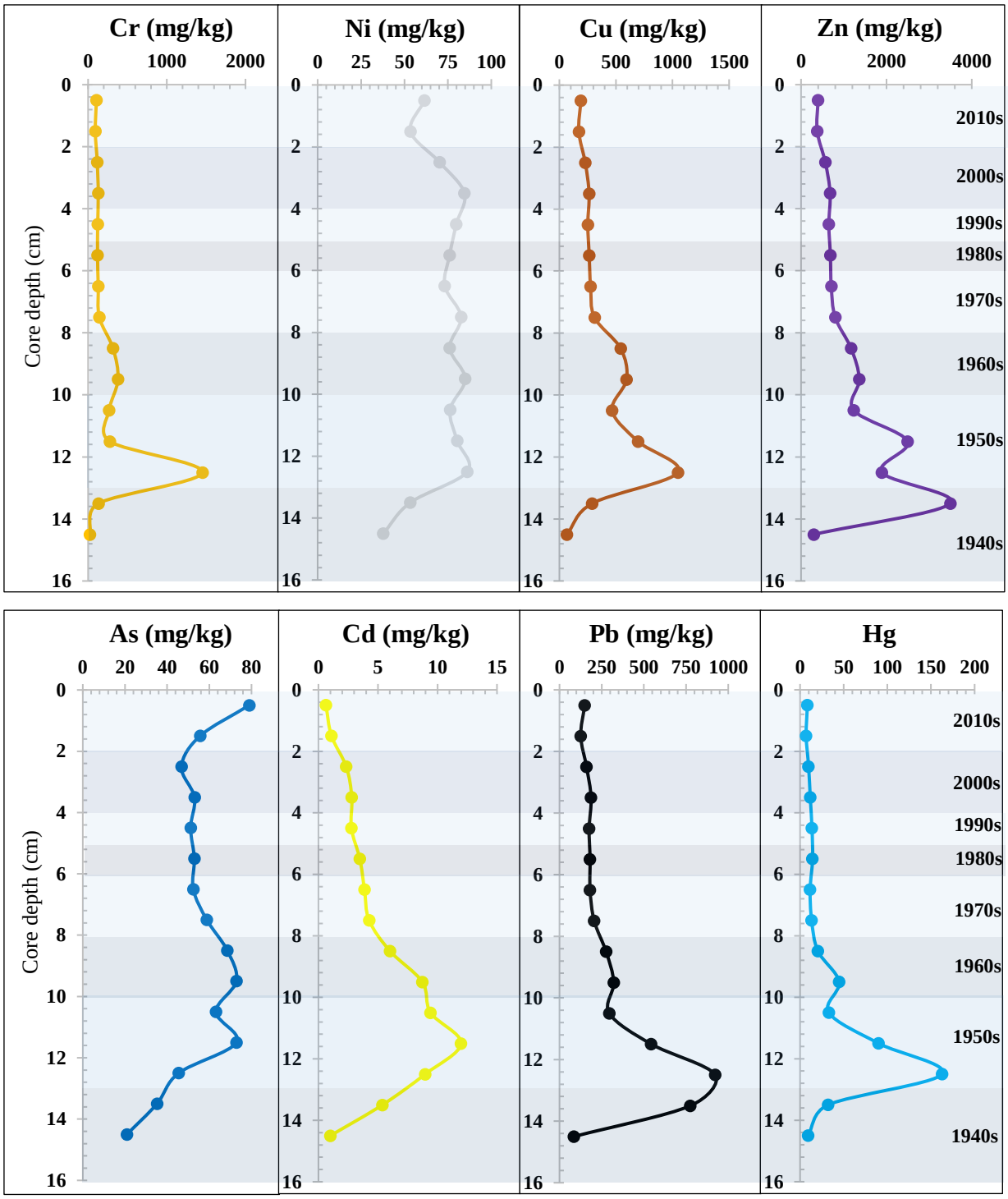

Figure 3.2d *– Profiles of the heavy metal content. The upper plots from left to right: chromium (Cr), nickel (Ni), copper (Cu) and zinc (Zn). The lower plots from left to right: arsenic (As), cadmium (Cd), lead (Pb) and mercury (Hg). The values are retrieved from Bjørneby (2019).*

3.2.7 Sediment preparation and separation/filtration

The sediment core samples from core BC-A were prepared and filtrated in the order from deep to shallow, from core interval 14-15 cm to 0-1 cm. The dry, homogenized sediment from core depth 14-15 cm was brown-grey, and it contained organic particles such as leaves, seeds and pieces of wood (Figure 3.2e). There were also some other particles that looked like waste (orange arrows in Figure 3.2e). There were a lot of low-density particles that had to be filtrated over to four steel mesh filters.

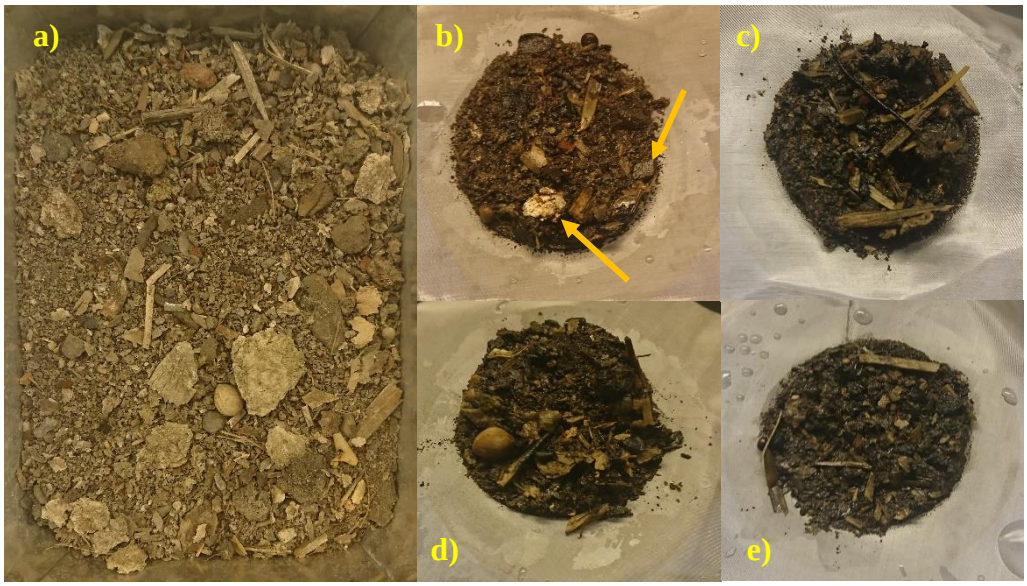

Figure 3.2e *– Introduction of sediment from core depth 14-15 cm from core BC-A to BMSS and separation/filtration. a) dry, homogenized sediment, b-e) low-density particles that have been separated from the sediment.*

The sample from core depth 13-14 cm was a mix of dry and homogenized light and dark grey sediment, and some organic material, such as particles of wood, was observed in the sediment. The low-density particles were filtrated over to one steel mesh filter (Figure 3.2f).

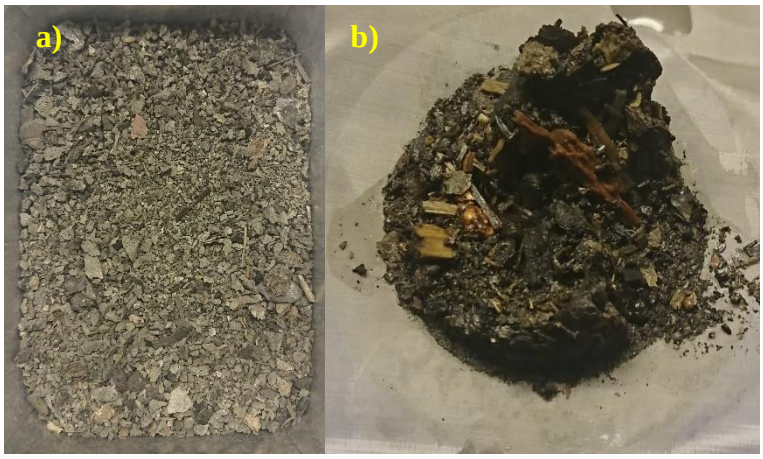

Figure 3.2f *– Introduction of sediment from core depth 13-14 cm from core BC-A to BMSS and separation/filtration. a) dry, homogenized sediment, b) low-density particles that have been separated from the sediment.*

The dry, homogenized sediment from core depth 5-6 cm was grey. There were a few big, white particles in the sediment that possibly were freeze-dried shrimp (orange arrow). This sediment contained less low-density particles than the sediment from the core interval 13-14 and 14-15 cm (Figure 3.2g).

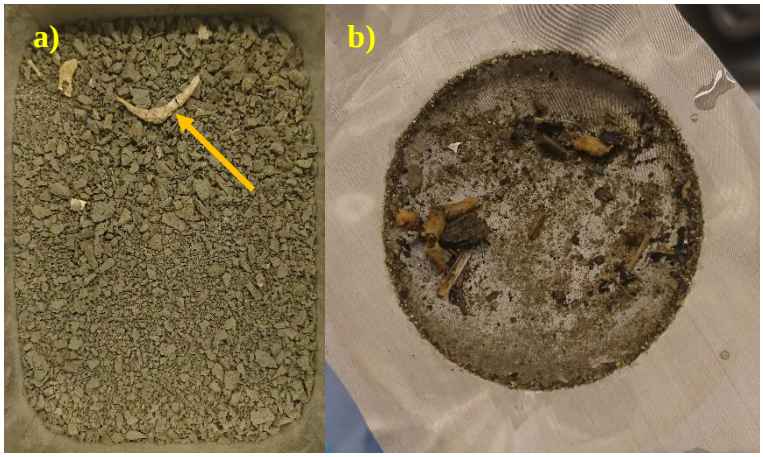

Figure 3.2g *– Introduction of sediment from core depth 5-6 cm from core BC-A to BMSS and separation/filtration. a) dry, homogenized sediment, b) low-density particles that have been separated from the sediment.*

3.2.8 Visual analysis

The results of the visual analysis are simplified, and the different categories are presented as distribution of shape, distribution of size and distribution of colour. The information on shape, size and colour of each particle can be seen in Appendix F, and a selection of particles identified as plastic is presented in Appendix G.

SHAPE (fibre, film, granulate) and SIZE (A, B, C and D)

The distribution of particles of different shape (fibre, film, granulate) shows that the fibres seem to increase from the bottom to the upper part of the core. The percentages of film and granulates are varying through the core (Figure 3.2h). The distribution of particle size (A, B, C, D) shows that there are most particles from the size category B (100-300 µm). There are second most particles from size category C, then A, and there are few particles from category D (see Table 2.10 for the size categories). Particles from category A, B and C seem to have a varying trend throughout the core, and particles from category D were only observed in the core depth interval 2.5-7.5 cm (Figure 3.2h).

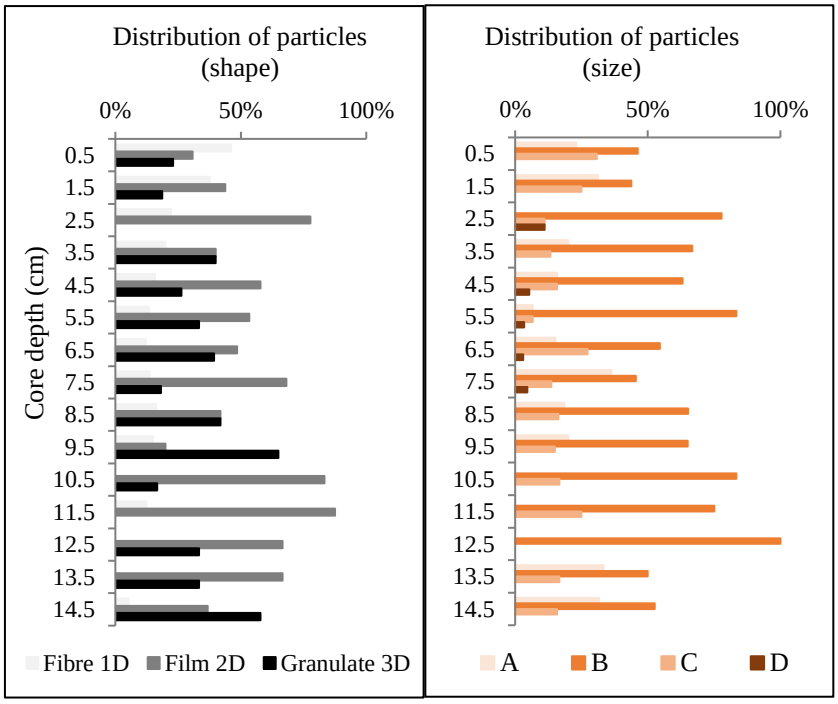

Figure 3.2h – *<u>Left</u>: distribution of particles of different shapes (fibre 1D, film 2D, granulate 3D) in core BC-A. <u>Right</u>: distribution of particles of different size (A: ≥45-100 µm, B: 100-300 µm, C: 300-1000 µm, D: 1-5 mm).*

COLOUR

The distribution of particles with different colours shows that the clear/white, brown and black particles were observed throughout the core. The black particles seem to have a decreasing trend from the bottom to the core surface, while the other colours are varying. The particles with the colours blue, red, green, orange and yellow do not seem to appear in the samples from every core interval. Yellow particles were first observed in the sample from core depth 14.5 cm, blue and green particles were first observed in the sample from core depth 9.5 cm, red particles were first observed in the sample from core depth 8.5, and orange particles were first observed in the sample from core depth 7.5 cm (Figure 3.2i).

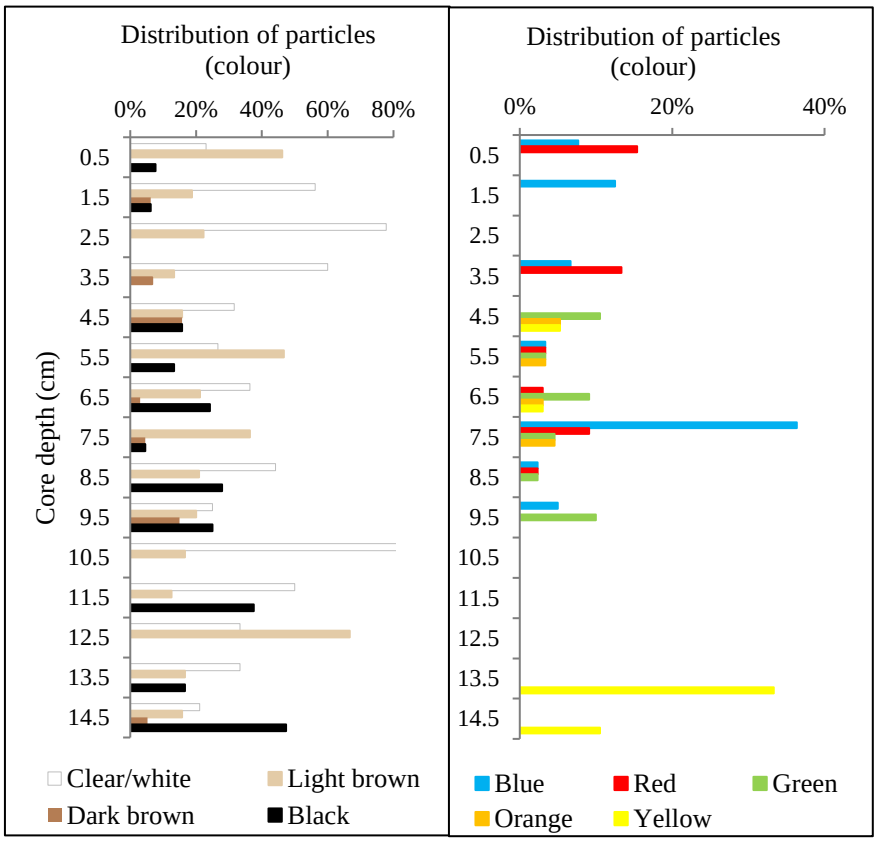

Figure 3.2i *– <u>Left</u>: distribution of particles with the colours clear/white, light brown, dark brown and black in core BC-A. <u>Right</u>: distribution of particles with the colours blue, red, green, orange and yellow.*

3.2.9 Microplastic, rubber, oxy-resin and petro-pyro

The plots of concentration (number of particles/ kg dry sediment) of oxy-resin, petro-pyro, plastic and rubber particles show that the highest concentration is in the bottom of the core, in the 1940s. It decreases towards the core surface, and it seems to increase in the upper 1.5 cm of the core. All four types of particles seem to have the same trend throughout the core (Figure 3.2j). The concentrations are listed in Appendix H.

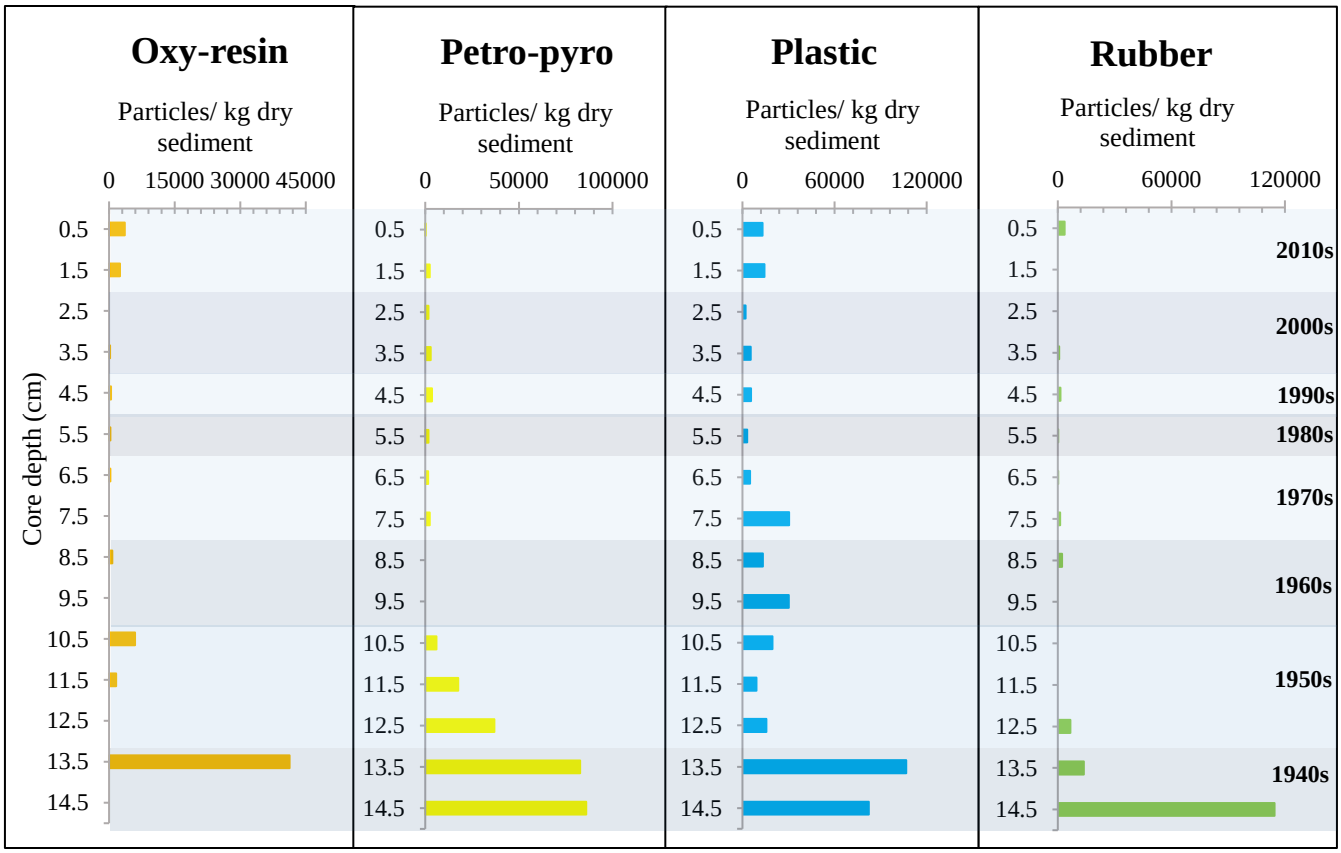

Figure 3.2j *– Plots of the concentration of oxy-resin, petro-pyro, plastic and rubber in core BC-A. The concentration is given as number of particles per kg dry sediment.*

All four particle types seem to have the same trend when the concentration is presented as weight in mg per kg dry sediment that was introduced to the BMSS. They all have high concentrations in the lower part of the core, in the 1940s, and the concentration decreases towards the core surface (Figure 3.2k). The trend of concentration in weight seems to be the same as the concentration presented as number of particles. The figures of both concentrations show a maximum in the deep part of the core, where the percentage of analysed material was very low, and the extrapolation factor was very high (see Table 2.13c).

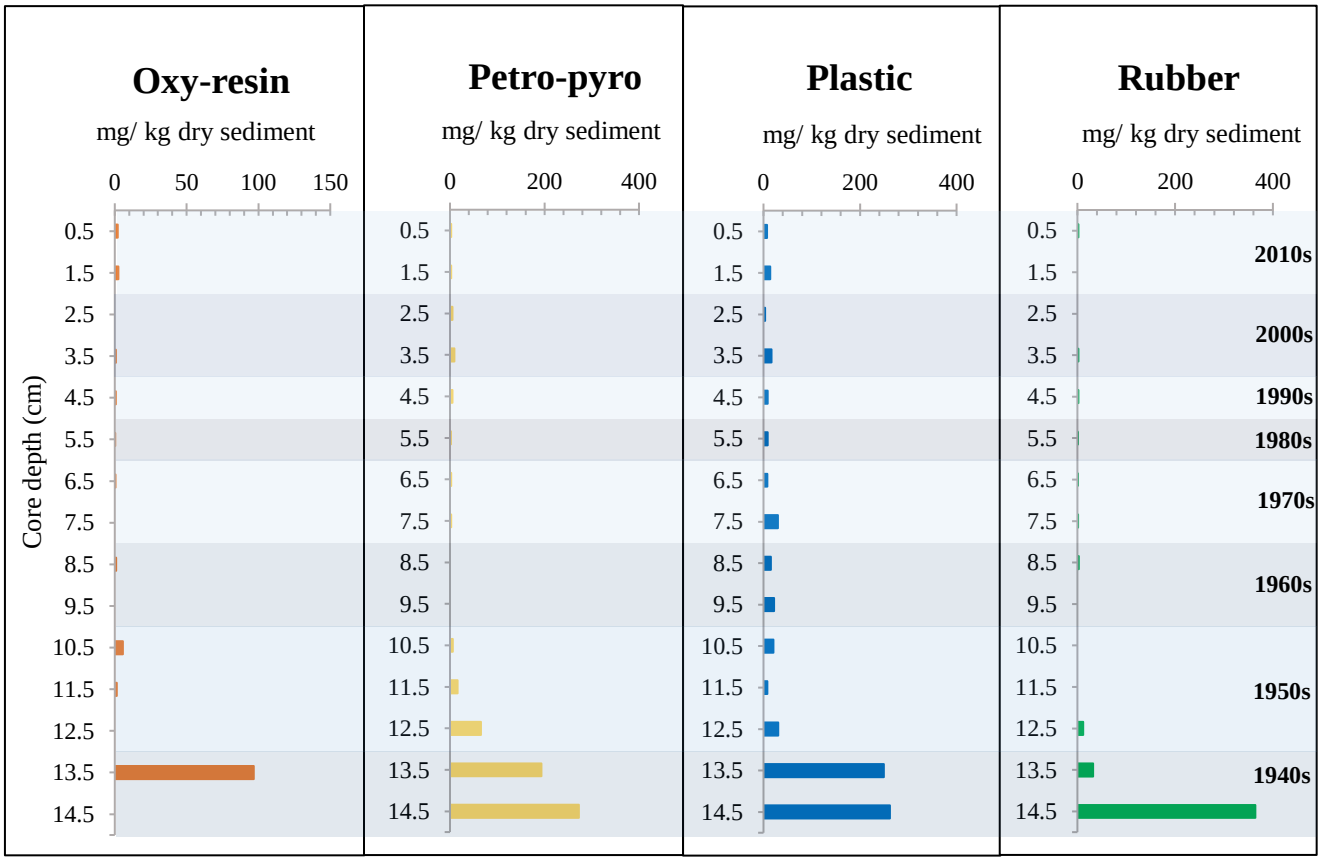

Figure 3.2k *– Plots of the concentration of oxy-resin, petro-pyro, plastic and rubber in core BC-A. The concentration is given as the weight of particles in mg per kg dry sediment.*

3.2.10 Plastic types

The percentages of the polyolefins (PE, PP, PE-oxidized and PE:PP) were merged and presented in a plot. The plot of polyolefins shows an increasing trend from the bottom to 3.5-5.5 cm core depth, and then it seems to decrease in the upper 0-3.5 cm. The chlorinated plastic types (PVC, PE-chlorinated and PP-chlorinated) were merged. The plot seems to increase in the deepest part of the core, from 12.5 to 3.5 cm core depth, from 1950s to the 2000s, and it seems to decrease in the upper 0-2 cm of the core. The percentage of the plastic types PS, PET, PU, PVF and nylon were merged and are presented in the same plot. The plot of these plastic types shows an increasing trend from the bottom of the core to 5.5 cm core depth and then it decreases towards the core surface (Figure 3.2l).

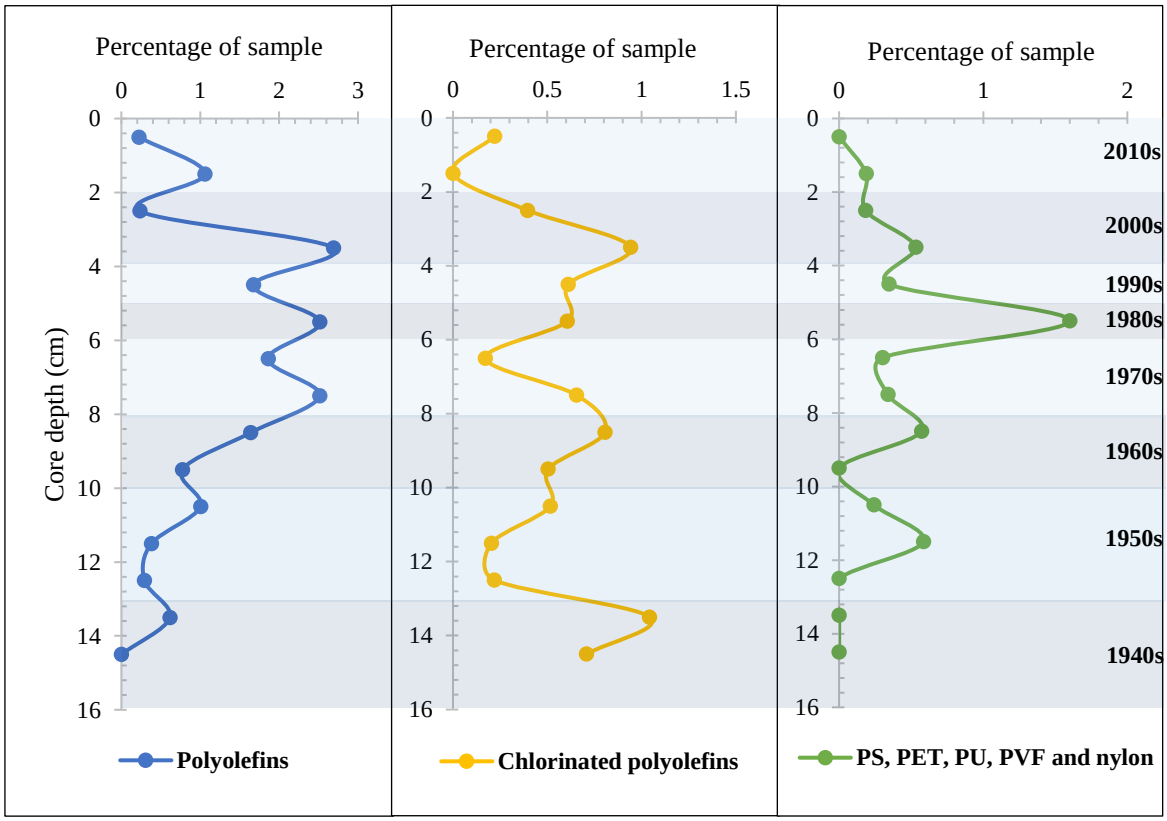

Figure 3.2l *– Left: plot of the percentage of polyolefins in core BC-A. Middle: the percentage of chlorinated polyolefins. Right: the percentage of PS, PET, PU, PVF and nylon (See Table 2.11b for the plastic abbreviations).*

The plot of PMMA, EVA and melamine shows an increase from 9.5 to 8.5 cm, in the 1960s, and a decrease from 6.5 to 5.5 cm, in the 1970s. It increases again in the upper 0-2 cm of the core. Less common polymers from the FT-IR analysis were merged with additives in a category called "unresolved plastic", and the plot shows that the percentage of these particles varies throughout the core (Figure 3.2m).

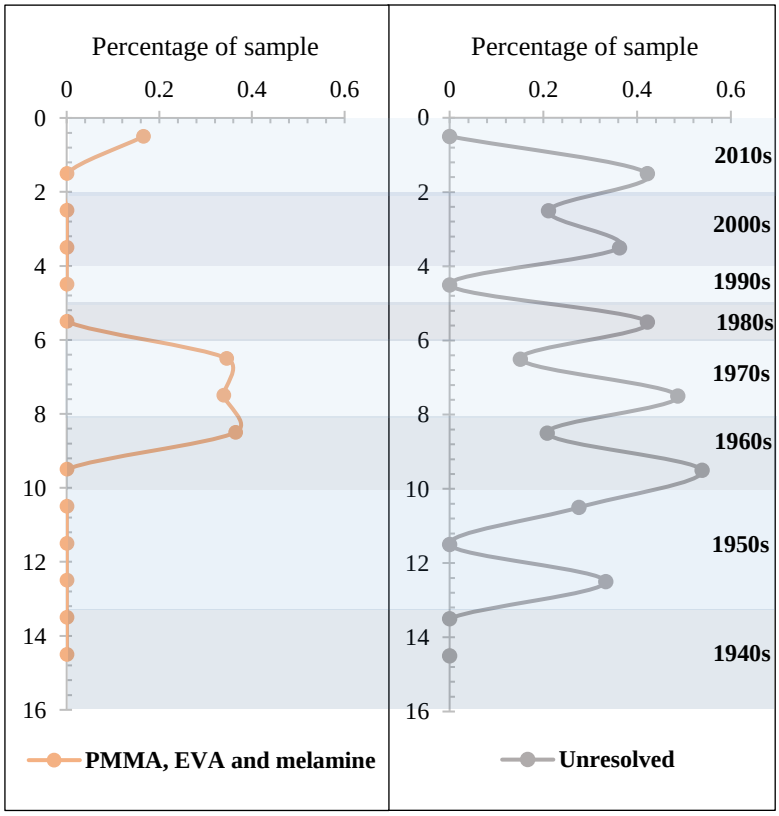

Figure 3.2m – *<u>Left</u>: plot of the percentage of PMMA, EVA and melamine in core BC-A. <u>Right</u>: the percentage of unresolved plastic (See Table 2.11b for the plastic abbreviations).*

3.2.11 Macroplastic

The results from the macroplastic analysis (Appendix I) are summarized in Table 3.2. There were no plastic particles big enough to be picked out with a tweezer, in the deepest core samples. There was also no plastic in some of the other core intervals, and the uppermost part of the core. PE and PP were the most frequent plastic types and they occurred in the core interval from 7 to 5 cm, and from 4 to 1 cm. The particles identified as plastic were 0.31 to 13.84 mm, they were mostly fibres and they had different colours, such as clear, white, black, dark brown, red, blue, green and orange (Table 3.2).

Table 3.2 *– Plastic types of particles that could be picked out by tweezer, in core BC-A (See Table 2.11b for the plastic abbreviation).*

Sample ID	Plastic type	Colour	Shape	Length (mm)
BC-A 0-1	-			-
BC-A 1-2	PP	White	Fibre	13.84
BC-A 2-3	PE	Grey	Fibre	1.03
	PP	Blue, clear	Fibre	0.85-6.12
BC-A 3-4	PE	White	Fibre	1.58
	PP	Blue, clear	Fibre	0.31-7.20
BC-A 4-5	-	-	-	-
BC-A 5-6	PE	White	Fibre, film	2.18-3.35
	PE-chlorosulfonated	White, green	Film, granule	0.31-3.21
	PP	Black/dark brown	Fibre	2.51
	PU	White	Film	2.32
BC-A 6-7	PP	Clear/white	Fibre	2.45
	Nylon	Clear/white	Fibre	6.70
BC-A 7-8	PP	Clear/white, green, red, black/dark brown	Fibre	1.39-5.68
BC-A 8-9	-	-	-	-
BC-A 9-10	-	-	-	-

BC-A 10-11	PE	Green	Film	2.26
BC-A 11-12	-	-	-	-
BC-A 12-13	PE-chlorinated	White, red, orange	Film, granule	0.68-1.39
BC-A 13-14	-	-	-	-
BC-A 14-15	-	-	-	-

3.3 CORE BC-B

The interval from 0 to 27 cm of the core was used for the microplastic analysis, and the same core was described. The data of grain size, TOC and heavy metals are from another core but from the same sampling station as BC-B.

3.3.1 Core description

The core is 75 cm long, and the sediment is grey-black from 75 to 55 cm. Shell fragments were observed in the sediment from 75 to 60 cm. The sediment is grey from 52 to 45 cm, and it seemed to have a high content of clay. The colour of the sediment changes to black, and it has a thin layer with grey sediment at 40 cm. A horizon with coarse material was observed between 35 and 30 cm. The colour of the sediment varies between grey and black from 30 to 6 cm, and there are several grey laminations with various thickness. The uppermost layer, 6 to 0 cm, is brown. The sediment was loose and seemed to have a high content of water (Figure 3.3a).

Figure 3.3a *– The core labelled "BL-B" is the same as the core named BC-B that was analysed for microplastic.*

3.3.2 Water content

The water content is also varying in this core. It starts with 76 % at the depth of 26 cm, and it decrease upwards and the water content is 68 % at 21 cm. Suddenly, there is a peak at 19 cm where the water content is 77 %. It decreases after this, but it starts to increase from 16.5 cm to 9.5 cm where it once more decrease, all the way up to the surface of the core (Figure 3.3b).

3.3.3 Total organic carbon and C/N

The TOC is varying substantially from 29 cm and upwards to the core surface. The general trend seems to be an increase of TOC with a value of 44 mg/g in the lower part and 61 mg/g in the upper part. There are peaks of TOC at the depths 27, 17.5, 11.5 and 4.5 cm, where the biggest peak is at 17.5 cm with a TOC of 97.6 mg/g (Figure 3.3b). The ratio of carbon and nitrogen seems to show a similar trend as the TOC, but it has less variations and it seems to stabilize in the upper part of the core. The biggest peak is at 17.5 cm with a carbon and nitrogen ratio of 15.4 (Figure 3.3b).

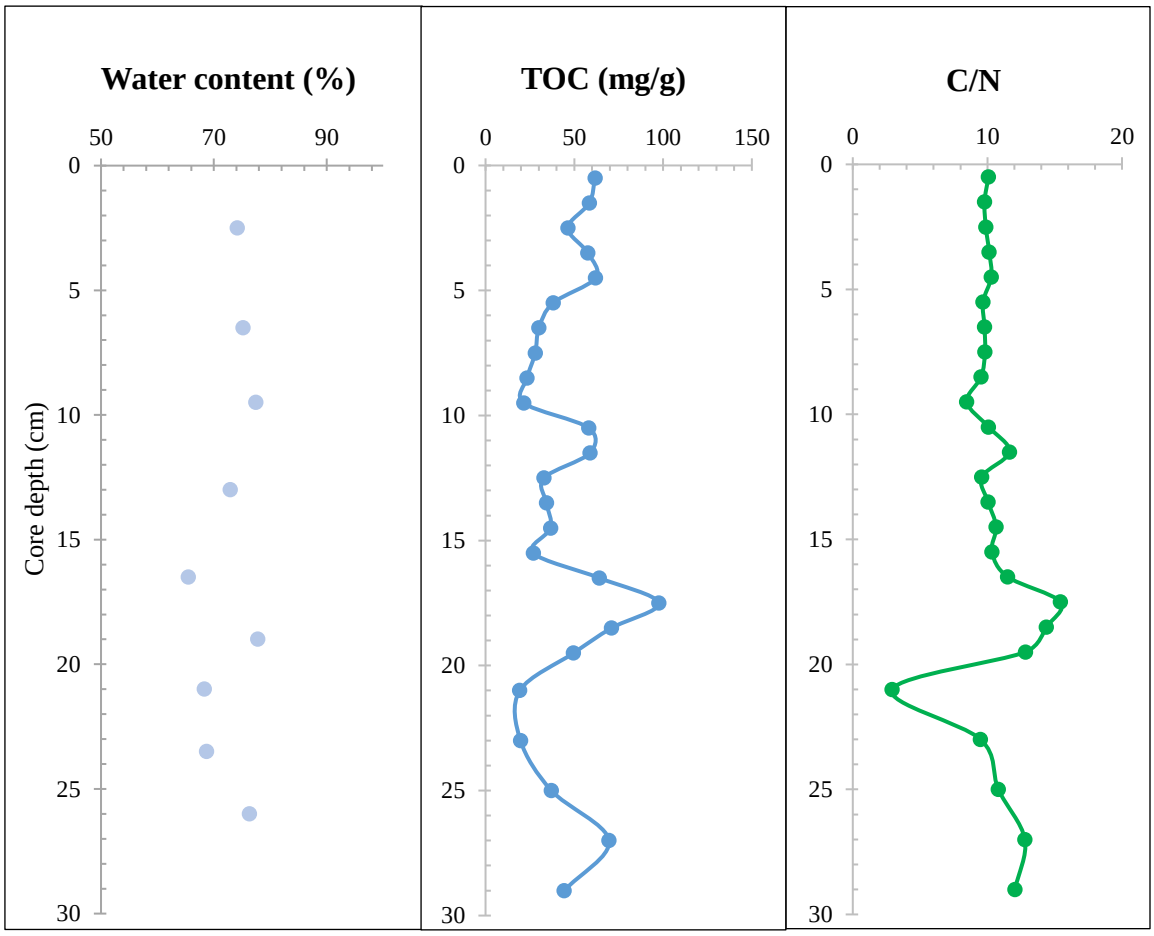

Figure 3.3b *– Left: water content in core BC-B. Middle: TOC (the values are retrieved from Bjørneby (2019). Right: C/N (the values are retrieved from Bjørneby (2019)).*

3.3.4 Grain size distribution

The full analysis of grain size distribution shows that all the core depths seem to have a very similar distribution of grains. There are two sample depths that differs from the rest, and these two are the samples from 17-18 cm and 20-22 cm. They seem to have a higher proportion of particles with a larger diameter (Figure 3.3c). Plot of the sand content shows that the amount of sand is more or less the same throughout the core, but the amount of sand is higher between the depth of 17 and 22 cm, and the amount is a little higher at 11.5 and 1.5 cm (Figure 3.3c).

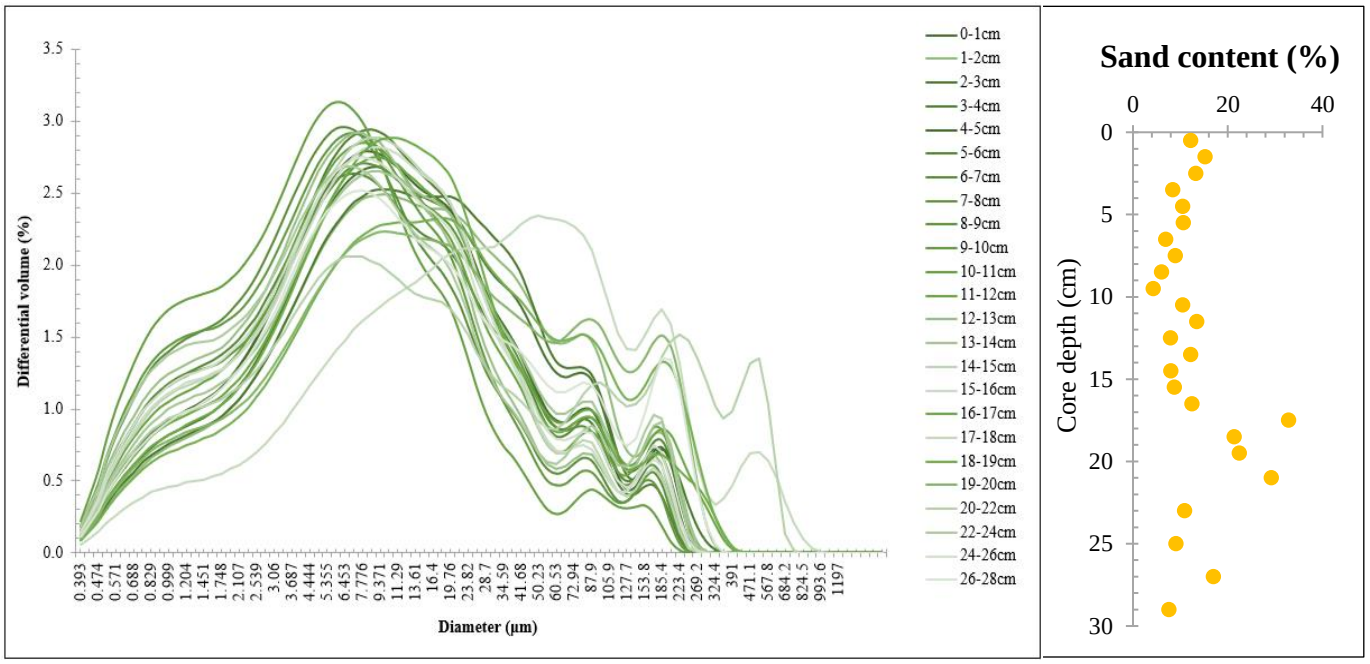

Figure 3.3c – *<u>Left</u>: distribution of grains with diameter from 0.393 to 1197 µm. <u>Right</u>: sand content (the values are retrieved from Bjørneby (2019)).*

3.3.5 Heavy metals

All the plots, except chromium and arsenic, seem to have the same pattern where they have a maximum concentration at 17.5 cm depth, and then it decreases and stabilizes towards the core surface. The plot of chromium shows a maximum concentration at 27 cm, and it seems to decrease towards the core surface. Arsenic has a maximum at 4.5 cm, and the overall pattern shows that the concentration is increasing from the bottom and towards the surface (Figure 3.3d).

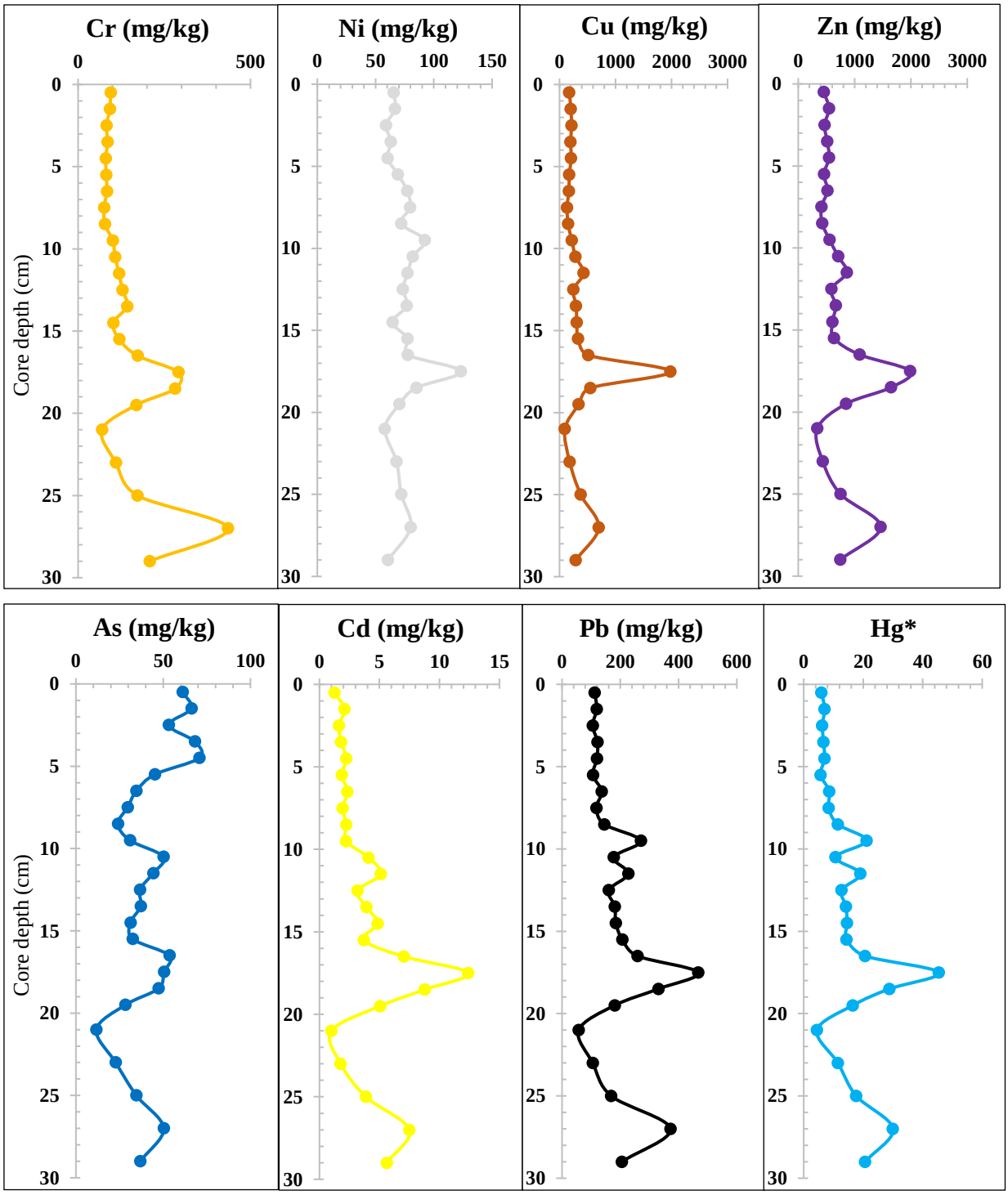

Figure 3.3d *– Profiles of the heavy metal content. The upper plots from left to right: chromium (Cr), nickel (Ni), copper (Cu) and zinc (Zn). The lower plots from left to right: arsenic (As), cadmium (Cd), lead (Pb) and mercury (Hg). The values are retrieved from Bjørneby (2019).*

3.3.6 Sediment preparation and separation/filtration

The sediment core samples from core BC-B were prepared and filtrated in the order from deep to shallow, from interval 25-27 cm to 0-5 cm. The dry, homogenized sediment from core depth 25-27 cm was grey. No organic particles were observed, and the low-density particles were filtrated over to two steel mesh filters (Figure 3.3e).

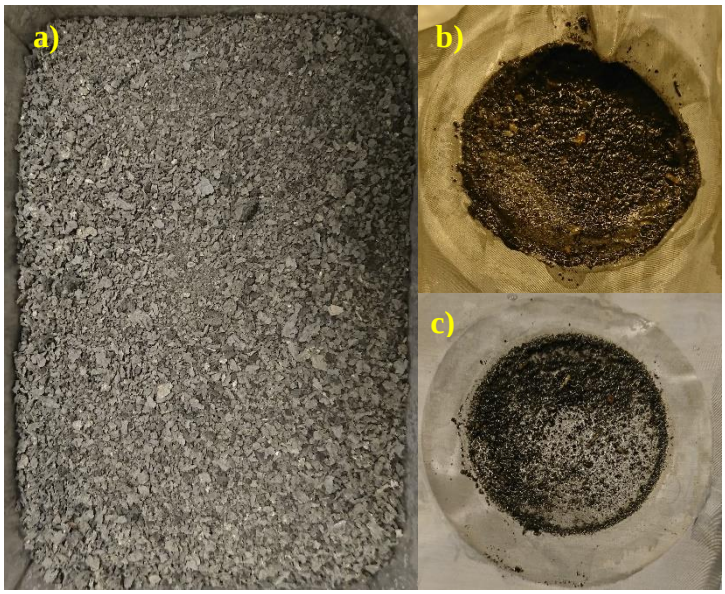

Figure 3.3e *– Introduction of sediment from core depth 25-27 cm from core BC-B to BMSS and separation/filtration. a) dry, homogenized sediment, b-c) low-density particles that have been separated from the sediment.*

The dry, homogenized sediment from core depth 20-22 cm was brown-grey, and no organic particles were observed in the sediment. Though, some organic particles were visible among the other light-density particles that were filtrated over to one steel mesh filter (Figure 3.3f).

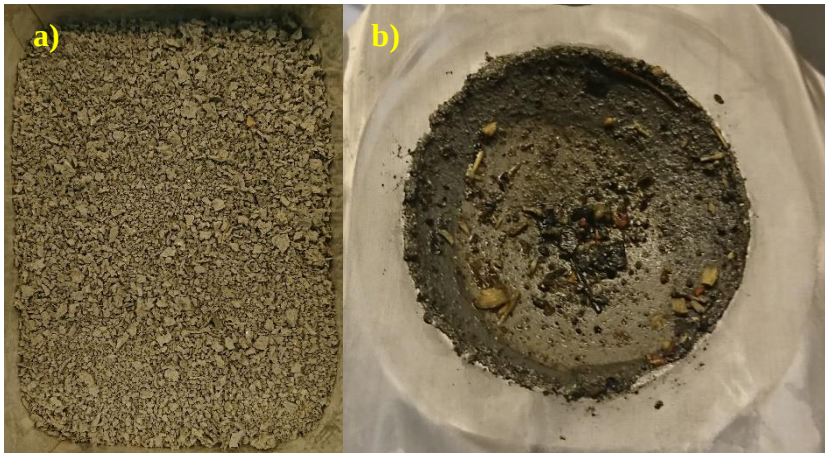

Figure 3.3f *– Introduction of sediment from core depth 20-22 cm from core BC-B to BMSS and separation/filtration. a) dry, homogenized sediment, b) low-density particles that have been separated from the sediment.*

The dry, homogenized sediment from core depth 0-5 cm was brown-grey. An organic particle that looked like wood was observed in the sediment (orange arrow). The sediment contained less low-density particles than the sediment from 25-27 and 20-22 cm (Figure 3.3g).

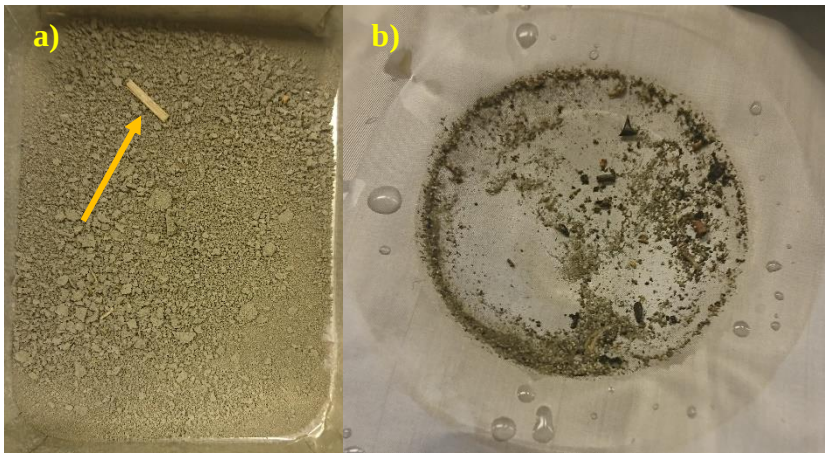

Figure 3.3g *– Introduction of sediment from core depth 0-5 cm from core BC-B to BMSS and separation/filtration. a) dry, homogenized sediment, b) low-density particles that have been separated from the sediment.*

3.3.7 Visual analysis

The results of the visual analysis are simplified, and the different categories are presented as distribution of shape, distribution of size and distribution of colour. The information on shape, size and colour of each particle can be seen in Appendix F, and a selection of particles identified as plastic is presented in Appendix G.

SHAPE (fibre, film, granulate) and SIZE (A, B, C and D)

The distribution of particles of different shape shows that the percentage of fibres seems to increase from the deepest part of the core to 6.5 cm core depth. The percentage of film seems to decrease from 26 to 9.5 cm core depth, and the percentage of granulates is varying throughout the core (Figure 3.3h). The distribution of particle size (A, B, C and D) shows that there are most particles from the size category B (100-300 µm). The second most abundant particle size is C, and then category A. There were only a few particles from category D (see Table 2.10 for the size categories). Particles from category A and C seem to have an increasing trend from the bottom to the upper part of the core. The particles from category B are varying throughout the core, and particles from category D were observed in the samples from core depths: 23.5, 16.5, 13, and 2.5 cm (Figure 3.3h).

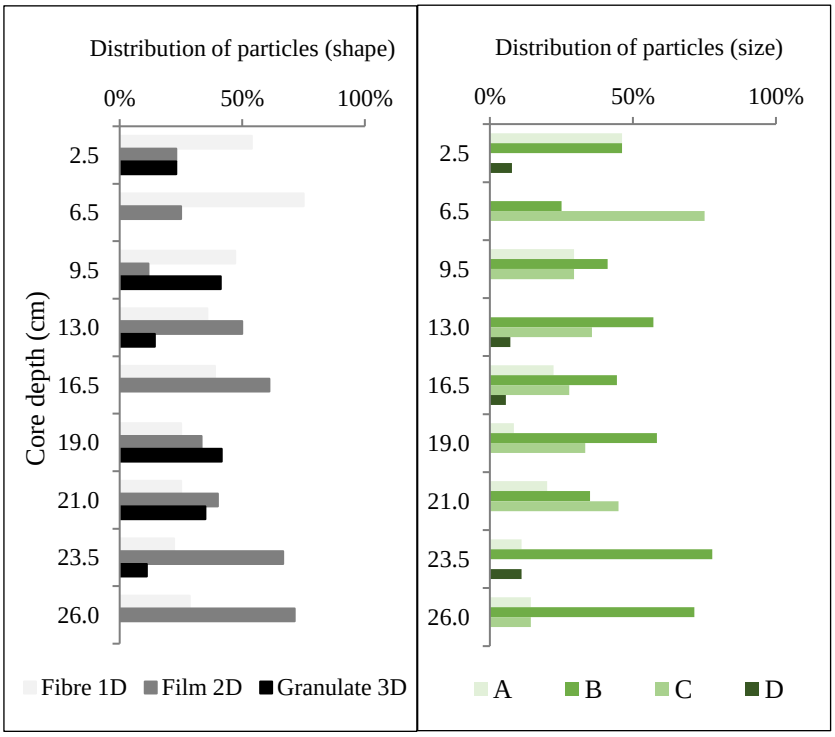

Figure 3.3h *– <u>Left</u>: distribution of particles of different shapes (fibre 1D, film 2D, granulate 3D) in core BC-B. <u>Right</u>: distribution of particles of different size (A: ≥45-100 µm, B: 100-300 µm, C: 300-1000 µm, D: 1-5 mm).*

COLOUR

The distribution of particles with different colours shows that the clear/white and black particles were observed throughout the core. The clear/white particles seem to decrease from the lower part of the core to the core surface, and the black particles seem increase from the bottom of the core to the core surface. The light and dark brown particles were only observed in some core depths. The light brown particles were observed in the core interval 13-23.5 cm, and the dark brown particles were observed in the core interval 21-26 cm. Blue particles were observed in the samples from almost every core depth, except 6.5 cm, and the percentage of blue particles is high in the bottom of the core, and it decrease to the middle of the core but it increases towards the core surface. Red particles were only observed in the samples from core depth 16.5 and 9.5 cm, and orange particles were only observed in the samples from core depth 21 and 2.5 cm. The percentage of green particles seem to increase from the bottom of the core towards the core surface, and yellow particles were only observed in the core interval 16.5-26 cm (Figure 3.3i).

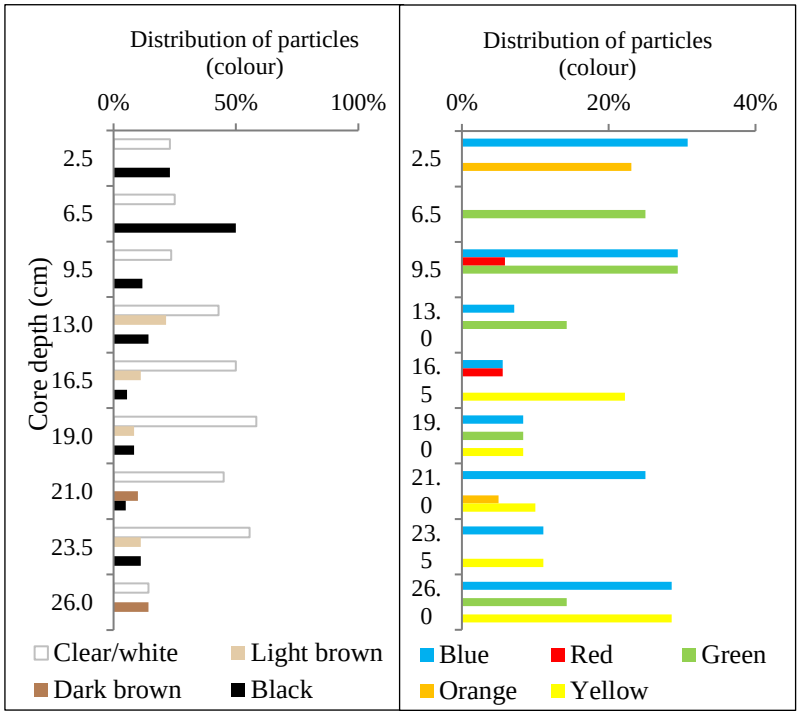

Figure 3.3i *– <u>Left</u>: distribution of particles with the colours clear/white, light brown, dark brown and black. <u>Right</u>: distribution of particles with the colours blue, red, green, orange and yellow.*

3.3.8 Microplastic, rubber, oxy-resin and petro-pyro

The plots of concentration (number of particles/ kg dry sediment) of oxy-resin, petro-pyro, plastic and rubber particles show different trends. The plot of the concentration of oxy-resin has a peak at 19 cm core depth, the plot of petro-pyro has a peak at the lowest part of the core, at 26 cm and the concentration decrease towards the core surface. The concentration of plastic seems to have a similar trend as petro-pyro but it seems to increase in the core surface. The concentration of rubber seems to vary, and it has a peak at 24 cm core depth. It has another peak at 17 cm core depth, and no rubber particles were found from 27 to 25 cm, and from 11 to 0 cm core depth (Figure 3.3j). The concentrations are listed in Appendix H.

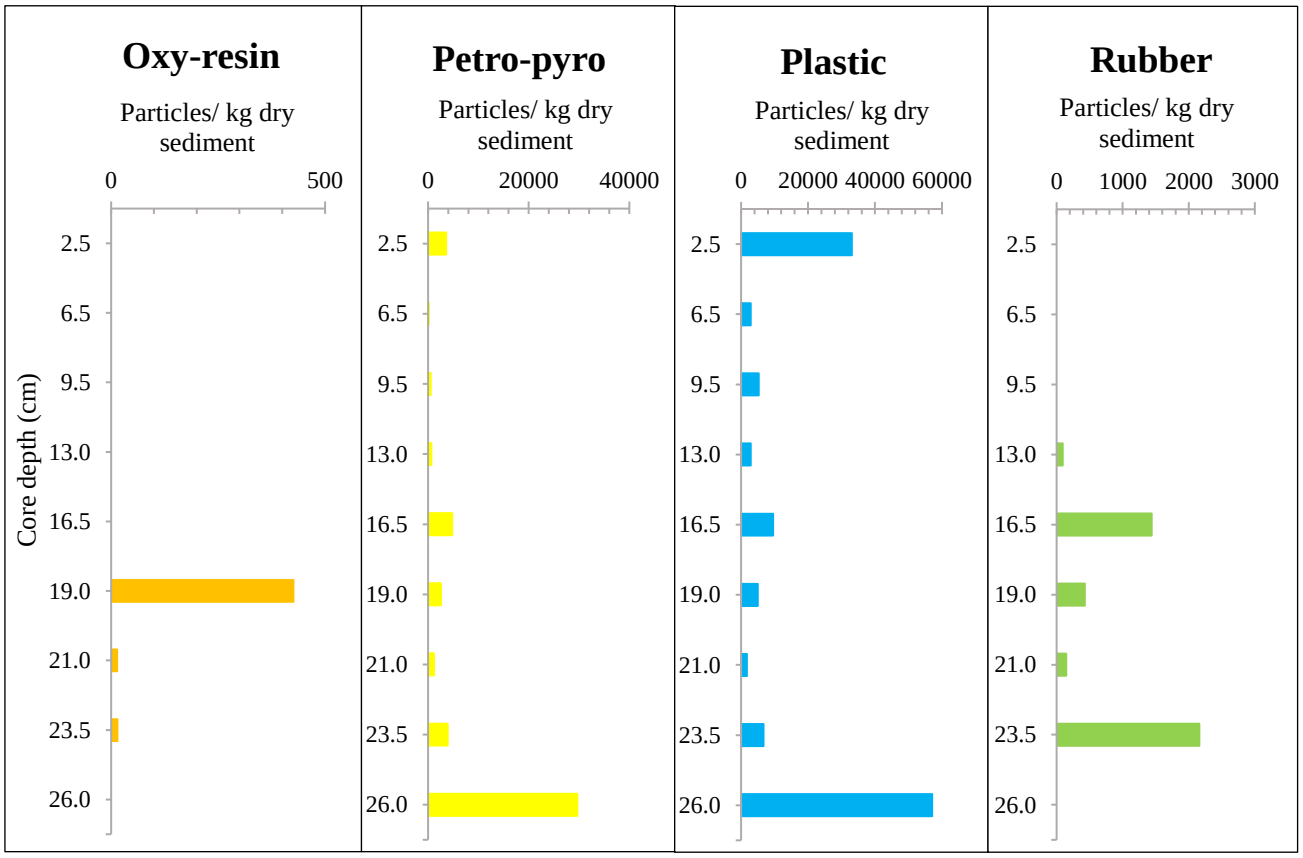

Figure 3.3j *– Plots of the concentration of oxy-resin, petro-pyro, plastic and rubber in core BC-B. The concentration is given as number of particles per kg dry sediment.*

The concentration given as weight of particles in mg per kg dry sediment seems to have the same trend as the concentration given as number of particles for all four types of particles. Though, the peak at 19 cm in the oxy-resin plot has decreased, and the same goes for the peak at 17 cm core depth in the rubber plot (Figure 3.3k).

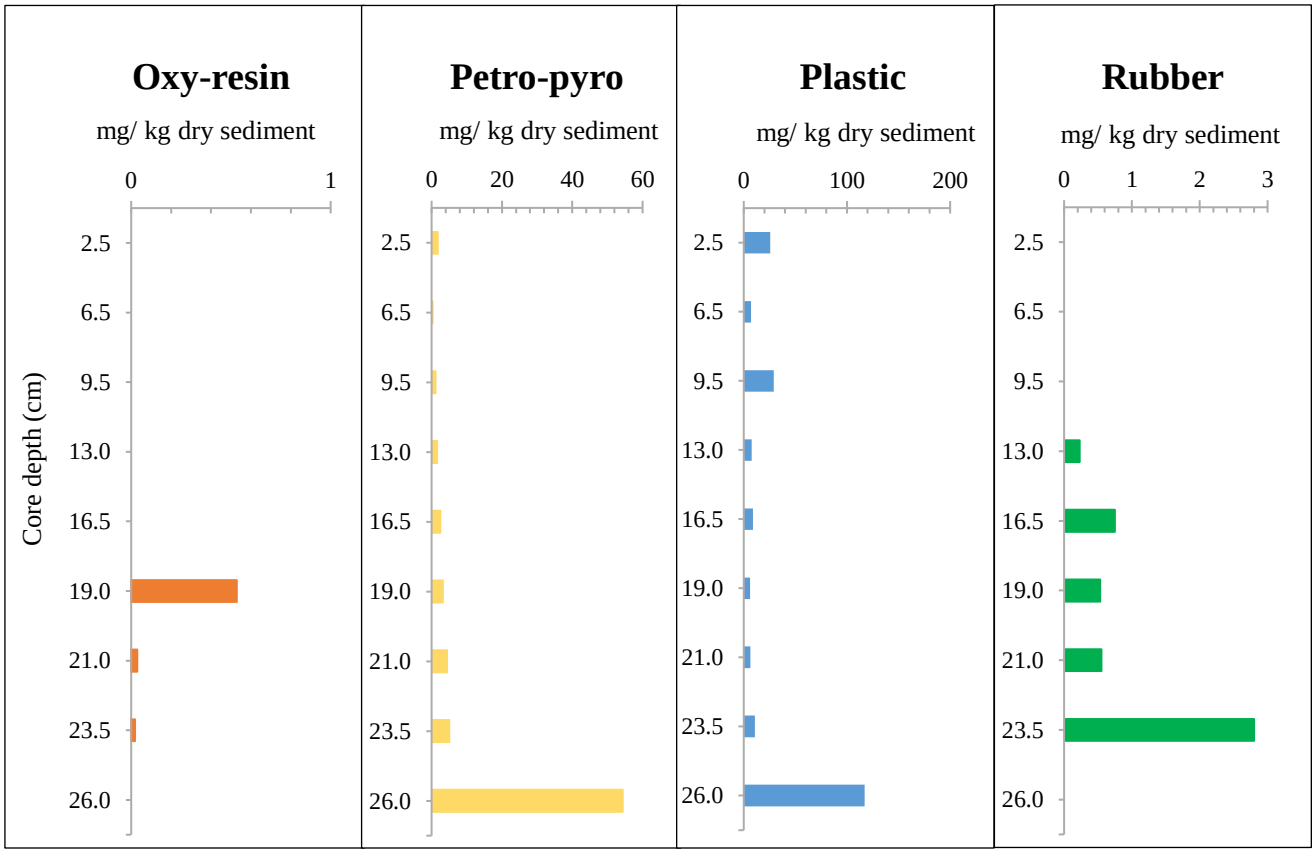

Figure 3.3k *– Plots of the concentration of oxy-resin, petro-pyro, plastic and rubber in core BC-B. The concentration is given as the weight of particles in mg per kg dry sediment.*

3.3.9 Plastic types

The percentages of the polyolefins (PE, PP, PE-oxidized and PE:PP) were merged and presented in a plot. The plot of polyolefins shows an increasing trend from the bottom to 9.5 cm, and then it seems to decrease in the upper 0-9.5 cm. The chlorinated plastic types (PVC, PE-chlorinated and PP-chlorinated) were merged. The plot shows varying percentages, but the overall trend seems to be increasing throughout the core. The percentage of the plastic types PS, PET, PU, PVF and nylon were merged and are presented in the same plot. This plot is also varying, and the overall trend seems to be increasing towards the core surface (Figure 3.3l).

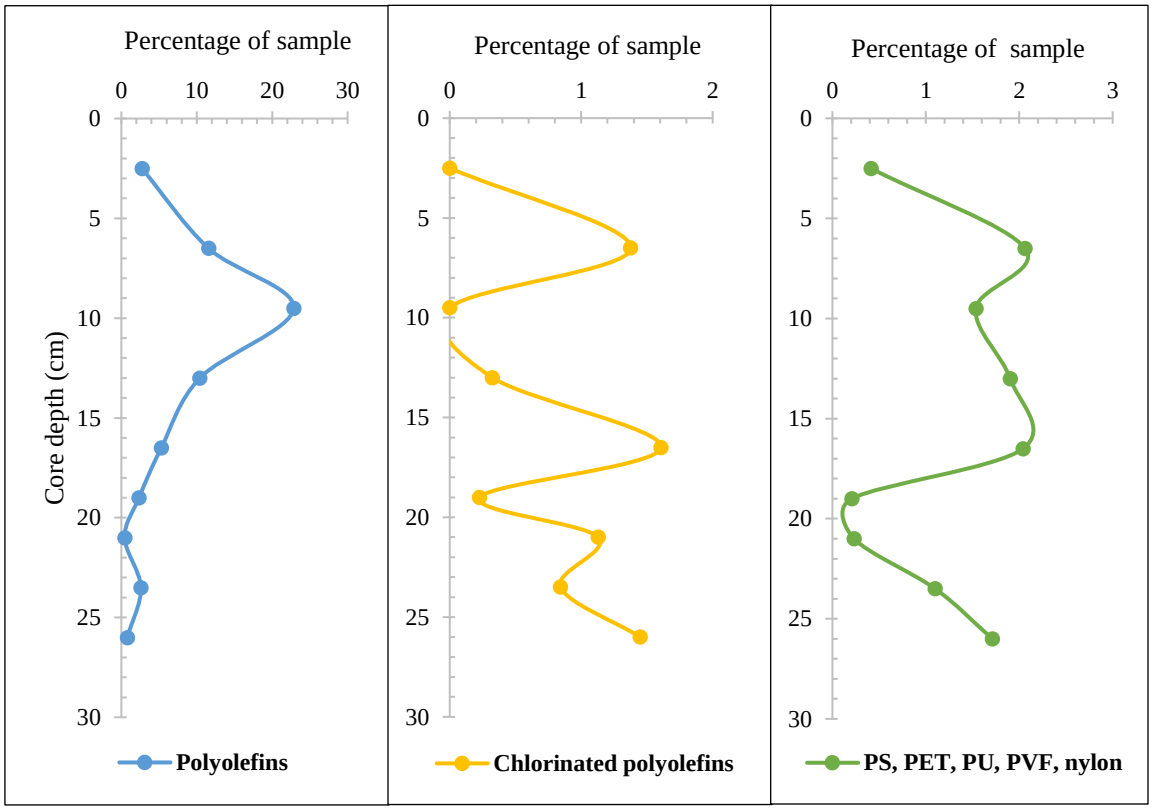

Figure 3.3l *– <u>Left</u>: plot of the percentage of polyolefins in core BC-B. <u>Middle:</u> the percentage of chlorinated polyolefins. Right: the percentage of PS, PET, PU, PVF and nylon (See Table 2.11b for the plastic abbreviations).*

The percentage of PMMA, EVA and melamine seems to be stable from the deepest part of the core to 9.5 cm core depth, and it is increasing in the upper 0-10 cm of the core. There were also particles categorized “unresolved plastic” in the samples from core BC-B, and the plot of unresolved plastic seems to decrease in the lower part of the core, and it increases from 13 cm core depth (Figure 3.3m).

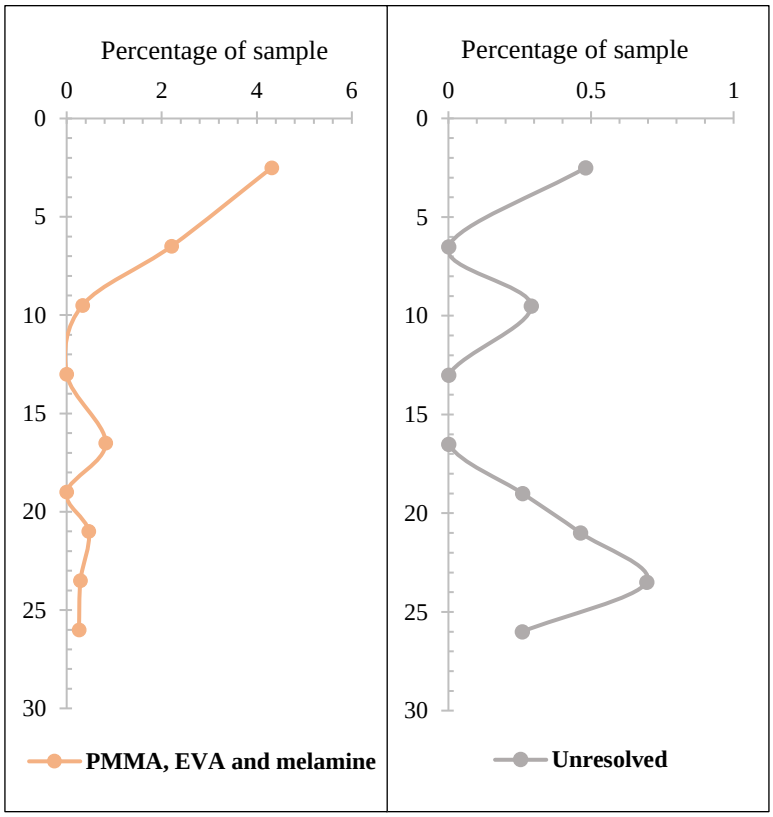

Figure 3.3m *– <u>Left</u>: plot of the percentage of PMMA, EVA and melamine in core BC-B. <u>Right</u>: the percentage of unresolved plastic (See Table 2.11b for the plastic abbreviations).*

3.3.10 Macroplastic

The results from the macroplastic analysis (Appendix I) are summarized in Table 3.3. Plastic particles were found in all core depth interval, from 25 to 0 cm. PE and PP were the most frequent plastic types. PP occurred in every core interval except 25-27 cm, and PE occurred in every core interval except 20-22 cm, 11-15 cm, 5-8 cm and 0-5 cm. The particles identified as plastic were 0.63 to 10.17 mm, they were mostly fibres and they had different colours, such as clear, white, black, grey, brown, light brown, red, blue, green and orange (Table 3.3).

Table 3.3 *– Plastic types of particles that could be picked out by tweezer, in core BC-B (See Table 2.11b for the plastic abbreviation).*

Sample ID	Plastic type	Colour	Shape	Length (mm)
BC-B 0-5	PP	White	Fibre	9.00
	PMMA	White	Granule	0.97
BC-B 5-8	PP	Black, blue, green/white	Fibre, granule	0.63-7.50
	Nylon	Light brown	Film	0.91
BC-B 8-11	PE	Black, green/white, white/light brown	Film	0.98-5.77
	PP	White	Fibre	2.66
BC-B 11-15	PP	Clear/white	Fibre	9.78
	PS	Orange	Film	1.53
BC-B 15-18	PE	White, green	Fibre, film, granule	1.02-2.39
	PP	Green	Fibre	1.26
	PS	White	Film	1.56
BC-B 18-20	PE	Red	Fibre	9.20
	PP	Green/white	Fibre	0.91
	Nylon	Brown	Fibre	2.60
BC-B 20-22	PP	Blue/white, blue	Fibre	0.93-1.32
BC-B 22-25	PE-chlorinated	White	Fibre	4.25
	PP	White	Fibre	10.17

	PS	White, white/light brown	Film	1.50-1.68
	Nylon	Brown	Fibre	2.26
	Other	White	Film	0.94
BC-B 25-27	PE	White, white/light brown	Fibre, film	1.90-2.19
	PE-chlorinated	White, black/grey	Film	1.48-1.63

3.4 SURFACE SAMPLES

3.4.1 Sample description

The uppermost 0-2 cm of the sea floor was collected for each of the surface samples. The only thing that differed was the water depth, and the sediment from each of the sample stations looked the same and had the same colour. They all had a brown colour, but a few things differed from one sample depth to another sample depth. Large objects or materials were observed in the grab at some depths. At 15 m, a shoe sole was stuck in the grab, and two large pieces of plastic were stuck in the grab with sediment from a 25 m depth. At 35 m depth, two large pieces of an unknown material was observed in the sediment inside the grab (Figure 3.4a). It looked like it could be material that are used on roofs, perhaps tar paper. There were a lot of polychaetes and some other living organisms in all the surface samples.

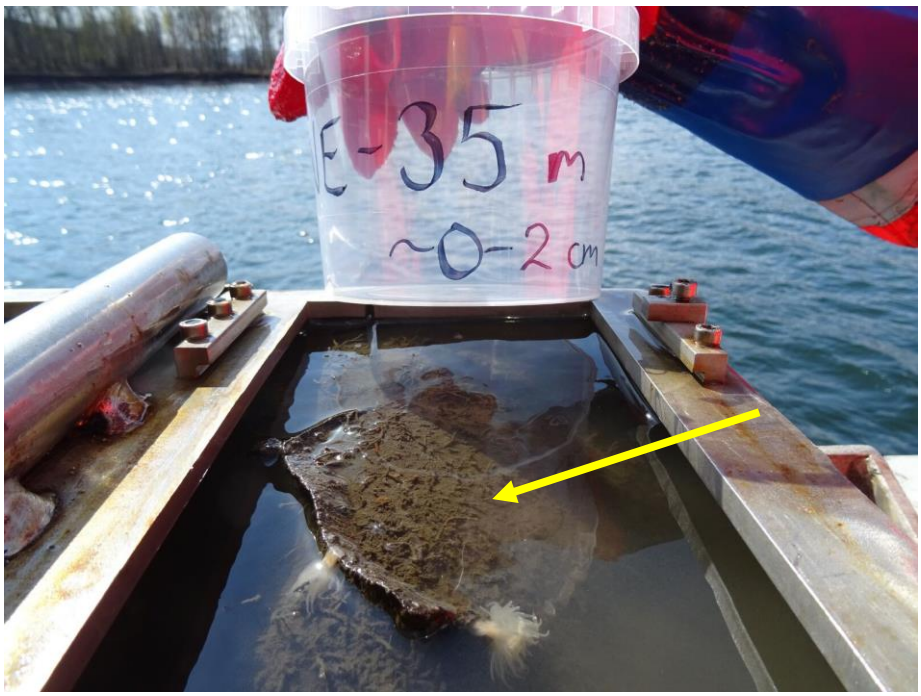

Figure 3.4a *– Van Veen grab full of sediment from 35 m water depth. There is a lot of polychaetes in the sediment, and two sea anemones were also observed. The strange material that resembles tar paper (yellow arrow) is also visible in the picture.*

3.4.2 Water content

Water depth 55 m is represented by the upper part of core BC-A. The upper plot in Figure 3.4b shows that the sediment from 15 m water depth has a high content of water, and then it decreases and seems to stabilize at a value of 71-72 % water. There is a peak at 55 m where the water content is 80 %, and this value differs from the rest of the samples. The water content at 65 m is similar to the ones from 25 m, 35 m and 45 m. Core BC-B is also from a depth of 65 m and it seems to have a water content that is similar to the grab sample from the same depth (Figure 3.4b), though the location of core BC-B is further away from Langøyene and the other grab samples.

3.4.3 Total organic carbon

The TOC seems to start with a high value at 15 m water depth and then it decreases as the water gets deeper. The value from 65 m is missing, but TOC from the upper part of the core from station BC-B (65) has a value that is similar to the grab sample from 45 m (Figure 3.4b).

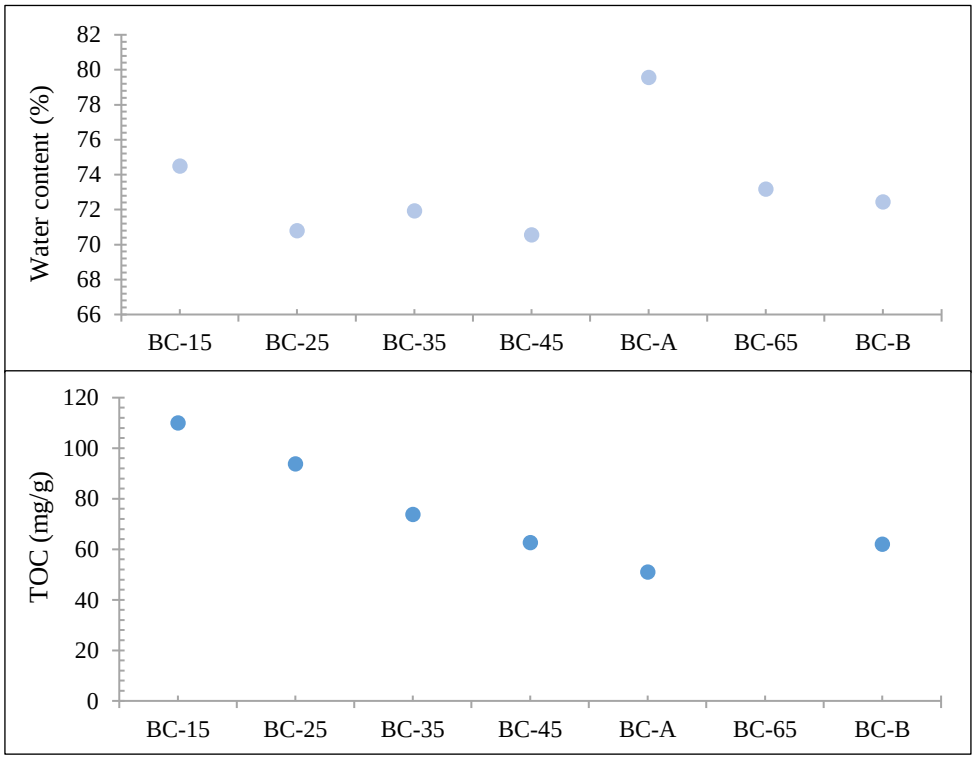

Figure 3.4b *– Upper plot: water content in the surface samples, including the upper part of the cores from station BC-A and BC-B. Lower plot: TOC in the surface samples (the values are retrieved from Bjørneby (2019)).*

3.4.4 Grain size distribution

The grain size distribution shows that the samples have a similar distribution. The sample from 15 m is a little different from the others and seems to have a higher amount of coarse material. The sample from 25 m and the core from station BC-B (65 m) have a very similar distribution, and the sample 45 m and the core from station BC-A (55 m) have a very similar distribution. The grain size distribution from 65 m depth from the transect is missing in the analysis (Figure 3.4c). The sand content confirms that 15 m has a higher amount of coarse material, and it decreases from 15 m to 35 m. After this depth, it slightly increases (Figure 3.4c).

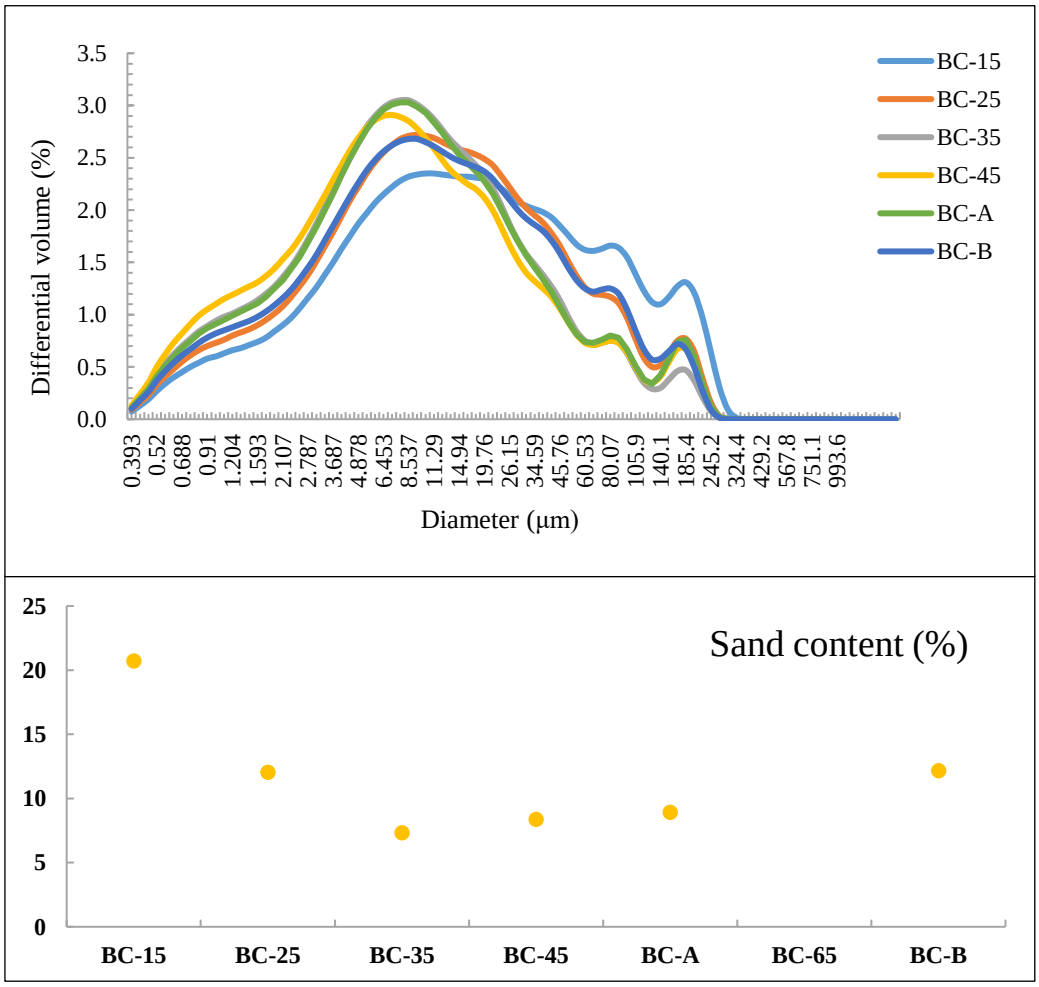

Figure 3.4c – *<u>Upper plot</u>: grain size distribution of the surface samples, including the upper part of the cores from station BC-A and BC-B. <u>Lower plot</u>: sand content in the surface samples (the values are retrieved from Bjørneby (2019)).*

3.4.5 Heavy metals

The bars representing copper, zinc and lead seems to decrease with the water depth, from 15 m to 65 m. Chromium, nickel and arsenic seem to be stable at every depth, and cadmium is not even visible in the plot. This does not mean that there was no cadmium in the sediment samples, but the values of this heavy metal are very low compared to the other metals. The distribution of the different heavy metals is similar in the upper part of the cores from station BC-A and BC-B (Figure 3.4d). Due to limitations in the method of analysis of mercury, the values of mercury are semi-quantitative. Therefore, it is not presented in the same figure as the other heavy metals, and without a y-axis label. The values of mercury are varying, and the sediment from shallower depths seem to have a higher content of mercury than the deeper sediment samples (Figure 3.4d).

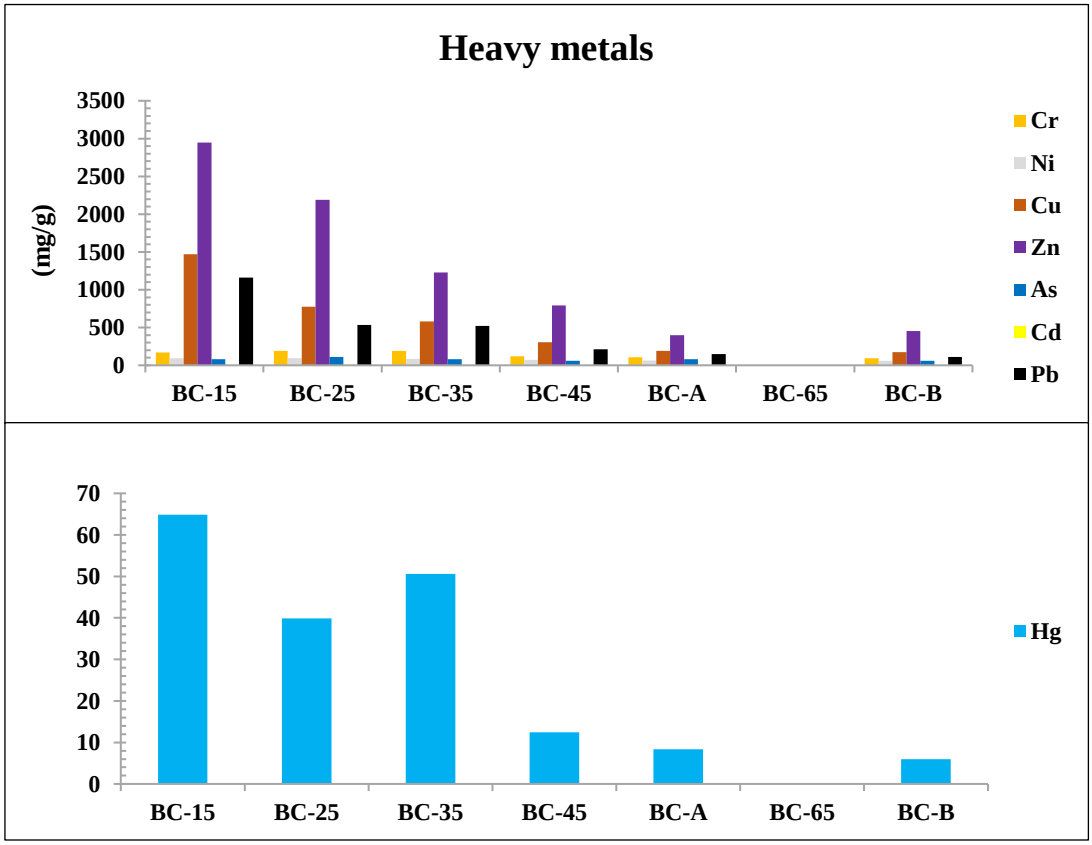

Figure 3.4d – *Upper plot: the content of the heavy metals chromium (Cr), nickel (Ni), copper (Cu), zinc (Zn), arsenic (As), cadmium (Cd) and lead (Pb), in the surface samples including the upper part of the cores from station BC-A and BC-B. Lower plot: the content of mercury (Hg). The values are retrieved from Bjørneby (2019).*

3.4.6 Sediment preparation and separation/filtration

The sediment samples collected with Van Veen Grab from different water depths were prepared and filtrated in the order from shallow to deep, from 15 m to 65 m. The dry, homogenized sediment from 15 m water depth was grey. There were some white particles that looked like waste (orange arrow), and there were some organic particles in the sediment (Figure 3.4e).

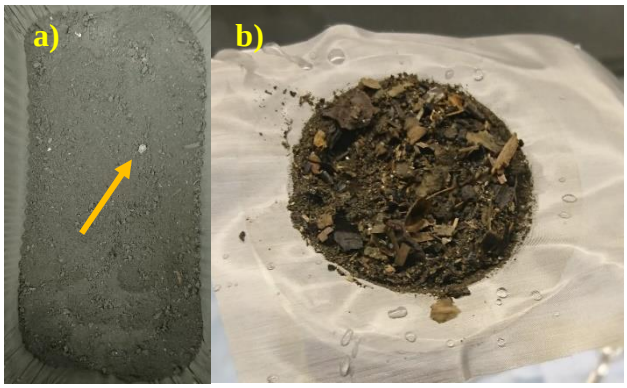

Figure 3.4e *– Introduction of sediment from water depth 15 m to BMSS and separation/filtration. a) dry, homogenized sediment, b) low-density particles that have been separated from the sediment.*

The dry, homogenized sediment from 45 m water depth was grey, and a large piece of an unknown material was observed in the sediment (orange arrow). A lot of small, white particles were observed in the separated low-density material (Figure 3.4f).

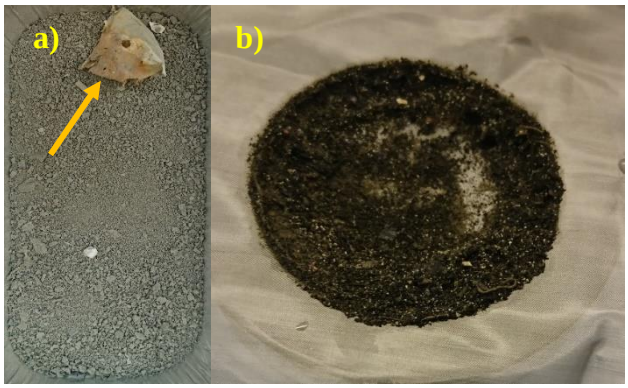

Figure 3.4f *– Introduction of sediment from water depth 45 m to BMSS and separation/filtration. a) dry, homogenized sediment, b) low-density particles that have been separated from the sediment.*

3.4.7 Visual analysis

The results of the visual analysis are simplified, and the different categories are presented as distribution of shape, distribution of size and distribution of colour. The information on shape, size and colour of each particle can be seen in Appendix F, and a selection of particles identified as plastic is presented in Appendix G.

SHAPE (fibre, film, granulate)

No fibres were observed in the surface sample from 15 m water depth, and the distribution of fibres seems to vary in the other surface samples. The percentage of fibres seems to decrease from 35 to 45 m, and it seems to increase from 45 to 65 m. The percentage of fibres in the surface sample from 65 m water depth is lower than the sample collected from station BC-B, further away from Langøyene. No particles with the shape of film were observed in the sample from 35 m water depth, and the percentage of film seems to increase with depth, from 15 to 55 m. It decreases from 55 to 65 m, and the percentage of film in the sample from 65 m is lower than the sample from the same water depth from station BC-B. There were no granulates that stood out in the sample from 25 m water depth and the sample from station BC-B. The percentage of granulates seems to decrease with depth, from 15 to 55 m, and it increase from 55 to 65 m (Figure 3.4g).

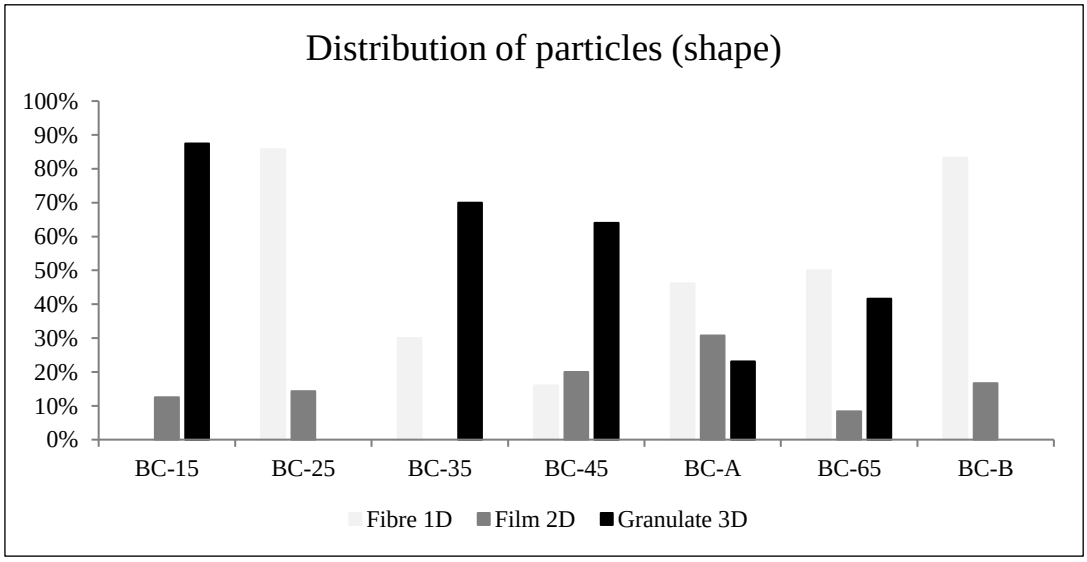

Figure 3.4g *– Distribution of particles of different shapes (fibre 1D, film 2D, granulate 3D) in the surface samples, including the upper part of core BC-A.*

SIZE (A, B, C, and D)

The distribution of particle size (A, B, C and D) shows that there are most particles from the size category B (100-300 µm). There are second most particles from size category C, then A and there are few particles from category D (see Table 2.10 for the size categories). Particles from category B seems to decrease with water depth, the particles from category A and C are varying with depth, and the particles from category D seems to decrease from 35 to 55 m, and the percentage of particles of category D is lower in the sample from 65 m in the transect than in the sample from station BC-B (Figure 3.4h).

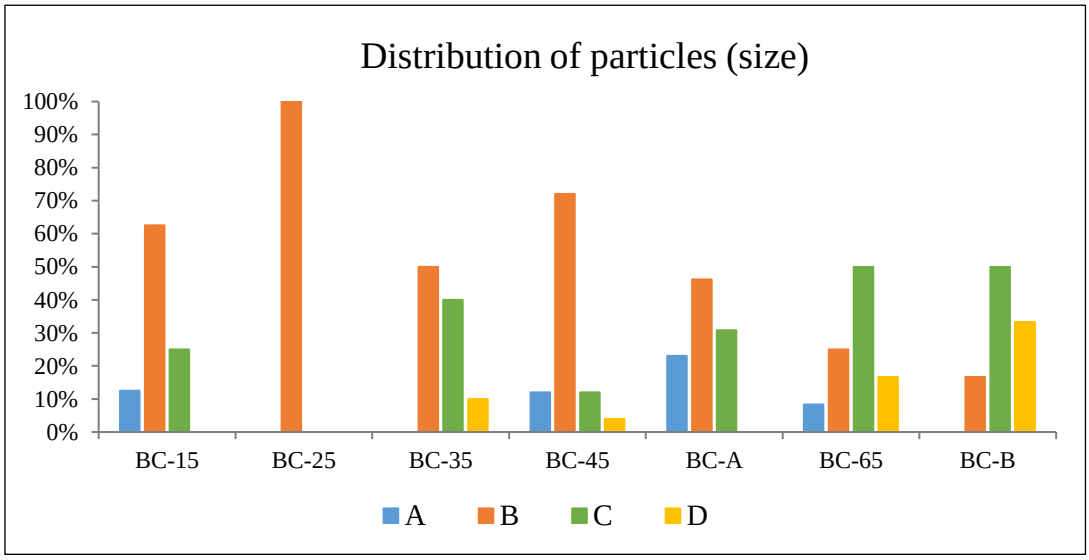

Figure 3.4h *– Distribution of particles of different sizes (A: ≥45-100 µm, B: 100-300 µm, C: 300-1000 µm, D: 1-5 mm) in the surface samples, including the upper part of core BC-A.*

COLOUR

The distribution of particles with different colours shows that particles that stood out in the surface samples were mostly clear/white. The percentage of clear/white particles seems to increase with depth, with 25 m as an exception as there is a peak in the sample from this depth. Light brown and black particles were observed in the samples from all water depths except 25 and 65 m (station BC-B). The percentage of light brown particles seems to increase from 15 to 55 m, and it decreases from 55 to 65 m. The percentage of black particles seems to decrease with depth, from 15 to 55 m, and it increases from 55 to 65 m. Dark brown particles were observed in only two surface samples: from depth 45 and 65 m, and the percentage of brown particles seems to increase with depth (Figure 3.4i).

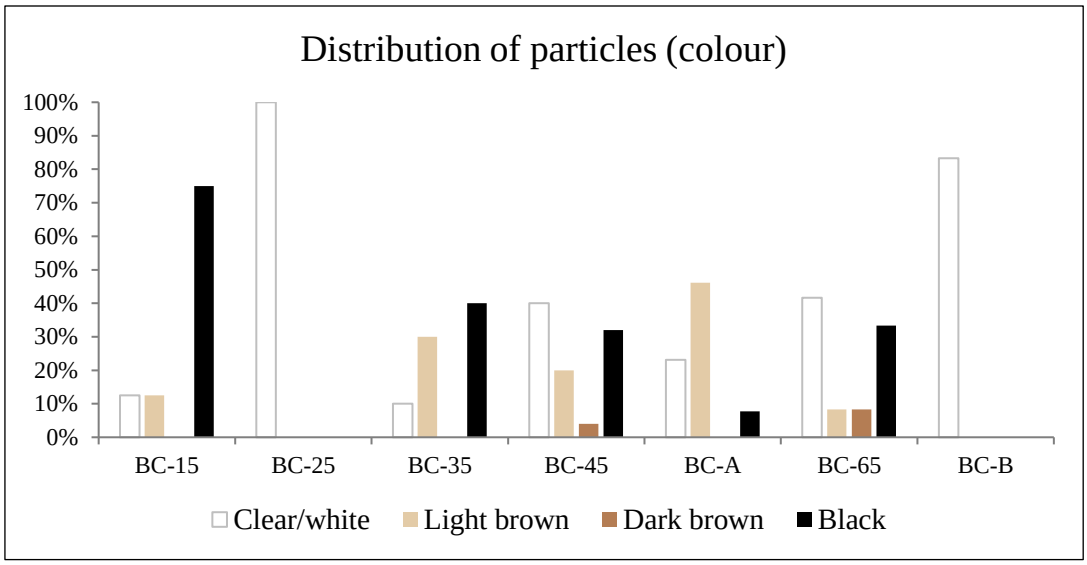

Figure 3.4i *– Distribution of particles with the colours clear/white, light brown, dark brown and black in the surface samples, including the upper part of core BC-A.*

Blue particles were only observed in the sample from water depth 35 to 55 m, and from 65 m (station BC-B). The percentage of blue particles is varying with higher percentage in the sample from 35 and 65 m, than 45 and 55 m. Red particles were only observed in the sample from 55 m, from the upper part of core BC-A, and yellow particles were only observed in the sample from 65 m water depth. No green or orange particles were observed (Figure 3.4j).

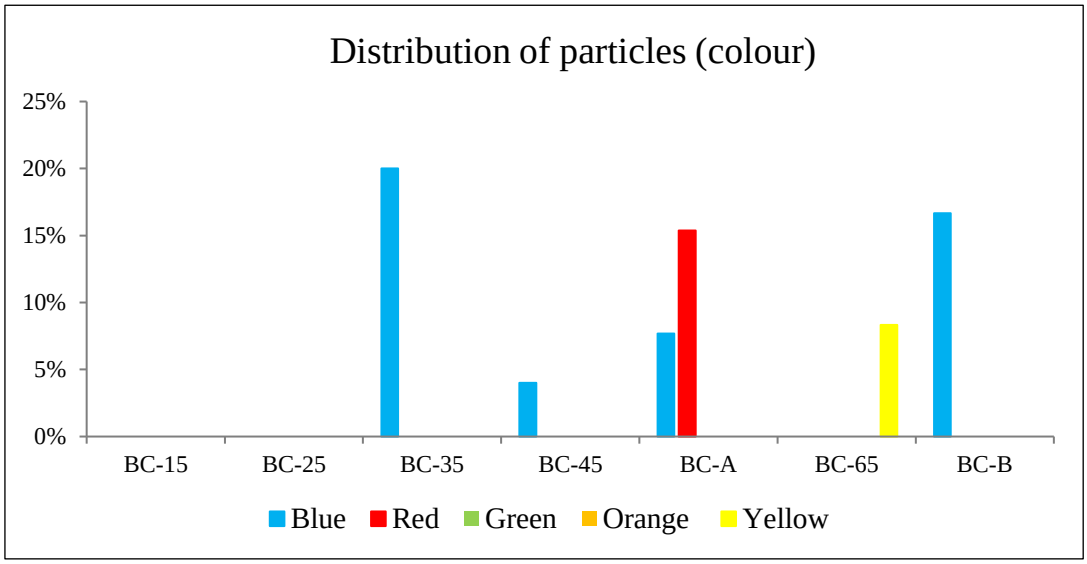

Figure 3.4j *–Distribution of particles with the colours blue, red, green, orange and yellow in the surface samples, including the upper part of core BC-A.*

3.4.8 Microplastic, rubber, oxy-resin and petro-pyro

No oxy-resin particles were found in the sediment surface samples. The only oxy-resin particles in the plot are from the uppermost core dept from BC-A that represents water depth 55 m in the transect (Figure 3.4k). The concentrations are listed in Appendix H.

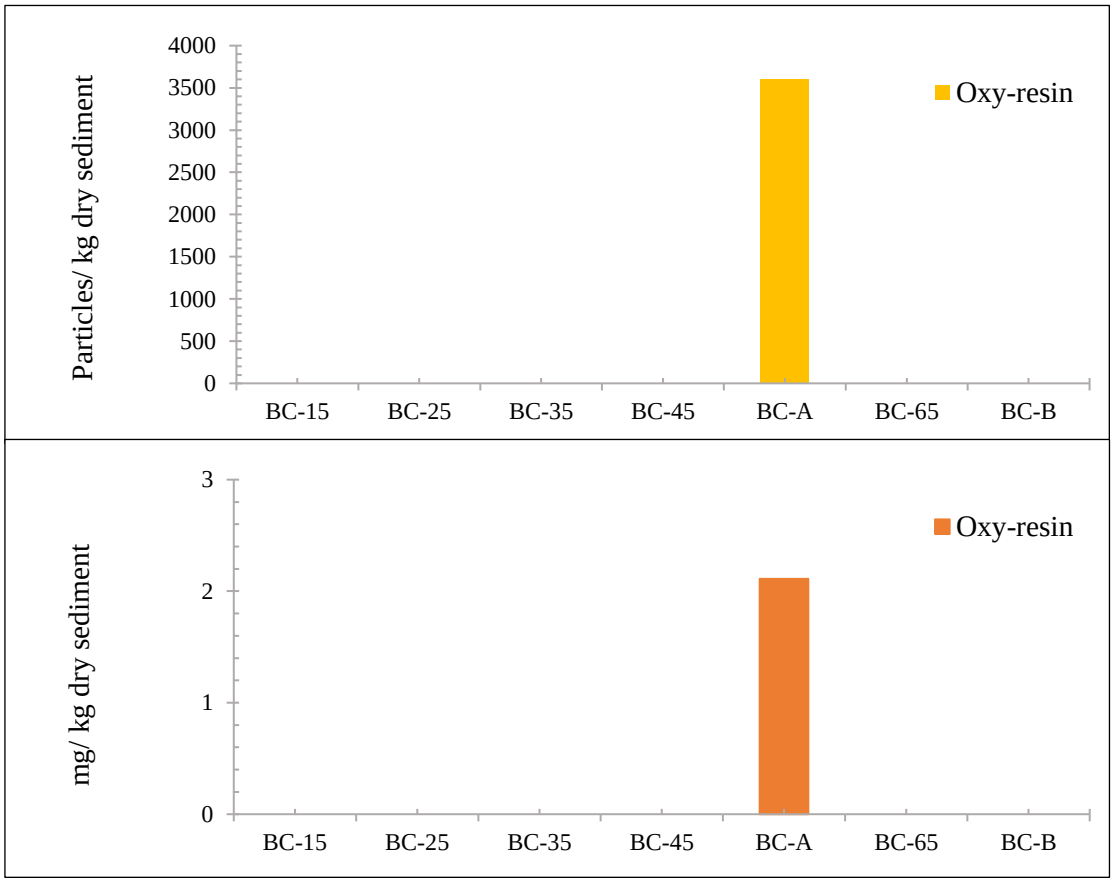

Figure 3.4k *– Upper plot: concentration of oxy-resin given as number of particles per kg dry sediment introduced to the BMSS. Lower plot: the concentration as weight in mg per kg dry sediment.*

The plots of petro-pyro concentrations show a peak at BC-35, the sample from 35 m water depth. The concentrations are low in the samples from deeper water depths. The concentration given as number of particles is bigger in BC-15 than BC-25, but it is opposite when looking at the concentration given as weight in mg (Figure 3.4l).

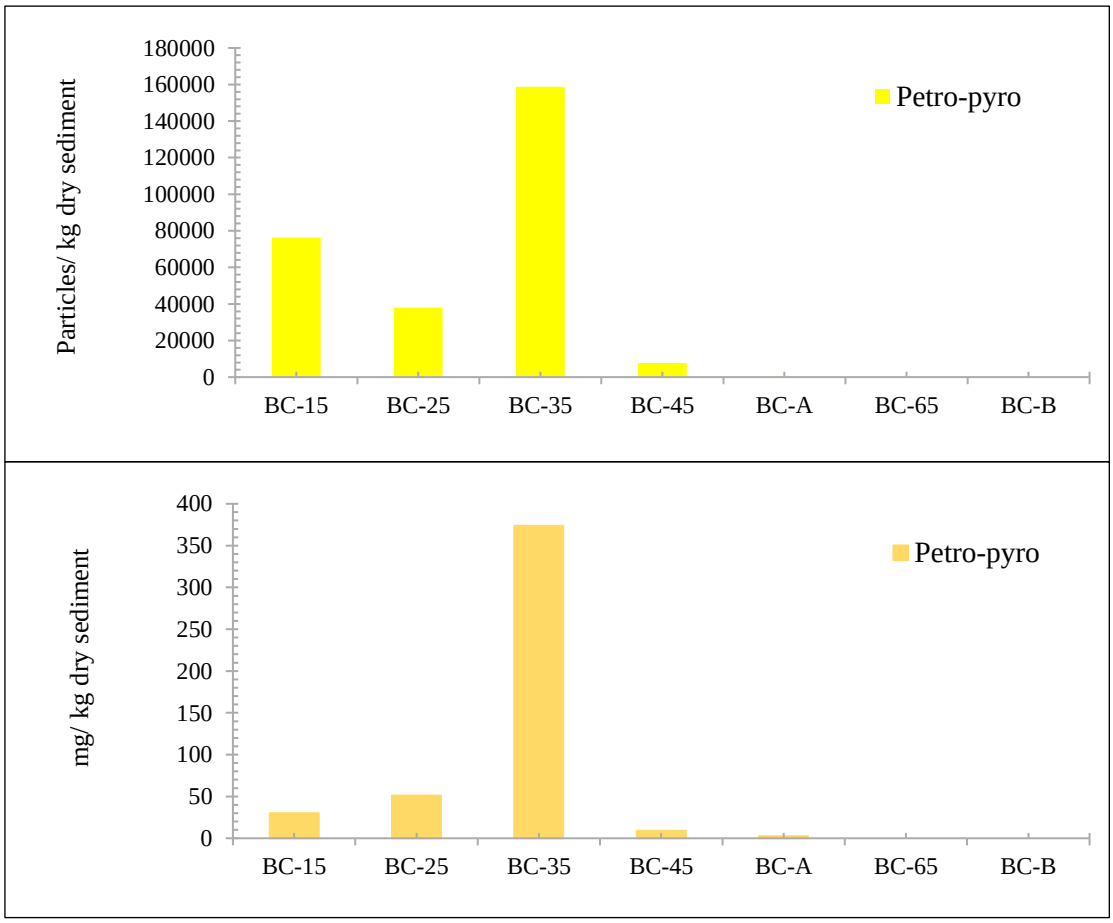

Figure 3.4l – *Upper plot: concentration of petro-pyro given as number of particles per kg dry sediment introduced to the BMSS. Lower plot: concentration as weight in mg per kg dry sediment.*

The concentration of plastic as number of particles seems to decrease with water depth. The sample from 15 m water depth seemed to have a bigger number of particles than the deeper samples. The concentration given as weight in mg shows another trend. The sample from 15 m had the highest number of particles, but the sample from 35 m has the highest weight, and the sample from 65 m depth has the second highest weight (Figure 3.4m).

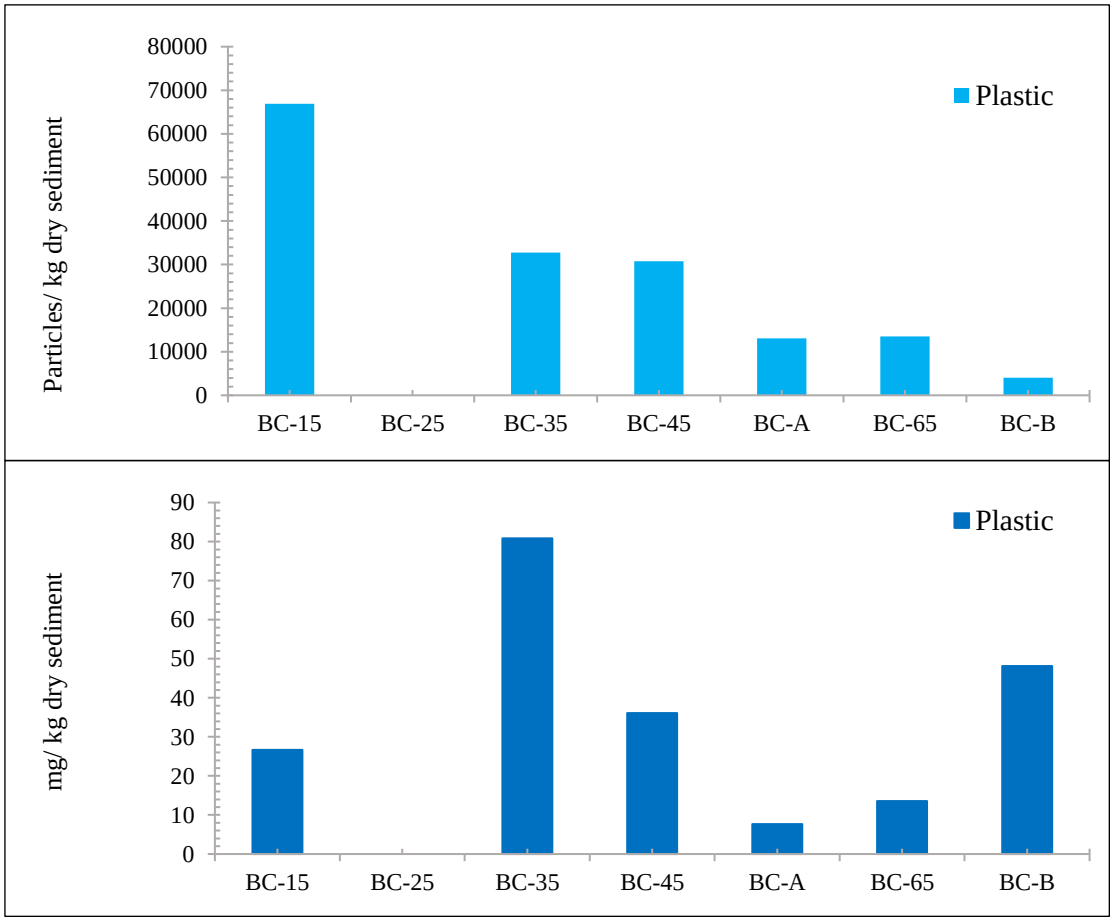

Figure 3.4m – *Upper plot: concentration of plastic given as number of particles per kg dry sediment introduced to the BMSS. Lower plot: concentration as weight in mg per kg dry sediment.*

The concentrations of rubber given as number of particles and weight seem to have same trend. The sample from 15 water depth seems to have the highest concentration, and it decrease with depth. No rubber was found in the sample from 65 m depth in the transect, but rubber was found in the sample from the sample from the same depth but further away from Langøyene (Figure 3.4n).

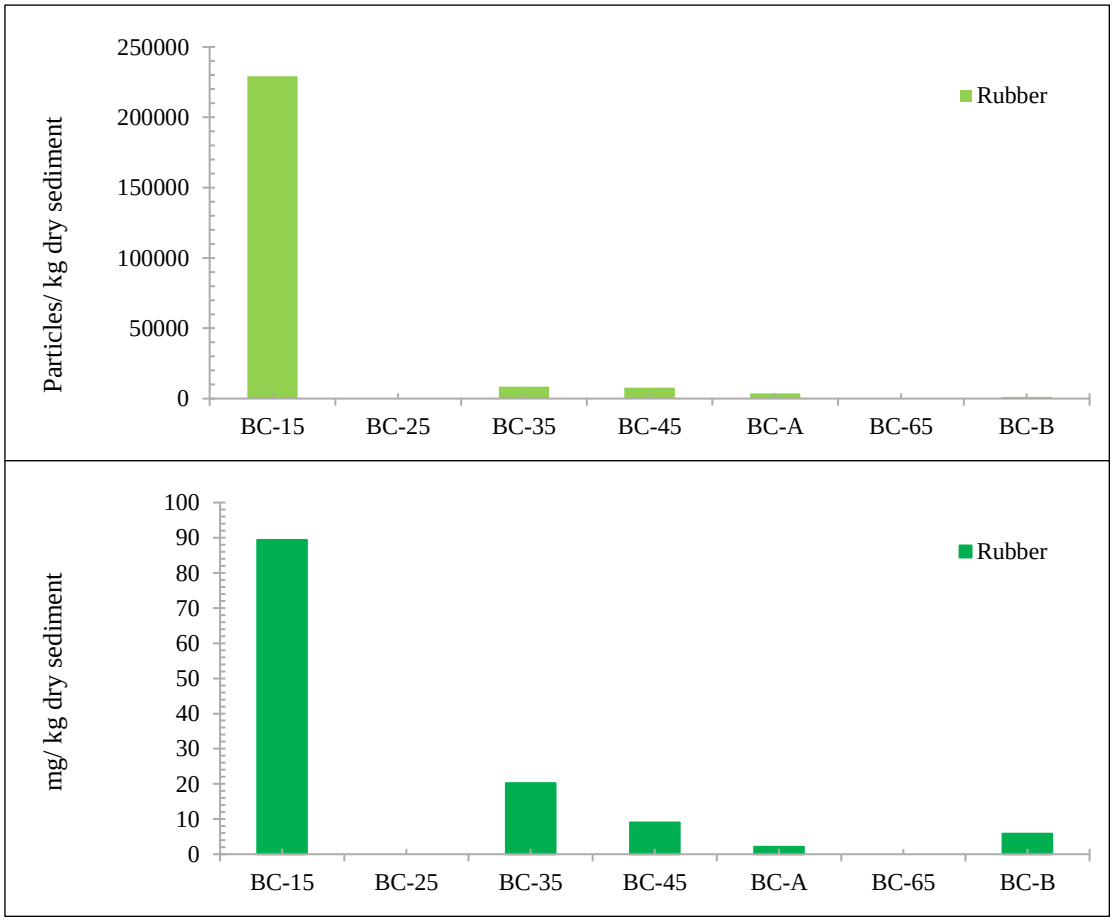

Figure 3.4n – *Upper plot: concentration of rubber given as number of particles per kg dry sediment introduced to the BMSS. Lower plot: concentration as weight in mg per kg dry sediment.*

3.4.9 Plastic types

The plot of polyolefins shows an increasing percentage to increase with water depth. There is a drop in the sediment from station BC-A from 55 m water depth, but it increases and reaches a maximum at 65 m water depth. The plot of chlorinated polyolefins shows an increasing trend, and the percentage is higher in the sediment from 65 m water depth from station BC-B that is close to Bekkelaget sewage treatment plant, than in the sediment from the same water depth closer to Langøyene. The plot of PS, PET, PU, PVF and nylon seems to have a similar trend as the polyolefins (Figure 3.4o).

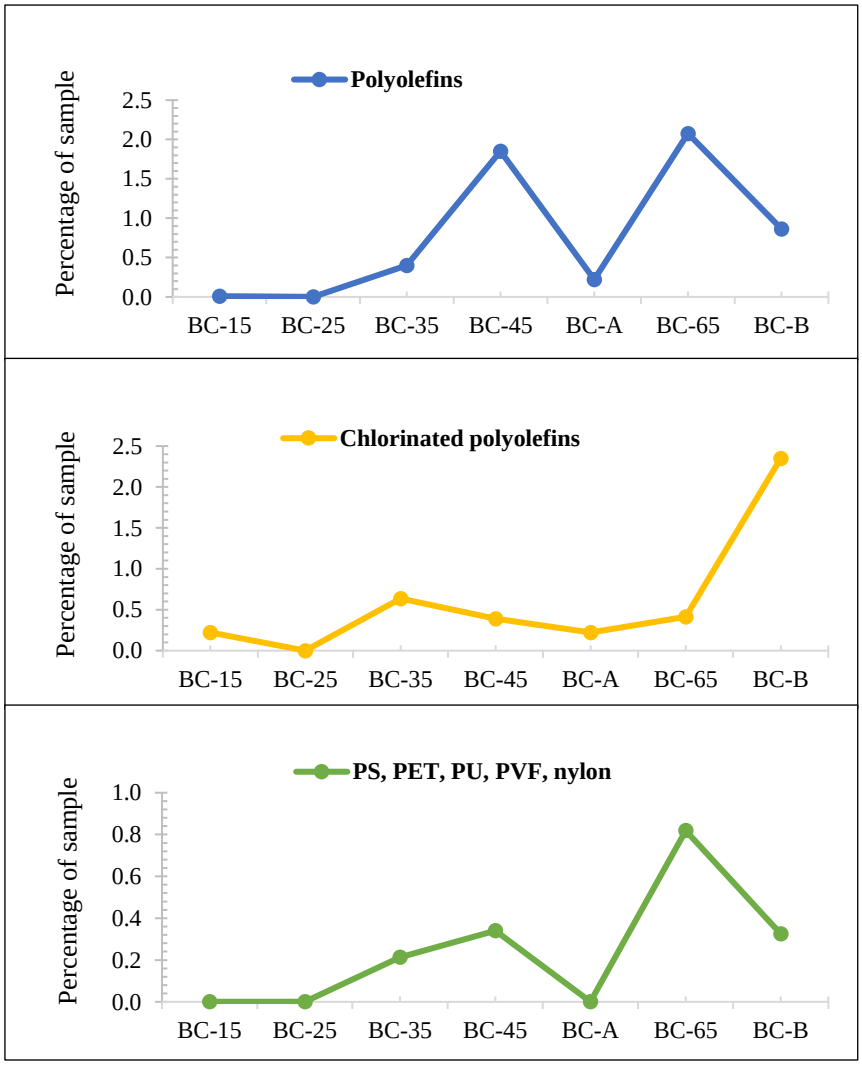

Figure 3.4o – *Upper plot: plot of the percentage of polyolefins in the surface samples, including the upper part of core BC-A. Middle plot: percentage of chlorinated polyolefins. Lower plot: percentage of PS, PET, PU, PVF and nylon (See Table 2.11b for the plastic abbreviations).*

The percentage of PMMA, EVA and melamine seems to increase from 25 to 35 m water depth, and then it decreases from 35 to 65 m. The percentage is lower in the sediment at 65 m depth from the station close to Bekkelaget sewage treatment plant than the sediment from the same water depth in the transect. The unresolved plastics seem to have a similar trend as the plot of polyolefins (Figure 3.4p).

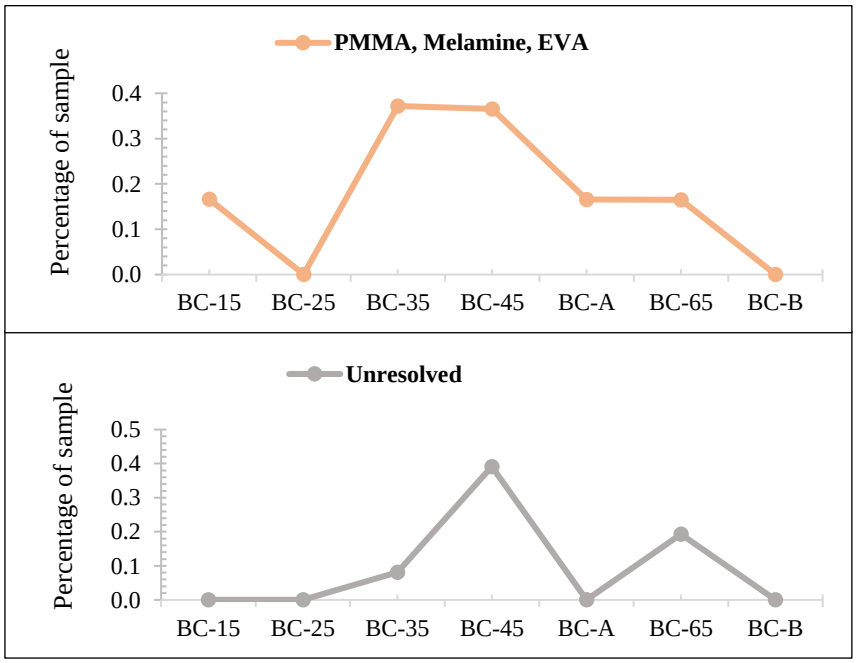

Figure 3.4p – *Upper plot: percentage of PMMA, EVA and melamine in the surface samples, including the upper part from core BC-A. Lower plot: percentage of the unresolved plastic (See Table 2.11b for the plastic abbreviations).*

3.4.10 Macroplastic

All data from the macroplastic analysis is listed in Appendix I and summarized in Table 3.4. Plastic particles were found in all of the sediment surface samples except the samples from 25 and 45 m water depth. The types of plastic, shape and colour varied, but the most frequent type seemed to be PE and PP, the most frequent shape seemed to be fibre, and the most frequent colour seemed to be white. The particles identified as plastic were from 0.44 to 5.60 mm, and there were also found black and green particles (Table 3.4).

Table 3.4 *– Plastic types of particles that could be picked out by tweezer, in the surface samples (See Table 2.11b).*

Sample ID	Plastic type	Colour	Shape	Length (mm)
BC-15	PE	Clear/white	Fibre	5.60
BC-25	-	-	-	-
BC-35	Other	White	Film	1.41
BC-45	-	-	-	-
BC-65	PE	Green	Granule	0.44
	PP	White	Fibre	17.62
	Nylon	Black	Fibre	8.51
BC-B	PE-chlorinated	White	Granule	2.00

4 DISCUSSION

4.1 DISCUSSION OF THE HYPOTHESES

I. The amount of microplastic will increase with time, so it would be expected to see an increasing amount of microplastic upward in the sediment cores.

The dating was performed on another core from station BC-A, so the core depths of the dated sediment core may not represent the exact same depths as the core that was used for the microplastic analysis. The core from station BC-B was not dated, so this core was indirectly dated by comparing the different parameters in the two cores.

Core BC-A

The margin of error was given for the core depth from 0 to 12 cm, and not from 12 to 15 cm, so the dating for the sediments beneath 12 cm is unreliable but it can be assumed that the sediments represents the 1940s (Appendix B). There was a rapid sedimentation rate between 12 and 15 cm, in the 1940s. The sedimentation rate varied from 0.36 to 0.47 cm y^{-1}, and the sediment was black and seemed to have traces of oil. The water content, TOC, C/N, grain size distribution, sand content, and the concentrations of oxy-resins, petro-pyro particles, plastic and rubber in the sediment from this depth differed from the overlying sediment that had a steady sedimentation rate that varied from 0.13 to 0.24 cm y^{-1}. It was also observed that the sediment from the depths 13-14 cm and 14-15 cm had coarser material than the rest of the core, and the sediment did also contain more organic material than the upper sediment layers. The sediment from 12-13 cm core depth had high value of TOC. It was 114.3 mg/g, and it varied from 41.6 to 87.7 mg/g in the core interval 0-12 cm (Figure 3.2b). The TOC in the sediment from 13-15 cm of the core was not possible to measure. The sediment could not be analysed because it was too coarse, but it was observed a lot of organic material compared to the other core depths when the sediment was prepared and introduced to the BMSS and separated (Figure 3.2e, Figure 3.2f). Based on the observations and results of the different parameters, it may be assumed that the rapid sedimentation in the core interval 13-15 cm is due to anthropogenic activity. This core was

collected outside the shoreline of Langøyene (Figure 1.4b), and the island was used as a landfill from 1908 to 1948, so it may seem that the rapid sedimentation rate and the high concentrations of oxy-resin, petro-pyro, plastic and rubber are due to the landfill.

The concentration of microplastic in the sediment from the core depth interval 13-14 cm is 106 745 particles per kg dry sediment, or 249.66 mg microplastic per kg dry sediment. The concentration in the sediment from core depth interval 14-15 cm is 823 68 particles per kg dry sediment or 261.62 mg per kg dry sediment. The concentration in the interval 13-15 cm is very high compared to the rest of the core, 0-13 cm where the concentration is 2 015 - 30 326 particles per kg dry sediment or 3.49 – 30.27 mg per kg dry sediment (Appendix H section H.1). The weight of the separated material that was analysed with microscope and FT-IR constituted a small percentage of the total weight of the material that was separated from the sediment from core depth 13-15 cm. 0.03 % of the separated material from core depth 14-15 cm was analysed, and 0.10 % of the separated material from core depth 13-14 cm was analysed. The percentage of the analysed material from the rest of the core, 0-13 cm was 0.34-5.67 % (Table 2.13c). A small percentage of material that was analysed leads to a high extrapolation factor, and therefore, it seems to be a high uncertainty in the concentration of microplastic in the sediment from 13-15 cm core depth. The exact concentration of microplastic in the sediment from 13-15 cm core depth seems to be very uncertain because of the high extrapolation factor, but it is not unlikely that there is a higher concentration of microplastic in this core depth interval due to the fact that the landfill was active from 1908 to 1948 and the sediment was probably deposited in the 1940s. The high concentration of the other anthropogenic particles (oxy-resin, petro-pyro and rubber) in the core depth interval 13-15 cm makes it more probable that the high concentrations of all four anthropogenic particles are due to the active period of the landfill (Figure 3.2j, Figure 3.2k).

Amount of microplastic over time

Concentration of microplastic in sediment is in general expected to increase with time due to the increasing production of plastic (Van Cauwenberghe et al., 2015), which means that an increasing concentration of microplastic from 13 cm core depth and upwards to the core surface was expected. The number of particles per kg dry sediment seemed to have an increasing trend from 12.5 to 7.5 cm, and from 6.5 to the core surface (Figure 3.2j). Plots of different plastic types

gives a different impression of the accumulation of plastic with time. The plot of polyolefins shows an increasing trend from the deepest part of the core to 3.5 cm core depth, and it decreases in the upper 0-3.5 cm of the core. The plot of chlorinated polyolefins seems to have a similar trend, but the percentage is increasing in the 1940s. The plot of PS, PET, PU, PVF and nylon has a similar trend as the polyolefins, but it has a peak in the core depth that represents the 1980s (Figure 3.2l). PMMA, EVA and melamine seems to be absent except in the 1960s and 70s, and the percentage of unresolved plastic is varying (Figure 3.2m). It seems that the high concentrations of plastic in the 13-15 cm core interval is due to particles of chlorinated polyolefins.

Core BC-B

The plot of the heavy metal concentrations in the core from station BC-A showed that Cr, Cu, Pb and Hg had a peak with a maximum concentration in the sediment from core depth 12.5 cm which, based on the results of the dating (Appendix B) represents the 1950s. As, and Cd had a peak with maximum concentration in the sediment from core depth 11.5 cm, which also represents the 1950s (Figure 3.2d). The plot of the heavy metal concentrations in the core from station BC-B showed that Ni, Cu, Zn, Pb and Hg had a peak with a maximum concentration in the sediment from core depth 17.5 cm (Figure 3.3d). By correlating the heavy metal peaks in the sediment core from station BC-A and BC-B, it seems that core depth 17.5 cm in the core from station BC-B represents the 1950s. The plots of the grain size distribution and sand content showed that the sediment from core depth interval 17.5-21 cm was coarser than the rest of the core, from 17.5 cm and upwards to the core surface (Figure 3.3c). A similar pattern was observed in the core interval 12.5-15 cm of the core from station BC-A and this core depth was dated back to the 1940/50s, so it could be assumed that 17.5-21 cm core depth in the core from station BC-B represents the 1940/50s.

Amount of microplastic over time

The concentration of microplastic seems to have a decreasing trend from 26 to 16.5 cm, and then it seems to increase from 16.5 cm to 0 cm (Figure 3.3j, Figure 3.3k). The maximum concentration of microplastic were found in the sediment from 26 cm core depth, and the concentration was 57 088 particles per kg dry sediment or 117.17 mg per kg dry sediment compared to a concentration of 9 554 particles per kg dry sediment or 8.9 mg per kg dry sediment in the sediment from 16.5 cm core depth (Appendix H section H.2). The concentration of microplastic seemed to increase from 13.5 cm to the core surface. Then, it increased from a concentration of 2 891 particles per kg dry sediment or 7.78 mg per dry sediment, to 33 075 particles per kg dry sediment or 25.61 mg per kg dry sediment in the core surface. Plots of the different plastic types gives a different impression of the amount of microplastic. The plot of polyolefins shows an increasing trend from 26 to 9.5 cm, and then it decreases in the upper 0-10 cm. The plot of chlorinated polyolefins varies but the overall trend seems to be decreasing. The same applies to the plot of PS, PET, PU, PVF and nylon (Figure 3.3l). PMMA, EVA and melamine seems to be stable from 26 to 13 cm and then it decreases in the upper 0-13 cm. The percentage of unresolved plastic is increasing from 26 to 23.5 cm and from 13 to 0 cm, and it decreases from 23.5 to 13 cm (Figure 3.3m). It seems that the high concentrations of plastic in the sediment from 26 cm core depth is due to chlorinated polyolefins and PS, PET, PU, PVF and nylon, and the results of the macroFT-IR analysis show that PE and PE-chlorinated were the most abundant plastic types in the deepest core interval (Table 3.3, Appendix I section I.2). The percentage of separated material that was analysed with microscope and FT-IR did also vary in this core. The highest concentration of microplastic was found in the sediment from 25-27 cm core depth interval, and only 0.62 % of the separated material was analysed, which was very little compared to the sediment from the core depth interval 5-8 cm. 18.75 % of the separated material from the sediment in this core depth interval was analysed. If the depth interval 17.5-21 cm represents the 1940/50s, then the sediment from 26 cm core depth is possibly deposited in the 1940s, during the active period of the landfill. Core BC-B was collected further away from Langøyene and it is unlikely that the landfill should have had any effect on this core, and the sediment from the core depth interval 25-27 cm did not look any different than the sediment from the upper parts of the core when it was prepared and introduced to the BMSS. The concentrations of oxy-resin and rubber do also show a different distribution than plastic and petro-pyro (Figure 3.3j, Figure 3.3k).

Waste management and coastal clean-ups

Both cores seemed to have an overall trend of decreasing concentration of microplastic. A possible to the high concentration of microplastic in the deeper part of the sediment cores could be that it was not illegal to dump waste into the ocean. It was assumed that 5.8 million tons of plastic waste was dumped from ship on a yearly basis in 1975, and dumping of plastic waste has been regulated by the international convention MARPOL since that time (Andersen, 2019, page 21). In the plots of polyolefins in core BC-A (Figure 3.2l), the percentage of polyolefins is clearly decreasing in the core depth 3.5 cm that represents the start of the 2000s. It is mentioned in Andersen (2019, page 60) that the production of plastic in Europe has been stable in the time period from 2006 to 2016, and the amount of recycled plastic waste increased with 79%, and the amount of plastic waste sent to landfills decreased with 43 %. A law regarding landfills was introduced in Norway in 2009. The law stated that no degradable waste should be sent to landfill, and since this time, the recycling of plastic waste has increased (Andersen, 2019, page 60-61). With a higher amount of plastic waste being recycled and managed properly, less waste would end up in the environment and this could be the explanation to the sudden decrease of polyolefins from the start of 2000s in core BC-A. A sudden decrease of polyolefins is also visible in core BC-B in the sediment from core depth 9.5 cm (Figure 3.3l), which could represent the 2000s because of the same clear trend as in the plot of polyolefins from core BC-A (Figure 3.2l). "Strandryddedagen" is a day with focus on coastal clean-up, and it has been arranged by "Hold Norge Rent" every year since 2011. This arrangement has been growing, and more and more people are joining in (Holdnorgerent, n.d.). According to the report by Eunomia (2016), 80 % of the plastic waste that ends up in the ocean are transported from land. The main contributor is everyday items such as plastic bottles and plastic packaging, which are usually made of polyolefins, so coast clean-ups that removes plastic items such as plastic packaging could explain the decrease of polyolefins in the upper 0-2 cm of the sediment core.

II. There will be no microplastic in the sediment representing the time before the start of the mass production of plastic.

There were found microplastic particles in all depths of core BC-A (Appendix H, section H.1) so it seems that the analysed core depths were not deep enough to see where the mass production of plastic started. It is mentioned in articles that the mass production started in the 1950s (Van Cauwenberghe et al., 2015), but according to the dating and the results of the microplastic analysis, it seems that the mass production may have started in the 1940s or earlier. PE, PP and PVC are the most common plastic types today. PP and PE were synthesised and produced in the 1940/50s, and the large-scale production of PVC started already in 1928, in Germany and USA (Crawford & Quinn, 2017), and the first products of PVC in Norway were made in 1950 (Nickelsen, 2015). The high weight of material after chemical digestion, and high extrapolation factor made it difficult to get accurate concentrations of microplastic. Sediment from deeper parts of the core should have been analysed to find a "reference condition" and to get an answer to this hypothesis. Analysis of the deeper core sediments would also have given a better impression of the effect of the landfill.

III. The concentration of microplastic is higher in the sediment closest to Langøyene than Bekkelaget sewage treatment plant.

Sediment samples were collected in a transect from a water depth of 15 to 65 m. These samples stations were close to Langøyene, and a sediment sample was also collected from 65 m water depth closer to Bekkelaget sewage treatment plant. The concentration of microplastic seems to be very high in the surface sample from 15 m water depth, and then it decreases with depth (Figure 3.4m). The concentration is 66 890 particles per kg dry sediment in the sediment from 15 m, and it decreases to 13 485 particles per kg dry sediment from 65 m water depth (Appendix H section H.3). The weight of microplastic seems to have a different trend. The sediment from 15 m water depth seems to have a lot of particles but the weight is 26.64 mg per kg dry sediment, and the highest weight of microplastic is from 35 m water depth with a concentration of 36.06 mg per kg dry sediment. The results of the visual analysis showed that the sediment from 15 m had a lot of low-density particles from size category A and B (≥45-300 µm) than the sediment sample from

35 m (Figure 3.4h), and this could be the reason why the weight of microplastic was higher in the sample from 35 m than 15 m. There is not a big difference in number and the weight of microplastic in the sediment from 45 to 65 m in the transect (Figure 3.4m). Oxy-resin particles were only found in the sample from 55 m water depth (represented by the upper 0-2 cm of core BC-A) (Figure 3.4k), and the plot of petro-pyro particles showed a concentration peak in the sediment sample from 35 m water depth (Figure 3.4l). When the sample from this depth was collected, a big piece of a material that looked like tar paper was observed in the surface of the sediment in the Van Veen grab (Figure 3.4a), this could probably be the cause of the high concentration. Rubber seemed to have the same trend as plastic, and the concentration seemed to decrease with water depth (Figure 3.4n). When looking at the plots of the different plastic types, it seems that the percentage of polyolefins, chlorinated polyolefins and PS, PET, PU, PVF and nylon increases with water depth (Figure 3.4o). PMMA, EVA and melamine seems to decrease with water depth, and the percentage of unresolved plastic seems to be increasing at first, from 15 to 45 m water depth, and then it decreases (Figure 3.4p). By looking at these plots, it seems that the high concentration of plastic in the sediment from 15 m water depth is because of PMMA, EVA and melamine.

Langøyene vs Bekkelaget sewage treatment plant

There were collected one sediment sample from 65 m water depth close to Langøyene, and one from 65 m water depth close to Bekkelaget sewage treatment plant. The concentration of microplastic in the sediment close to Bekkelaget is 4 030 particles per kg dry sediment, which is lower than the sediment sample close to Langøyene where the concentration was 13 485 particles per kg dry sediment. Though, the weight concentration shows the opposite. The sediment close to Bekkelaget has a weight concentration of 48.13 mg per kg dry sediment, while 13.54 mg per kg dry sediment of microplastic was found in the sample from the transect (Appendix H section H.3). This could mean that the sample from the transect contains microplastic particles of a smaller size, and this can be seen in the plot of the size distribution of particles (Figure 3.4h). The types of plastic particles that were found in the sediment from those two sample stations were different. The sediment from the transect had a higher percentage of polyolefins, PS, PET,

melamine and unresolved plastic, while the sediment close to Bekkelaget had a higher percentage of chlorinated polyolefins and nylon (Figure 3.4o, Figure 3.4p, Appendix H section H.3).

4.2 LITERATURE COMPARISON

A selection of different studies of microplastic in sediment samples from different parts of the world, is listed in Table 4.2. Different methods of sampling and separation makes it difficult to compare the results from this study to the findings in other studies. As seen in Table 4.2, the concentration of microplastic varies a lot because of different separation techniques, use of density solutions, and different size interval.

Some studies present the concentration as number of particles per kg sediment or mg microplastic per kg sediment, some others present the concentration as number of particles per m^2 sediment. Concentrations of microplastic presented differently could make it difficult to compare if there is not enough data to convert to a microplastic concentration with the same unit. It was observed in Bergmann et al. (2017) that the number of microplastic particles increased drastically with decreasing particle size. So, the bigger the particle size interval, the bigger the concentration of microplastic as number of particles. Different density solutions have been used in the studies (Table 4.2). Some of the studies have used NaCl with a density around 1.2 g/cm^3, and using a density solution with this density, plastic types with higher density, such as higher density than NaCl, such as PET, PVC, PVF, melamine (Table 2.11b) would not be separated. This would lead to an underestimation of microplastic concentration. However, it is also important that the density of the density solution is not too high as this will cause sediment particles, with a density around 2.6 g/cm^3 (Møskeland et al., 2018), to float as well.

Table 4.2 *– Relevant studies with information on particle size range, separation technique, and microplastic concentration (Møskeland et al., 2018; Lilleeng, 2018).*

Location	Location specification	Separation technique	Particle size	Measured concentration	Reference
Chile	Beach	Sieving	1 - 4.75 mm	<1 – 805 items/m^2	Hidalgo-Ruz & Thiel (2013)
India	Ship-breaking yard	Sieving and density separation: NaCl (30%)	1.6µm – 5 mm	81.4 mg/kg	Reddy et al. (2006)
India	Beach	Sieving and density separation: NaCl (1.40 g/l)	1 – 5 mm	10 – 180 items/m^2	Jayasiri et al. (2013)
Singapore	Mangrove	Density separation: NaCl (1.18 g/l)	1.6µm – 5 mm	36.8 items/kg	Nor & Obbard (2014)
NW Pacific	Deep sea trench	Sieving	300 µm – 5 mm	60 – 2 020 items/m^2	Fisher et al. (2015)
South Korea	Beach	Sieving and density separation: NaCl (2.16 g/cm^3)	50 µm – 5 mm	56 – 285 673 items/m^2	Kim et al. (2015)
Belgium	Continental Shelf	*Unknown*	38 µm – 1 mm	97.2 items/kg	Claessens et al. (2011)
Italy	Subtidal	Density separation: NaCl (1.2 g/mL)	0.7 µm – 1 mm	672 – 2 175 items/kg	Vianello et al. (2013)
Worldwide	Deep sea	Sieving and density separation: NaI (1.6 g/cm^3)	5 µm – 1 mm	50 items/m^2	Van Cauwenberghe et al. (2013)
Arctic	Deep sea	Density separation: ZnCl (1.7-1.8 g/cm^3)	10 µm – 5 mm	42 – 6 595 items/kg dry	Bergman et al. (2017)
Norway	Oslo beach	Density separation: $ZnCl_2$-$CaCl_2$ (1.57 g/cm^3)	45 µm – 5 mm plus fibres	500 – 9800 mg/kg	Mahat (2017)
Norway	Oslo sediment	Density separation: $ZnCl_2$-$CaCl_2$ (1.57 g/cm^3)	45 µm – 5 mm plus fibres	20 – 90 mg/kg	Mahat (2017)
Norway	Reference areas in the Norwegian coastal shelf	Density separation: NaI (~1.6 g/mL)	5 µm – 1 mm	23-391 items/kg	Jensen & Cramer (2017) (MAREANO)
Norway	Norwegian Continental Shelf	Density separation: $ZnCl_2$-$CaCl_2$ (1.53 g/cm^3)	45 µm – 5 mm plus fibres	< LOD - ≤ 410 (60) max mg/kg ≤ 180 - ≤ 31 000 (4 900) max items/kg	Møskeland, et al. (2018)
Norway (this study)	Bekkelaget basin, inner Oslofjord	Density separation: $ZnCl_2$-$CaCl_2$ (1.53 g/cm^3)	45 µm – 5 mm plus fibres	13.54 – 80.83 mg/kg 4 030 – 66 890 items/kg	*This thesis*
Norway (this thesis)	Sediment core samples, Bekkelaget basin, inner Oslofjord	Density separation: $ZnCl_2$-$CaCl_2$ (1.53 g/cm^3)	45 µm – 5 mm plus fibres	3.49 – 261.62 mg/kg 2 015 – 106 745 items/kg	*This thesis*

4.2.1 Beach samples, and sediment from Bekkelaget sewage treatment plant

The study by Mahat (2017) separated microplastic from sediment by using a high-density solution, and particles from the same size interval were studied. The results of this study showed a concentration that varied from 500 to 9 800 mg microplastic per kg dry sediment in beach samples collected from Bygdøy, which is a higher concentration compared to microplastic concentration of 14-81 mg per kg dry sediment in the sediment collected from the seabed from 15 to 65 m water depth. Sediment samples from Bekkelaget sewage treatment plant were also analysed in Mahat (2017), and the results showed a concentration of 20 to 90 mg microplastic per kg dry sediment. The microplastic concentration in the sediment collected close to Bekkelaget sewage treatment plant in this thesis was 48 mg per kg sediment, and it was within the range of microplastic concentration in sediment from the same location in Mahat (2017), and the higher density of the $ZnCl_2$-$CaCl_2$ (1.57 g/cm^3) could explain the maximum concentration of 90 mg per kg sediment, which is higher than the concentration of 48 mg per kg sediment in this thesis. The mean density of the density solution in this thesis was 1.53 g/cm^3, and the higher the density, the more particles with a high density would be separated. It is also uncertain from what water depth the sediment sample in Mahat (2017) were collected and the concentration of microplastic is based on the weight of low-density particles that survived chemical digestion, and this could explain the difference of maximum concentration from Bekkelaget sewage treatment plant.

4.2.2 Norwegian Continental Shelf

The separation technique, type of density solution and particle size interval in the study by Møskeland et al. (2018) were the same as in this thesis. Sediment from three different locations: central North Sea, northern North Sea and Barents Sea, from the Norwegian Continental Shelf was studied. The results showed that the concentration of microplastic with mean and standard deviation from the central North Sea varied from 412±770 to 6155±7003 number of particles per kg dry sediment. The concentration from the northern North Sea varied from 677±1064 to 2333±2920 number of microplastic particles, and the concentration from Barents Sea varied from 452±385 to 1570±1157 number of particles per kg dry sediment. The concentration in the upper 0-2 cm of the seabed in this thesis, varied from 4 030 to 66 890 microplastic particles per kg dry sediment. The concentration was relatively higher in the sediment from 15 to 65 m water depths

from the Bekkelaget basin compared to water depths of 66 to 80 m (central North Sea), 137 to 400 m (northern North Sea), and 242 to 508 m (Barents Sea) (Møskeland et al., 2018). The different water depths, distance from mainland and different sources of plastic contamination could explain the different microplastic concentrations. The identified particles with a search score ≥0.6 from the FT-IR analysis in the study of sediment from the Norwegian Continental Shelf, were accepted. Particles with a search score ≥0.7 were accepted in this thesis. With 0.7 as a cut-off compared to 0.6, fewer particles would have been accepted, and the concentration of microplastic could have been smaller. When looking at the concentration of microplastic as mg per kg dry sediment, the concentration in the sediment from the central North Sea vary from 5±10 to 81±93 mg per kg dry sediment. The concentration in the sediment from the northern North Sea vary from 9±15 to 31±40 mg, and the concentration in the sediment from the Barents Sea vary from 6±5 to 21±15 mg per kg dry sediment. The concentration of microplastic in the sediment from Bekkelaget basin vary from 13.54 to 80.83 mg per kg dry sediment. It seems that the weight of microplastic is in general lower in the sediment from the Norwegian Continental Shelf, but the maximum weight of microplastic from the central North Sea is almost the same weight as the maximum from Bekkelaget basin. The weight of microplastic in this thesis was calculated by combining the density of the plastic types that were detected in the FT-IR analysis, and extrapolation of the weight of low-density particles that were analysed. This could have led to an underestimation or overestimation of the weight of microplastic in the sediment from Bekkelaget.

5 CONCLUSION

- The maximum concentration of microplastic in core BC-A is in the depth interval where the dating is uncertain, but it is likely that this high concentration is due to the time period when waste was dumped and Langøyene went from being two islands to one.

- The concentration decreases over time in both cores, which could be explained by the increased focus on plastic waste and the improvement of waste management in the recent years. More plastic is being produced but the amount of recycled plastic waste has increased.

- PE and PP were the most abundant plastic types in all the sediment samples, and the plots of polyolefins in the sediment cores seem to reflect the time period when the focus on plastic waste in the environment started.

- Sediment from the deeper parts of the cores should have been analysed in order to get a better impression of the time when plastic became popular to use as material in various products.

- The decreasing concentration of microplastic with water depth, in the sediment samples from the transect gives a strong indication that most plastic waste that ends up in the ocean origin from land. The concentration of microplastic in the sediment sample from 65 m water depth in the transect (close to Langøyene) was higher than the concentration in the sediment sample from 65 m water depth close to the outlets of Bekkelaget sewage treatment plant.

REFERENCES

Andersen, G. S. (2019) *Å se en havhest dø. Forestillinger og fakta om plast i havet*. Spartacus Forlag AS.

Barnes, D. K. A., Galgani, F., Thompson, R. C. & Barlaz, M. (2009) *Accumulation and fragmentation of plastic debris in global environments*. Philosophical Transactions of the Royal Society of London B: Biological Sciences 364, pp 1985-1998. https://doi.org/10.1098/rstb.2008.0205

Bekkelagetvel (2011) *Informasjonsmøte 4.mai*. Selskapet til Bekkelaget vel. Available at: https://www.bekkelagetvel.org/2011/04/informasjonsmøte-4-mai/ Accessed [06.02.2019]

Bergmann, M., Wirzberger, V., Krumpen, T., Lorenz, C., Primpke, S., Tekman, M. B. & Gerdts, G. (2017) *High Quantities of Microplastic in Arctic Deep-Sea Sediments from the HAUSGARTEN Observatory*. Environmental Science & Technology 51, pp 11000-11010. https://doi.org/10.1021/acs.est.7b03331

Bjørneby, L. (2019) *Den historiske utviklingen av miljøtilstanden i Bekkelagsbassenget, Indre Oslofjord, En geokjemisk og mikropaleontologisk studie* [Master thesis] University of Oslo

Claessens, M., De Meester, S., Van Landuyt, L., De Clerck, K. & Janssen, C. R. (2011) *Occurrence and distribution of microplastics in marine sediments along the Belgian coast*. Marine Pollution Bulletin 62, pp. 2199-2204. https://doi.org/10.1016/j.marpolbul.2011.06.030

Crawford, C. B. & Quinn, B. (2017) *Microplastic Pollutants*. 1st edition. Published in Amsterdam (Netherlands)/Oxford (UK)/Cambridge (USA). Elsevier Inc.

Dolven, J. K., Alve, E., Rygg, B. & Magnusson, J. (2013) *Defining past ecological status and in situ reference conditions using benthic foraminifera: A case study from the Oslofjord, Norway*. Ecological Indicators, 29, 219-233

Eunomia (2016) *Plastics in the Marine Environment*. Available at: https://holdnorgerent.no/wp-content/uploads/2016/09/Plastics-in-the-Marine-Environment_Eunomia_Report.pdf Accessed [30.09.2019]

Fisher, V., Elsner, N. O., Brenke, N., Schwabe, E. & Brandt, A. (2015) *Plastic pollution of the Kuril-Kamchatka Trench area (NW Pacific)*. Deep Sea Research II, 111, 399-405. https://doi.org/10.1016/j.dsr2.2014.08.012

Hidalgo-Ruz, R. & Thiel, M. (2013) *Distribution and abundance of small plastic debris on beaches in the SE Pacific (Chile): A study supported by a citizen science project.* Marine Environmental Research, 87-88, 12-18. https://doi.org/10.1016/j.marenvres.2013.02.015

Holdnorgerent (n.d.) *Om hold norge rent*. Available from: https://holdnorgerent.no/om-hold-norge-rent/ Accessed [28.09.2019]

Hudgins, C. M. (1964) *Solubility and Density Studies of the $CaCl_2$-$ZnCl_2$-H_2O System at 0 and 25 C*. Journal of Chemical & Engineering Data, 9(3), 434-436. https://doi.ord/10.1021/je60022a045

Imhof, H. K., Schmid, J., Niessner, R., Ivleva, N. P. & Laforsch, C. (2012) *A novel, highly efficient method for the separation and quantification of plastic particles in sediments of aquatic environments*. Limnology and Oceanography: Methods 10: pp 524-537 https://doi.org/10.4319/lom.2012.10.524

Ivar do Sul, J. A., Spengler, Â., Costa, M. F. (2009) *Here, there and everywhere. Small plastic fragments and pellets on beaches of Fernando de Noronha (Equatorial Western Atlantic).* Marine Pollution Bulletin, 58, 1236-1238. https://doi.org/10.1016/j.marpolbul.2009.05.0004

Ivar do Sul, J. A. & Costa, M. F. (2013) *The present and future of microplastic pollution in the marine environment*. Environmental Pollution 185, pp 352-364. https://doi.org/10.1016/j.envpol.2013.10.036

Jambeck, J. R., Geyer, R., Wilcox, C., Siegler, T. R., Perryman, M., Andrady, A., Narayan, R. & Law, K. L. (2015) *Plastic waste inputs from land into the ocean*. Science 347, pp 768-771. https://doi.org/10.1126/science.1260352

Jayasiri, H. B., Porushothaman, C. S., Vennila, A. (2013) *Quantitative analysis of plastic debris on recreational beaches in Mumbai, India*. Marine Bulletin, 77, 107-112. https://doi.org/10.1016/j.marpolbul.2013.10.024

Jensen, H. K. B. & Cramer, J. (2017) *MAREANOs pilotprosjekt på mikroplast – resultater og forslag til videre arbeid. Norges Geologiske Undersøkelse* (NGU). Available at: http://www.ngu.no/upload/Publikasjoner/Rapporter/2017/2017_043.pdf Accessed [28.09.19]

Kim, I. S., Chae, D. H., Kim, S. K., Choi, S. & Woo, S. B. (2015) *Factors influencing the spatial variation of microplastics on high-tidal coastal beaches in Korea. Archives of Environmental Contamination and Toxicology*. https://doi.org/10.10007/s00244-015-0155-6

Lilleeng, Ø. (2018) *The presence of microplastics on the Norwegian Continental Shelf and the coast of Havana* [Master thesis] Norwegian University of Life Sciences

Mahat, S. (2017) *Separation and quantification of Microplastics from Beach and Sediment samples using the Bauta microplastic-sediment separator* [Master thesis] Norwegian University of Life Sciences

Miljødirektoratet (2019a) *Langøyene – tillatelse til opprydding*. Available at: https://www.miljodirektoratet.no/aktuelt/nyheter/2019/juli-2019/langoyene---tillatelse-til-opprydding/ [Accessed 01.09.2019].

Miljødirektoratet (2019b) Miljøstatus. Forsøpling av havet. Available at: https://miljostatus.miljodirektoratet.no/tema/avfall/forsopling-av-havet/ [Accessed 29.09.19]

Multiconsult (2013) *Langøyene avfallsdeponi*. Miljøteknisk undersøkelse. Report no. 124728-RIGm-RAP-01. 34 pages.

Multiconsult (2014) *Langøyene avfallsdeponi*. Miljøtekniske sedimentundersøkelser og risikovurdering. Report no. 124728- RIGm-RAP-004. 45 pages.

Møskeland, T., Knutsen, H., Arp, H. P., Lilleeng, Ø., & Pettersen, A. (2018) *Microplastics in sediments on the Norwegian Continental Shelf*. Miljødirektoratet. Available at: https://www.miljodirektoratet.no/publikasjoner/2018/mars-2018/microplastics-in-sediments-on-the-norwegian-continental-shelf/

Nickelsen, T. (2015) *Då plasten kom til Noreg*. Apollon. Available at: https://www.apollon.uio.no/artikler/2015/1_plasten.html [Accessed 29.09.19]

Nor, N. H. M. & Obbard, J. P. (2014) *Microplastics in Singapore's coastal mangrove ecosystems.* Marine Pollution Bulletin, 79, 278-283. https://doi.org/10.1016/j.marpolbul.2013.11.025

Olsen, L. M., Mahat, S. & Arp, H. P. (in preparation) *A solvation-digestion method for the isolation of microplastics from organic matter collected from surface-water trawls, coastlines and sediments.*

Oslobilder (2010) *Søppelfyllingen på Langøyene* [Photo] Available at: http://oslobilder.no/OMU/OB.Y6644 Owned by Oslo Museum, published on Oslobilder.

Oslo kommune (n.d.) *Langøyene – opprydding*. Available at: https://www.oslo.kommune.no/politikk-og-administrasjon/slik-bygger-vi-oslo/langoyene/#gref Accessed [09.05.2019]

Reddy, M. S., Basha, S., Adimurthy, S. & Ramachandraiah, G. (2006) *Description of the small plastic fragments in marine sediments along the Alang-Sosiya ship-breaking yard, India.* Estaurine Coastal and Shelf Science, 68, 656-660. https://doi.org/10.1016/j.ecss.2006.03.018

Scientific Polymer Products, Inc. (2013) Density of polymers (by density) [Webpage] Available at: https://scientificpolymer.com/density-of-polymers-by-density/ [Accessed 24.09.19]

Song, Y-K., Hong, S. H., Jang, M., Han, G. M., Rani, M., Lee, J. & Shim, W. J. (2015) *A comparison of microscopic and spectroscopic identification methods for analysis of microplastics in environmental samples*. Marine Pollution Bulletin 93, pp. 202-209 https://doi.org/10.1016/j.marpolbul.2015.01.015

Staalstrøm, A. & Røed, L. P. (2016) *Vertical mixing and internal wave energy fluxes in a sill fjord*. Journal of Marine Systems, 159, 15-32. https://dx.doi.org/10.1016/j.jmarsys.2016.02.005

Thompson, A. (2018) *From Fish to Humans, A Microplastic Invasion May Be Taking a Toll*. Scientific American. Available at: https://www.scientificamerican.com/article/from-fish-to-humans-a-microplastic-invasion-may-be-taking-a-toll/# [Accessed 29.11.18].

Thompson, R. C., Olsen, Y., Mitchell, R. P., Davis, D., Rowland, S. J., John, A. W. G., McGonigle, D & Russel, A. E. (2004) Lost at Sea: Where Is All the Plast? Science 304, pp 838-838. https://doi.org/10.1126/science.1094559

Van Cauwenberghe, L., Devriese, L., Galgani, F., Robbens, J. & Janssen, C. R. (2015) *Microplastics in sediments: A review of techniques, occurrence and effects*. Marine Environmental Research 111, pp 5-17. https://doi.org/10.1016/j.marenvres.2015.06.007

Vianello, A., Boldrin, A., Guerriero, P., Moschino, V., Rella, R., Sturaro, A. & Da Ros., L. (2013) *Microplastic particles in sediments of Lagoon of Venice, Italy: First observations on occurrence, spatial patterns and identification.* Estaurine, Coastal ad Shelf Science, 130, 54-61. https://doi.org/10.1016/j.ecss.2013.03.022

Ziccardi, L. M., Edgington, A., Hentz, K., Kulacki, K. J. & Driscoll, S. K. (2016) *Microplastics as vectors for bioaccumulation of hydrophobic organic chemicals in the marine environment*: A state-of-the-science-review. Environmental Toxicology and Chemistry 35 (7), pp 1667-1676. https://doi.org/10.1002/etc.3461

APPENDICES

APPENDIX A – SAMPLE WEIGHTS AND WATER CONTENT

A.1 – CORE BC-A

Core	Core interval (cm)	Core depth (cm)	Wet sample weight (g)	Dry sample weight (g)	% Water	Salt corrected dry sample weight (g)	% Water (salt corrected)
BC-A	0-1	0.5	221.42	51.03	77.0	45.24	79.57
BC-A	1-2	1.5	233.24	62.33	73.3	56.52	75.77
BC-A	2-3	2.5	243.67	76.26	68.7	70.57	71.04
BC-A	3-4	3.5	244.67	83.56	65.8	78.08	68.09
BC-A	4-5	4.5	248.54	85.38	65.6	79.83	67.88
BC-A	5-6	5.5	232.68	75.55	67.5	70.21	69.83
BC-A	6-7	6.5	163.10	50.66	68.9	46.84	71.28
BC-A	7-8	7.5	222.70	60.36	72.9	54.84	75.37
BC-A	8-9	8.5	235.05	57.37	75.6	51.33	78.16
BC-A	9-10	9.5	216.40	48.27	77.7	42.55	80.34
BC-A	10-11	10.5	211.51	48.54	77.1	43.00	79.67
BC-A	11-12	11.5	222.57	51.83	76.7	46.02	79.32
BC-A	12-13	12.5	225.69	55.37	75.5	49.58	78.03
BC-A	13-14	13.5	249.63	76.36	69.4	70.47	71.77
BC-A	14-15	14.5	306.18	126.93	58.5	120.84	60.53

A.2 – CORE BC-B

Core	Core interval (cm)	Core depth (cm)	Wet sample weight (g)	Dry sample weight (g)	% Water	Salt corrected dry sample weight (g)	% Water (salt corrected)
BC-B	0-5	2.5	58.88	16.64	71.7	15.25	74.11
BC-B	5-8	6.5	138.75	37.83	71.7	34.50	75.14
BC-B	8-11	9.5	171.75	43.10	74.9	38.85	77.38
BC-B	11-15	13	220.24	64.92	70.5	59.79	72.85
BC-B	15-18	16.5	231.73	84.92	63.4	80.08	65.44
BC-B	18-20	19	199.53	49.31	75.3	44.35	77.77
BC-B	20-22	21	209.20	70.94	66.1	66.38	68.27
BC-B	22-25	23.5	200.45	67.21	66.5	62.81	68.66
BC-B	25-27	26	184.59	48.31	73.8	43.81	76.26

A.3 – SURFACE SAMPLES

Core	Core interval (cm)	Core depth (m)	Wet sample weight (g)	Dry sample weight (g)	% Water	Salt corrected dry sample weight (g)	% Water (salt corrected)
BC-15	0-2	15	1 131.09	311.02	72.5	288.47	74.50
BC-25	0-2	25	1 147.57	360.40	68.6	335.21	70.79
BC-35	0-2	35	1 063.60	322.55	69.7	298.47	71.94
BC-45	0-2	45	1 262.84	400.20	68.3	371.73	70.56
BC-65	0-2	65	1 136.47	331.43	70.8	304.86	73.17
BC-B	0-2	65	1 150.42	343.61	70.1	316.99	72.45

APPENDIX B – ^{210}PB DATING OF SEDIMENT CORE

Radiometric dating of a marine sediment core from inner Oslofjord, Norway

P.G.Appleby and G.T.Piliposian
Environmental Radioactivity Research Centre
University of Liverpool

Methods

Dating by ^{210}Pb and ^{137}Cs was carried out on a marine sediment core from the inner Oslofjord, LØ55. Sub-samples from each core were analysed for ^{210}Pb, ^{226}Ra, and ^{137}Cs by direct gamma assay in the Liverpool University Environmental Radioactivity Laboratory, using Ortec HPGe GWL series well-type coaxial low background intrinsic germanium detectors (Appleby et al. 1986). ^{210}Pb was determined via its gamma emissions at 46.5 keV, and ^{226}Ra by the 295 keV and 352 keV γ-rays emitted by its daughter radionuclide ^{214}Pb following 3 weeks storage in sealed containers to allow radioactive equilibration. ^{137}Cs was measured by its emissions at 662 keV. The absolute efficiencies of the detectors were determined using calibrated sources and sediment samples of known activity. Corrections were made for the effect of self-absorption of low energy γ-rays within the sample (Appleby et al. 1992).

Results

The results of the radiometric analyses carried out on the core is given in Table 1 and shown graphically in Figure 1.i. Supported ^{210}Pb activity was assumed to be equal to the measured ^{226}Ra activity, and unsupported ^{210}Pb activity calculated by subtracting supported ^{210}Pb from the measured total ^{210}Pb activity. ^{210}Pb dates were calculated using both the CRS and CIC models (Appleby & Oldfield 1978) where appropriate, and possible 1963 and 1986 depths determined from the ^{137}Cs record. Best chronology for the core was determined following an assessment of all the data using the methods outlined in Appleby (2001). The result is shown in Figure 1.ii and given in detail in Table 3.

Core LØ55 (Bekkelag basin)

Lead-210 Activity

This core has an unusual ^{210}Pb record in that although total ^{210}Pb activity (Figure 1.i(a)) in the upper half of the core declines in a fairly regular way to reach values close to equilibrium with the supporting ^{226}Ra at a depth of around 12 cm, there are large variations in the deeper layers. These are however largely driven by unusual variations in the supported activity, particularly in sediments between 12-17 cm. ^{226}Ra concentrations are relatively uniform in sediments below 17 cm and above 12 cm, with mean values of 44 Bq kg-1 and 61 Bq kg-1 respectively. Between these two values, in sediments immediately above 17 cm they initially fall steeply to a minimum value of just 14 Bq kg-1 in the 14-15 cm sample, but then rise abruptly to a peak value of 125 Bq kg-1 in the 12-13 cm slice. The latter result was confirmed by repeat analyses carried out on a second aliquot from that slice. Possible causes of these variations are deposition at this site of allochthonous material from two different sources, one of which was ^{226}Ra poor and the other ^{226}Ra rich. Sediments within this section, particularly between 11-16 cm, also have a higher dry bulk density.

Unsupported (total minus supported) ^{210}Pb activity declines more or less regularly with depth in the uppermost 12 cm of the core (Figure 1.i(b)), but is close to the limit of detection throughout the anomalous 12-17 cm section. Deeper in the core, a small but significant unsupported 210Pb concentration in the 18-19 cm sample may indicate that sediments at this depth are relatively modern.

Artificial Fallout Radionuclides

^{137}Cs concentrations (Figure 1.i(c)) have a well-defined peak in the 5-6 cm. The proximity of this peak to the surface of the core suggests that it is more likely to be a record of fallout from the 1986 Chernobyl accident, though that is not certain. There are two smaller peaks, at 9-10 cm and 14-15 cm though it is not clear whether they are true records of atmospheric fallout. The latter feature may be associated with the events responsible for the ^{226}Ra anomalies between 12-17 cm.

Core Chronology

^{210}Pb dates calculated using the CRS model place 1986 at a depth of 6.5 cm and 1963 at a depth of 10 cm. These results suggest that the ^{137}Cs peaks at 5.5 cm and 9.5 cm may well be associated with the 1986 and 1963 fallout events. The calculations also suggest that the 210Pb anomalies between 12-17 cm record an episode of rapid sedimentation in the 1940s. Although irregularities in the ^{210}Pb record preclude detailed use of the alternative CIC model, it can be used to help date individual samples that appear to have been unaffected by those events, such as that at 18-19 cm. Both ^{210}Pb models date this sample to around 1940. Revised ^{210}Pb dates calculated by applying the CRS model in a piecewise using the ^{137}Cs dates as reference points suggest that sedimentation rates were relatively constant from the late 1950s through to the end of the 20th century with a mean sedimentation rate during that time of 0.056 g cm^{-2} y^{-1} (0.17 cm y^{-1}). There may have been a small increase in the sedimentation rate in recent years. Dates for sediments below 12 cm are highly uncertain because of the very low ^{210}Pb concentrations in the anomalous section. The raw calculations suggest they record an episode of rapid sedimentation in the 1940s or early 1950s. The 12-13 cm sample with the unusually high ^{226}Ra concentration is dated 1951. The 14-15 cm sample with the unusually low value is dated 1946. All the results are shown in Figure 1.ii and given in detail in Table 3.

References

Appleby P.G., 2001. Chronostratigraphic techniques in recent sediments, in *Tracking Environmental Change Using Lake Sediments Volume 1: Basin Analysis, Coring, and Chronological Techniques*, (eds W M Last & J P Smol), Kluwer Academic, pp171-203.

Appleby, P.G., P.J.Nolan, D.W.Gifford, M.J.Godfrey, F.Oldfield, N.J.Anderson & R.W.Battarbee, 1986. 210Pb dating by low background gamma counting. *Hydrobiologia*, **141**:21-27.

Appleby, P.G. & F.Oldfield, 1978. The calculation of 210Pb dates assuming a constant rate of supply of unsupported 210Pb to the sediment. *Catena*, **5**:1-8

Appleby, P.G., N.Richardson, & P.J.Nolan, 1992. Self-absorption corrections for well-type germaniun detectors. *Nucl. Inst.& Methods B*, **71**: 228-233.

Table 1. Fallout radionuclide concentrations in the Oslofjord sediment core LØ55.

Depth		^{210}Pb						^{137}Cs	
		Total		Unsupported		Supported			
cm	g cm^{-2}	Bq kg^{-1}	±	Bq kg^{-1}	±	Bq kg^{-1}	±	Bq kg^{-1}	±
0.5	0.13	178.9	10.8	126.0	11.0	52.9	2.2	25.5	1.6
2.5	0.74	197.4	9.5	138.1	9.8	59.3	2.2	21.8	1.6
3.5	1.13	180.0	14.5	108.1	14.9	71.9	3.2	24.3	2.0
4.5	1.56	152.9	10.3	88.4	10.6	64.5	2.5	34.4	1.9
5.5	1.98	150.6	14.0	88.5	14.4	62.2	3.4	52.3	3.0
6.5	2.36	160.2	10.2	95.3	10.5	64.8	2.5	31.9	1.9
7.5	2.72	143.4	9.6	87.2	9.9	56.1	2.4	22.5	1.7
8.5	3.01	140.1	9.2	79.5	9.4	60.7	2.2	19.5	1.7
9.5	3.26	107.9	10.9	54.1	11.2	53.8	2.5	21.3	1.9
10.5	3.51	73.7	5.6	33.6	5.8	40.1	1.4	12.6	1.0
11.5	3.77	86.3	7.1	39.0	7.3	47.3	1.6	6.0	1.0
12.5	4.09	133.5	13.5	8.1	13.9	125.4	3.5	3.2	1.4
13.5	4.48	45.6	7.5	9.8	7.8	35.9	1.9	3.5	0.7
14.5	4.98	19.7	3.4	5.5	3.5	14.1	0.8	12.6	0.7
15.5	5.44	33.4	7.8	7.7	8.0	25.7	1.8	5.4	1.2
16.5	5.74	33.2	6.1	7.8	6.3	25.3	1.4	1.2	0.7
17.5	6.02	47.5	5.7	8.1	5.9	39.4	1.4	3.3	0.8
18.5	6.30	59.5	5.7	15.6	5.9	44.0	1.5	0.0	0.0
19.5	6.60	45.0	5.7	1.3	5.9	43.7	1.5	0.7	0.8
21.0	7.08	51.8	7.1	8.6	7.3	43.2	1.8	0.2	1.0

Table 3 ^{210}Pb chronology of the Oslofjord sediment core LØ55

Depth		Chronology			Sedimentation Rate		
cm	g cm^{-2}	Date AD	Age y	±	g cm^{-2} y^{-1}	cm y^{-1}	± (%)
0.0	0.00	2018	0	0			
0.5	0.13	2017	1	1	0.072	0.24	10.7
2.5	0.74	2008	10	2	0.065	0.20	10.5
3.5	1.13	2001	17	2	0.058	0.14	11.5
4.5	1.56	1994	24	3	0.056	0.13	11.5
5.5	1.98	1986	32	3	0.056	0.14	11.5
6.5	2.36	1979	39	4	0.056	0.15	11.5
7.5	2.72	1973	45	4	0.056	0.17	11.5
8.5	3.01	1968	50	5	0.056	0.21	11.5
9.5	3.26	1963	55	5	0.056	0.23	11.5
10.5	3.51	1959	59	6	0.056	0.22	11.5
11.5	3.77	1954	64	8	0.071	0.24	14.6
12.5	4.09	1951	67		0.128	0.36	
13.5	4.48	1949	69		0.205	0.46	
14.5	4.98	1946	72		0.223	0.47	
15.5	5.44	1944	74		0.209	0.54	
16.5	5.74	1943	75		0.176	0.61	
17.5	6.02	1941	77		0.134	0.48	
18.5	6.30	1939	79		0.070	0.46	

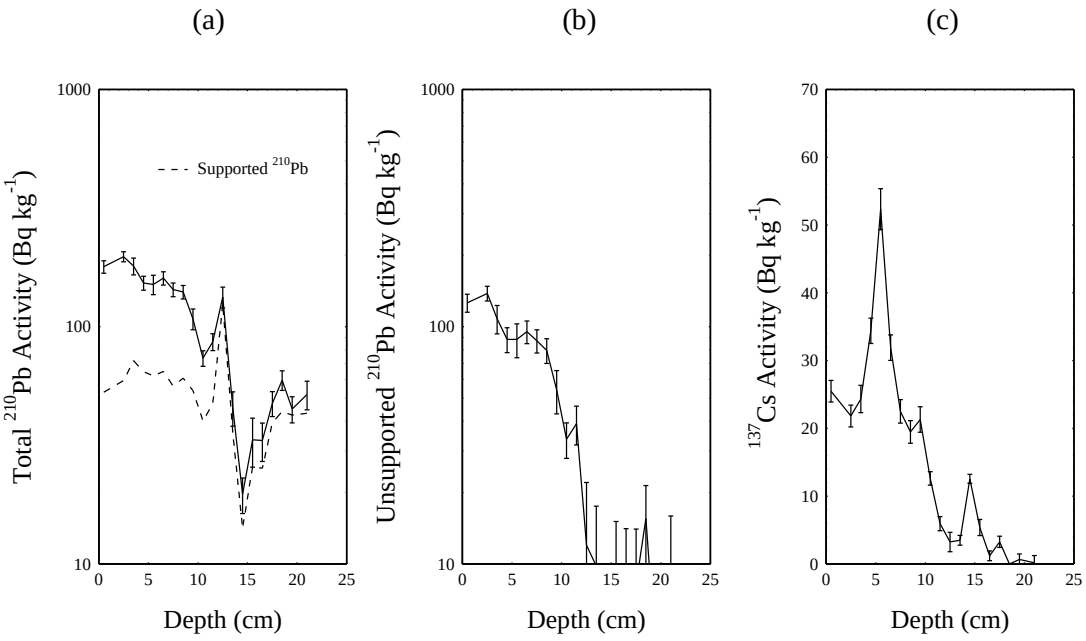

Figure 1.i. Fallout radionuclides in the Oslofjord sediment core LØ55 showing (a) total and supported ^{210}Pb, (b) unsupported ^{210}Pb, (c) ^{137}Cs concentrations versus depth.

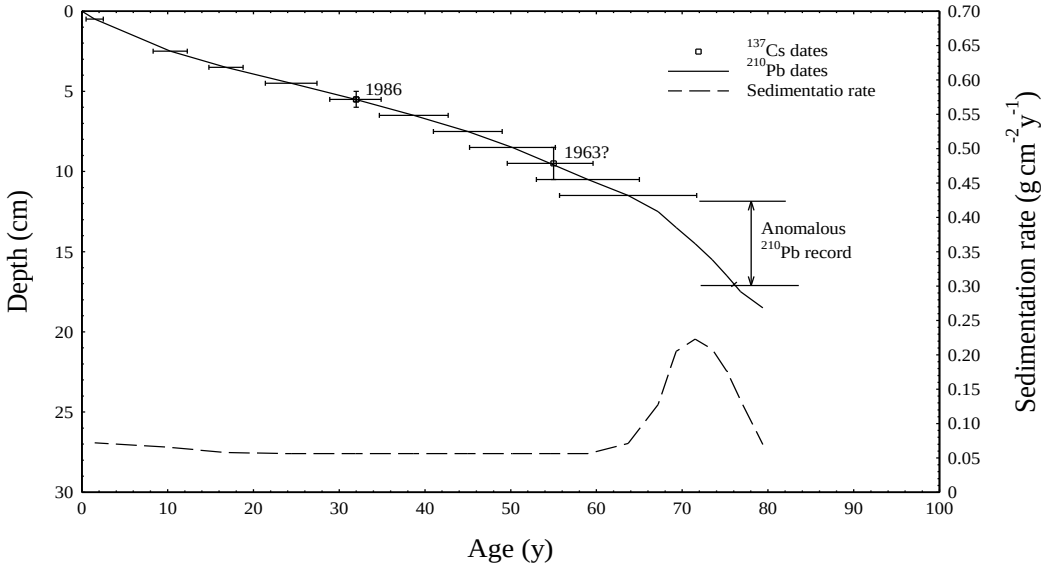

Figure 1.ii. Radiometric chronology of the Oslofjord sediment core LØ55 showing the ^{210}Pb dates and sedimentation rates and the 1986 and 1963 depths suggested by the ^{137}Cs record. A small adjustment to the ^{210}Pb dates has been made using the ^{137}Cs dates as reference points.

APPENDIX C – SEDIMENT PREPARATION

C.1 – CORE BC-A

Sample ID	Date	Density of $ZnCl_2$-$CaCl_2$ (g/cm^3)	Aluminium tray (g)	Aluminium tray + dry sediment (g)	Dry sediment (g) added to BMSS
BC-A 0-1	07.03.2019	1.54	6.70	58.62	51.92
BC-A 1-2	01.03.2019	1.55	6.67	70.12	63.45
BC-A 2-3	26.02.2019	1.55	6.62	83.44	76.82
BC-A 3-4	22.02.2019	1.55	6.69	91.40	84.71
BC-A 4-5	21.02.2019	1.55	6.73	93.04	86.31
BC-A 5-6	19.02.2019	1.55	6.77	83.74	76.97
BC-A 6-7	13.02.2019	1.55	6.62	58.33	51.71
BC-A 7-8	04.02.2019	1.57	6.64	67.71	61.07
BC-A 8-9	01.02.2019	1.57	6.59	65.40	58.81
BC-A 9-10	31.01.2019	1.53	6.75	56.46	49.71
BC-A 10-11	30.01.2019	1.53	6.66	56.18	49.52
BC-A 11-12	28.01.2019	1.53	6.69	60.09	53.40
BC-A 12-13	23.01.2019	1.53	6.69	63.25	56.56
BC-A 13-14	22.01.2019	1.53	6.67	84.98	78.31
BC-A 14-15	17.01.2019	1.53	6.66	136.24	129.58

C.2 – CORE BC-B

Sample ID	Date	Density of $ZnCl_2$-$CaCl_2$ (g/cm^3)	Aluminium tray (g)	Aluminium tray + dry sediment (g)	Dry sediment (g) added to BMSS
BC-B 0-5	14.01.2019	1.53	6.66	23.56	16.90
BC-B 5-8	09.01.2019	1.53	6.63	45.16	38.53
BC-B 8-11	03.01.2019	1.53	6.64	50.79	44.15
BC-B 11-15	02.01.2019	1.53	6.59	72.98	66.39
BC-B 15-18	26.11.2018	1.53	6.66	92.72	86.06
BC-B 18-20	19.11.2018	1.53	6.67	56.87	50.20
BC-B 20-22	01.11.2018	1.54	6.64	78.36	71.72
BC-B 22-25	30.10.2018	1.54	6.64	74.59	67.95
BC-B 25-27	22.10.2018	1.53	6.69	55.70	49.01

C.3 – SURFACE SAMPLES

Sample ID	Date	Density of $ZnCl_2$-$CaCl_2$ (g/cm^3)	Aluminium tray (g)	Aluminium tray + dry sediment (g)	Dry sediment (g) added to BMSS
BC-15	27.09.2018	1.57	6.59	42.83	36.24
BC-25	01.10.2018	1.53	6.63	47.83	41.20
BC-35	02.10.2018	1.53	6.65	50.16	43.51
BC-45	03.10.2018	1.53	6.66	50.76	44.10
BC-65	09.10.2018	1.53	6.72	52.92	46.20
BC-B	15.10.2018	1.54	6.72	49.05	42.33

APPENDIX D – MATERIAL WEIGHT*

*Total weight of the separated material (not blank corrected).

D.1 – CORE BC-A

Sample ID	Date	Weight before separation (g)			Weight after separation (after drying in oven at 60 °C)	Separated material (g)
		Steel filter	Steel wire	Total weight	Total weight	
BC-A 0-1	08.03.2019	1.6342	0.2968	1.9310	2.9720	1.0410
BC-A 1-2	04.03.2019	1.3062	0.3071	1.6133	2.0604	0.4471
BC-A 2-3	01.03.2019	1.6235	0.3502	1.9737	2.1966	0.2229
BC-A 3-4	25.02.2019	1.1184	0.3675	1.4859	1.6075	0.1216
BC-A 4-5	22.02.2019	1.3692	0.2165	1.5857	1.7453	0.1596
BC-A 5-6	21.02.2019	1.1245	0.3178	1.4423	1.5034	0.0611
BC-A 6-7	18.02.2019	1.1703	0.2659	1.4362	1.5071	0.0709
BC-A 7-8	05.02.2019	1.8538	0.3142	2.1680	2.4304	0.2624
BC-A 8-9	04.02.2019	1.2125	0.3304	1.5429	1.7573	0.2144
BC-A 9-10	01.02.2019	1.3305	0.1863	1.5168	1.7898	0.2730
BC-A 10-11	31.01.2019	1.1766	0.2409	1.4175	1.5484	0.1309
BC-A 11-12	29.01.2019	1.3475	0.3527	1.7002	1.9025	0.2023
BC-A 12-13	25.01.2019	1.6721	0.2905	1.9626	2.4070	0.4444
BC-A 13-14	23.01.2019	1.8044	0.3188	2.1232	4.8148	2.6916
BC-A 14-15 (1/4)	21.01.2019	1.7776	0.3512	2.1288	4.8133	2.6845
BC-A 14-15 (2/4)	21.01.2019	1.8222	0.2799	2.1021	4.3205	2.2184
BC-A 14-15 (3/4)	21.01.2019	1.7502	0.2345	1.9847	4.4320	2.4473
BC-A 14-15 (4/4)	21.01.2019	1.3245	0.3241	1.6486	3.2762	1.6276

Sample ID	Weight (g) of material picked out with tweezer	Weight (g) of material separated onto steel filter	Total weight (g) of low-density particles
BC-A 0-1	-	1.0410	1.0410
BC-A 1-2	-	0.4471	0.4471
BC-A 2-3	0.0517	0.2229	0.2746
BC-A 3-4	0.2162	0.1216	0.3378
BC-A 4-5	0.0417	0.1596	0.2013
BC-A 5-6	0.0422	0.0611	0.1033
BC-A 6-7	-	0.0709	0.0709
BC-A 7-8	-	0.2624	0.2624
BC-A 8-9	-	0.2144	0.2144
BC-A 9-10	-	0.2730	0.2730
BC-A 10-11	-	0.1309	0.1309
BC-A 11-12	-	0.2023	0.2023
BC-A 12-13	-	0.4444	0.4444
BC-A 13-14	0.4415	2.6916	3.1331
BC-A 14-15	0.74030	8.9778	9.7181

D.2 – CORE BC-B

Sample ID	Date	Weight before separation (g)			Weight after separation (after drying in oven at 60 °C)	Separated material (g)
		Steel filter	Steel wire	Total weight	Total weight	
BC-B 0-5	16.01.2019	1.3285	0.3125	1.6410	1.6733	0.0323
BC-B 5-8	11.01.2019	1.2824	0.3547	1.6371	1.6677	0.0306
BC-B 8-11	04.01.2019	1.3303	0.2558	1.5861	1.6425	0.0564
BC-B 11-15	03.01.2019	2.0523	0.7645	2.8168	2.8634	0.0466
BC-B 15-18	27.11.2018	2.3101	0.3586	2.6687	2.7941	0.1254
BC-B 18-20	20.11.2018	1.6093	0.4024	2.0117	2.0942	0.0825
BC-B 20-22	05.11.2018	1.4980	0.3874	1.8853	2.0324	0.1471
BC-B 22-25	01.11.2018	1.7634	0.4605	2.2238	2.3800	0.1561
BC-B 25-27 (1/2)	24.10.2018	1.5004	0.4968	1.9973	2.6364	0.6391
BC-B 25-27 (2/2)	24.10.2018	1.5911	0.3561	1.9472	2.0203	0.0730

Sample ID	Weight (g) of material picked out with tweezer	Weight (g) of material separated onto steel filter	Total weight (g) of low-density particles
BC-B 0-5	-	0.0323	0.0323
BC-B 5-8	-	0.0306	0.0306
BC-B 8-11	-	0.0564	0.0564
BC-B 11-15	-	0.0466	0.0466
BC-B 15-18	-	0.1254	0.1254
BC-B 18-20	-	0.0825	0.0825
BC-B 20-22	-	0.1471	0.1471
BC-B 22-25	-	0.1561	0.1561
BC-B 25-27	-	0.7122	0.7122

D.3 – SURFACE SAMPLES

Sample ID	Date	Weight before separation (g)			Weight after separation (after drying in oven at 60 °C)	Separated material (g)
		Steel filter	Steel wire	Total weight	Total weight	
BC-15	01.10.2018	1.4927	0.1616	1.6543	3.3656	1.7113
BC-25	02.10.2018	1.4590	0.1920	1.6510	2.2960	0.6450
BC-35	03.10.2018	1.5129	0.1753	1.6882	2.3781	0.6898
BC-45	05.10.2018	1.8236	0.1402	1.9638	2.1969	0.2331
BC-65	11.10.2018	1.3958	0.3169	1.7128	1.8903	0.1777
BC-B	16.10.2018	1.9428	0.2467	2.1895	2.4103	0.2208

Sample ID	Weight (g) of material picked out with tweezer	Weight (g) of material separated onto steel filter	Total weight (g) of low-density particles
BC-15	-	1.7113	1.7113
BC-25	-	0.6450	0.6450
BC-35	-	0.6898	0.6898
BC-45	0.1190	0.3521	0.4712
BC-65	-	0.1777	0.1777
BC-B	-	0.2208	0.2208

APPENDIX E – CHEMICAL DIGESTION AND BLANK CORRECTION

E.1 – CORE BC-A

Sample ID	Weight (g) before digestion	Weight (g) after digestion	Rounds of digestion	Method blank and recovery corrected (g)
BC-A 0-1	1.0410	0.0443	2	0.0497
BC-A 1-2	0.4471	0.0632	2	0.0715
BC-A 2-3	0.2229	0.0232	2	0.0263
BC-A 3-4	0.1216	0.0276	2	0.0313
BC-A 4-5	0.1596	0.0250	2	0.0283
BC-A 5-6	0.0611	0.0112	2	0.0126
BC-A 6-7	0.0709	0.0125	2	0.0141
BC-A 7-8	0.2624	0.0369	2	0.0418
BC-A 8-9	0.2144	0.0226	2	0.0256
BC-A 9-10	0.2730	0.0533	2	0.0602
BC-A 10-11	0.1309	0.0448	2	0.0508
BC-A 11-12	0.2023	0.0335	2	0.0380
BC-A 12-13	0.4444	0.1790	2	0.2031
BC-A 13-14	2.6916	1.0394	2	1.1797
BC-A 14-15	8.9778	4.2168	2	4.7860

E.2 – CORE BC-B

Sample ID	Weight (g) before digestion	Weight (g) after digestion	Rounds of digestion	Method blank and recovery corrected (g)
BC-B 0-5	0.0323	0.0049	2	0.0055
BC-B 5-8	0.0306	0.0015	2	0.0016
BC-B 8-11	0.0564	0.0046	2	0.0051
BC-B 11-15	0.0466	0.0037	2	0.0041
BC-B 15-18	0.1254	0.0070	2	0.0078
BC-B 18-20	0.0825	0.0091	2	0.0102
BC-B 20-22	0.1471	0.0150	2	0.0169
BC-B 22-25	0.1561	0.0117	2	0.0132
BC-B 25-27	0.7122	0.1139	2	0.1289

E.3 – SURFACE SAMPLES

Sample ID	Weight (g) before digestion	Calculated weight (g) after digestion	Rounds of digestion	Method blank and recovery corrected (g)
BC-15	1.7113	0.2156	3	0.2437
BC-25	0.6450	0.1233	2	0.1397
BC-35	0.6898	0.1825	3	0.2069
BC-45	0.4712	0.0421	3	0.0477
BC-65	0.1777	0.0151	3	0.0171
BC-B	0.2208	0.0508	1	0.0576

APPENDIX F – VISUAL ANALYSIS

F.1 – CORE BC-A

Date	ID	Colour	Fibre 1D				Film 2D				Granulate 3D			
			A	B	C	D	A	B	C	D	A	B	C	D
10.05.2019	BC-A 0-1	Clear/white	1					1					1	
		Light brown		1	3			1				1		
		Dark brown												
		Black						1						
		Blue									1			
		Red		1			1							
		Green												
		Orange												
		Yellow												
		Sum	1	2	3	0	1	3	0	0	1	1	1	0
		Fraction of total	6		46.2 %		4		30.8 %		3		23.1 %	
		SUM									13			

Date	ID	Colour	Fibre 1D				Film 2D				Granulate 3D			
			A	B	C	D	A	B	C	D	A	B	C	D
10.05.2019	BC-A 1-2	Clear/white	3				1	4				1		
		Light brown		1	1								1	
		Dark brown											1	
		Black						1						
		Blue			1		1							
		Red												
		Green												
		Orange												
		Yellow												
		Sum	3	1	2	0	2	5	0	0	0	1	2	0
		Fraction of total	6		37.5 %		7		43.8 %		3		18.8 %	
		SUM									16			

Date	ID	Colour	Fibre 1D				Film 2D				Granulate 3D			
			A	B	C	D	A	B	C	D	A	B	C	D
25.04.2019	BC-A 2-3	Clear/white				1		5	1					
		Light brown		1				1						
		Dark brown												
		Black												
		Blue												
		Red												
		Green												
		Orange												
		Yellow												
		Sum	0	1	0	1	0	6	1	0	0	0	0	0
		Fraction of total	2		22.2 %		7		77.8 %		0		0.0 %	
		SUM									9			

Date	ID	Colour	Fibre 1D				Film 2D				Granulate 3D			
			A	B	C	D	A	B	C	D	A	B	C	D
25.04.2019	BC-A 3-4	Clear/white			1		1	1	1			5		
		Light brown		1				1						
		Dark brown					1							
		Black												
		Blue						1						
		Red		1							1			
		Green												
		Orange												
		Yellow												
		Sum	0	2	1	0	2	3	1	0	1	5	0	0
		Fraction of total	3		20.0 %		6		40.0 %		6		40.0 %	
		SUM									15			

Date	ID	Colour	Fibre 1D				Film 2D				Granulate 3D			
			A	B	C	D	A	B	C	D	A	B	C	D
16.05.2019	BC-A 4-5	Clear/white			1	1		2				1	1	
		Light brown						2	1					
		Dark brown						3						
		Black						2				1		
		Blue												
		Red												
		Green		1							1			
		Orange					1							
		Yellow									1			
		Sum	0	1	1	1	1	9	1	0	2	2	1	0
		Fraction of total	3		15.8 %		11		57.9 %		5		26.3 %	
		SUM									19			

Date	ID	Colour	Fibre 1D				Film 2D				Granulate 3D			
			A	B	C	D	A	B	C	D	A	B	C	D
16.05.2019	BC-A 5-6	Clear/white				1		5				2		
		Light brown		2				8	1			2	1	
		Dark brown												
		Black						1				3		
		Blue		1										
		Red									1			
		Green									1			
		Orange						1						
		Yellow												
		Sum	0	3	0	1	0	15	1	0	2	7	1	0
		Fraction of total	4		13.3 %		16		53.3 %		10		33.3 %	
		SUM									30			

Date	ID	Colour	Fibre 1D				Film 2D				Granulate 3D			
			A	B	C	D	A	B	C	D	A	B	C	D
20.05.2019	BC-A 6-7	Clear/white			2		2	3	1			4		
		Light brown						3	2			2		
		Dark brown											1	
		Black					1	3	1			2	1	
		Blue												
		Red									1			
		Green			1	1						1		
		Orange									1			
		Yellow												
		Sum	0	0	3	1	3	9	4	0	2	9	2	0
		Fraction of total	4		12.1 %		16		48.5 %		13		39.4 %	
		SUM									33			

Date	ID	Colour	Fibre 1D				Film 2D				Granulate 3D			
			A	B	C	D	A	B	C	D	A	B	C	D
29.05.2019	BC-A 7-8	Clear/white			1		1	4	1			1		
		Light brown					1							
		Dark brown				1								
		Black					5	2				1		
		Blue						1				1		
		Red									1			
		Green			1									
		Orange												
		Yellow												
		Sum	0	0	2	1	7	7	1	0	1	3	0	0
		Fraction of total	3		13.6 %		15		68.2 %		4		18.2 %	
		SUM									22			

Date	ID	Colour	Fibre 1D				Film 2D				Granulate 3D			
			A	B	C	D	A	B	C	D	A	B	C	D
31.05.2019	BC-A 8-9	Clear/white		1	2		2	11			1	2		
		Light brown		1	1						1	4	2	
		Dark brown												
		Black		1				2	2		2	5		
		Blue		1										
		Red									1			
		Green					1							
		Orange												
		Yellow												
		Sum	0	4	3	0	3	13	2	0	5	11	2	0
		Fraction of total	7		16.3 %		18		41.9 %		18		41.9 %	
		SUM									43			

Date	ID	Colour	Fibre 1D				Film 2D				Granulate 3D			
			A	B	C	D	A	B	C	D	A	B	C	D
02.06.2019	BC-A 9-10	Clear/white			1			2			2			
		Light brown							1		1	2		
		Dark brown		1								2		
		Black						1				4		
		Blue			1									
		Red												
		Green									1	1		
		Orange												
		Yellow												
		Sum	0	1	2	0	0	3	1	0	4	9	0	0
		Fraction of total	3		15.0 %		4		20.0 %		13		65.0 %	
		SUM									20			

Date	ID	Colour	Fibre 1D				Film 2D				Granulate 3D			
			A	B	C	D	A	B	C	D	A	B	C	D
27.03.2019	BC-A 10-11	Clear/white						4	1					
		Light brown										1		
		Dark brown												
		Black												
		Blue												
		Red												
		Green												
		Orange												
		Yellow												
		Sum	0	0	0	0	0	4	1	0	0	1	0	0
		Fraction of total	0		0.0 %		5		83.3 %		1		16.7 %	
		SUM									6			

Date	ID	Colour	Fibre 1D				Film 2D				Granulate 3D			
			A	B	C	D	A	B	C	D	A	B	C	D
27.03.2019	BC-A 11-12	Clear/white						4						
		Light brown						1						
		Dark brown												
		Black			1			1	1					
		Blue												
		Red												
		Green												
		Orange												
		Yellow												
		Sum	0	0	1	0	0	6	1	0	0	0	0	0
		Fraction of total	1		12.5 %		7		87.5 %		0		0.0 %	
		SUM									8			

Date	ID	Colour	Fibre 1D				Film 2D				Granulate 3D			
			A	B	C	D	A	B	C	D	A	B	C	D
04.04.2019	BC-A 12-13	Clear/white						1						
		Light brown						1				1		
		Dark brown												
		Black												
		Blue												
		Red												
		Green												
		Orange												
		Yellow												
		Sum	0	0	0	0	0	2	0	0	0	1	0	0
		Fraction of total	0		0.0 %		2		66.7 %		1		33.3 %	
		SUM									3			

Date	ID	Colour	Fibre 1D				Film 2D				Granulate 3D			
			A	B	C	D	A	B	C	D	A	B	C	D
04.04.2019	BC-A 13-14	Clear/white						1	1					
		Light brown										1		
		Dark brown												
		Black										1		
		Blue												
		Red												
		Green												
		Orange												
		Yellow					2							
		Sum	0	0	0	0	2	1	1	0	0	2	0	0
		Fraction of total	0		0.0 %		4		66.7 %		2		33.3 %	
		SUM									6			

Date	ID	Colour	Fibre 1D				Film 2D				Granulate 3D			
			A	B	C	D	A	B	C	D	A	B	C	D
02.06.2019	BC-A 14-15	Clear/white						1				1	2	
		Light brown					1					2		
		Dark brown					1							
		Black	1					1	1		1	5		
		Blue												
		Red												
		Green												
		Orange												
		Yellow					2							
		Sum	1	0	0	0	4	2	1	0	1	8	2	0
		Fraction of total	1		5.3 %		7		36.8 %		11		57.9 %	
		SUM	19											

F.2 – CORE BC-B

Date	ID	Colour	Fibre 1D				Film 2D				Granulate 3D			
			A	B	C	D	A	B	C	D	A	B	C	D
27.02.2019	BC-B 0-5	Clear/white		1			1	1						
		Light brown												
		Dark brown												
		Black	1	2										
		Blue		2		1	1							
		Red												
		Green												
		Orange									3			
		Yellow												
		Sum	1	5	0	1	2	1	0	0	3	0	0	0
		Fraction of total	7		53.8 %		3		23.1 %		3		23.1 %	
		SUM	13											

Date	ID	Colour	Fibre 1D				Film 2D				Granulate 3D			
			A	B	C	D	A	B	C	D	A	B	C	D
01.03.2019	BC-B 5-8	Clear/white						1						
		Light brown												
		Dark brown												
		Black			2									
		Blue												
		Red												
		Green			1									
		Orange												
		Yellow												
		Sum	0	0	3	0	0	1	0	0	0	0	0	0
		Fraction of total	3		75.0 %		1		25.0 %		0		0.0 %	
		SUM	4											

Date	ID	Colour	Fibre 1D				Film 2D				Granulate 3D			
			A	B	C	D	A	B	C	D	A	B	C	D
28.02.2019	BC-B 8-11	Clear/white			2			1	1					
		Light brown												
		Dark brown												
		Black		1								1		
		Blue		3	1						1			
		Red									1			
		Green		1							3		1	
		Orange												
		Yellow												
		Sum	0	5	3	0	0	1	1	0	5	1	1	0
		Fraction of total	8		47.1 %		2		11.8 %		7		41.2 %	
		SUM	17											

Date	ID	Colour	Fibre 1D				Film 2D				Granulate 3D			
			A	B	C	D	A	B	C	D	A	B	C	D
01.03.2019	BC-B 11-15	Clear/white			1	1		2	2					
		Light brown		2					1					
		Dark brown												
		Black						2						
		Blue			1									
		Red												
		Green										2		
		Orange												
		Yellow												
		Sum	0	2	2	1	0	4	3	0	0	2	0	0
		Fraction of total	5		35.7 %		7		50.0 %		2		14.3 %	
		SUM									14			

Date	ID	Colour	Fibre 1D				Film 2D				Granulate 3D			
			A	B	C	D	A	B	C	D	A	B	C	D
04.03.2019	BC-B 15-18	Clear/white			4	1	1	2	1					
		Light brown						2						
		Dark brown												
		Black					1							
		Blue		1										
		Red		1										
		Green												
		Orange												
		Yellow					2	2						
		Sum	0	2	4	1	4	6	1	0	0	0	0	0
		Fraction of total	7		38.9 %		11		61.1 %		0		0.0 %	
		SUM									18			

Date	ID	Colour	Fibre 1D				Film 2D				Granulate 3D			
			A	B	C	D	A	B	C	D	A	B	C	D
07.03.2019	BC-B 18-20	Clear/white			2			2	1			2		
		Light brown			1									
		Dark brown												
		Black										1		
		Blue						1						
		Red												
		Green									1			
		Orange												
		Yellow										1		
		Sum	0	0	3	0	0	3	1	0	1	4	0	0
		Fraction of total	3		25.0 %		4		33.3 %		5		41.7 %	
		SUM									12			

Date	ID	Colour	Fibre 1D				Film 2D				Granulate 3D			
			A	B	C	D	A	B	C	D	A	B	C	D
07.03.2019	BC-B 20-22	Clear/white						3	4			1	1	
		Light brown												
		Dark brown		1				1						
		Black											1	
		Blue	1								3	1		
		Red												
		Green												
		Orange			1									
		Yellow			2									
		Sum	1	1	3	0	0	4	4	0	3	2	2	0
		Fraction of total	5		25.0 %		8		40.0 %		7		35.0 %	
		SUM									20			

Date	ID	Colour	Fibre 1D				Film 2D				Granulate 3D			
			A	B	C	D	A	B	C	D	A	B	C	D
19.03.2019	BC-B 22-25	Clear/white				1		3				1		
		Light brown						1						
		Dark brown												
		Black						1						
		Blue		1										
		Red												
		Green												
		Orange												
		Yellow					1							
		Sum	0	1	0	1	1	5	0	0	0	1	0	0
		Fraction of total	2		22.2 %		6		66.7 %		1		11.1 %	
		SUM									9			

Date	ID	Colour	Fibre 1D				Film 2D				Granulate 3D			
			A	B	C	D	A	B	C	D	A	B	C	D
19.03.2019	BC-B 25-27	Clear/white						1						
		Light brown												
		Dark brown						1						
		Black												
		Blue		1	1									
		Red												
		Green						1						
		Orange												
		Yellow					1	1						
		Sum	0	1	1	0	1	4	0	0	0	0	0	0
		Fraction of total	2		28.6 %		5		71.4 %		0		0.0 %	
		SUM									7			

F.3 – SURFACE SAMPLES

Date	ID	Colour	Fibre 1D				Film 2D				Granulate 3D			
			A	B	C	D	A	B	C	D	A	B	C	D
03.08.2019	BC-15	Clear/white					1							
		Light brown										1		
		Dark brown												
		Black										4	2	
		Blue												
		Red												
		Green												
		Orange												
		Yellow												
		Sum	0	0	0	0	1	0	0	0	0	5	2	0
		Fraction of total	0		0.0 %		1		12.5 %		7		87.5 %	
		SUM									8			

Date	ID	Colour	Fibre 1D				Film 2D				Granulate 3D			
			A	B	C	D	A	B	C	D	A	B	C	D
20.02.2019	BC-25	Clear/white		6				1						
		Light brown												
		Dark brown												
		Black												
		Blue												
		Red												
		Green												
		Orange												
		Yellow												
		Sum	0	6	0	0	0	1	0	0	0	0	0	0
		Fraction of total	6		85.7 %		1		14.3 %		0		0.0 %	
		SUM									7			

Date	ID	Colour	Fibre 1D				Film 2D				Granulate 3D			
			A	B	C	D	A	B	C	D	A	B	C	D
03.08.2019	BC-35	Clear/white				1								
		Light brown										3		
		Dark brown												
		Black										2	2	
		Blue			2									
		Red												
		Green												
		Orange												
		Yellow												
		Sum	0	0	2	1	0	0	0	0	0	5	2	0
		Fraction of total	3		30.0 %		0		0.0 %		7		70.0 %	
		SUM									10			

Date	ID	Colour	Fibre 1D				Film 2D				Granulate 3D			
			A	B	C	D	A	B	C	D	A	B	C	D
11.08.2019	BC-45	Clear/white		4			1					4	1	
		Light brown					1	1		1		2		
		Dark brown											1	
		Black						1			1	5	1	
		Blue										1		
		Red												
		Green												
		Orange												
		Yellow												
		Sum	0	4	0	0	2	2	0	1	1	12	3	0
		Fraction of total	4		16.0 %		5		20.0 %		16		64.0 %	
		SUM									25			

Date	ID	Colour	Fibre 1D				Film 2D				Granulate 3D			
			A	B	C	D	A	B	C	D	A	B	C	D
25.08.2019	BC-65	Clear/white			2	1		1					1	
		Light brown										1		
		Dark brown									1			
		Black			1	1						1	1	
		Blue												
		Red												
		Green												
		Orange												
		Yellow			1									
		Sum	0	0	4	2	0	1	0	0	1	2	2	0
		Fraction of total	6		50.0 %		1		8.3 %		5		41.7 %	
		SUM									12			

Date	ID	Colour	Fibre 1D				Film 2D				Granulate 3D			
			A	B	C	D	A	B	C	D	A	B	C	D
25.01.2019	BC-B	Clear/white			3	1				1				
		Light brown												
		Dark brown												
		Black												
		Blue		1										
		Red												
		Green												
		Orange												
		Yellow												
		Sum	0	1	3	1	0	0	0	1	0	0	0	0
		Fraction of total	5		83.3 %		1		16.7 %		0		0.0 %	
		SUM									6			

APPENDIX G – PICTURES OF MICROPLASTIC PARTICLES

G.1 – CORE BC-A

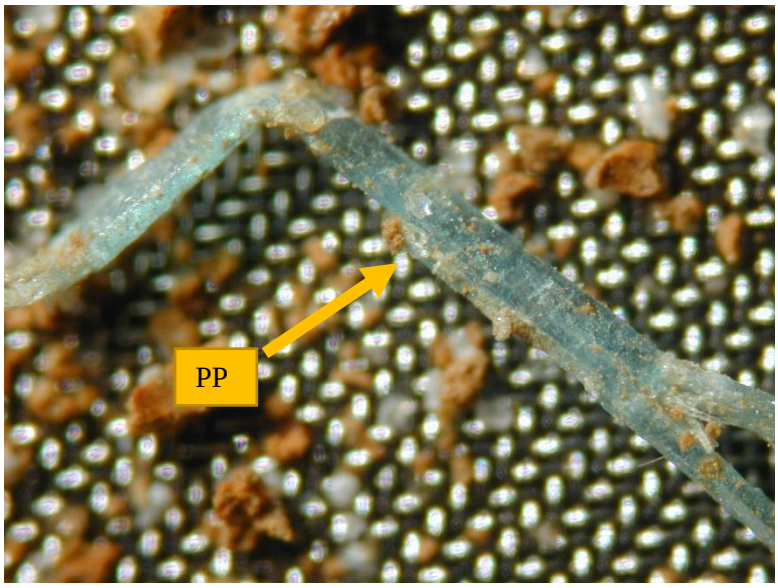

Core depth: 1-2 cm

Shape: fibre

Size: 832 µm (size category C)

Colour: blue

FT-IR identification: polypropylene (PP)

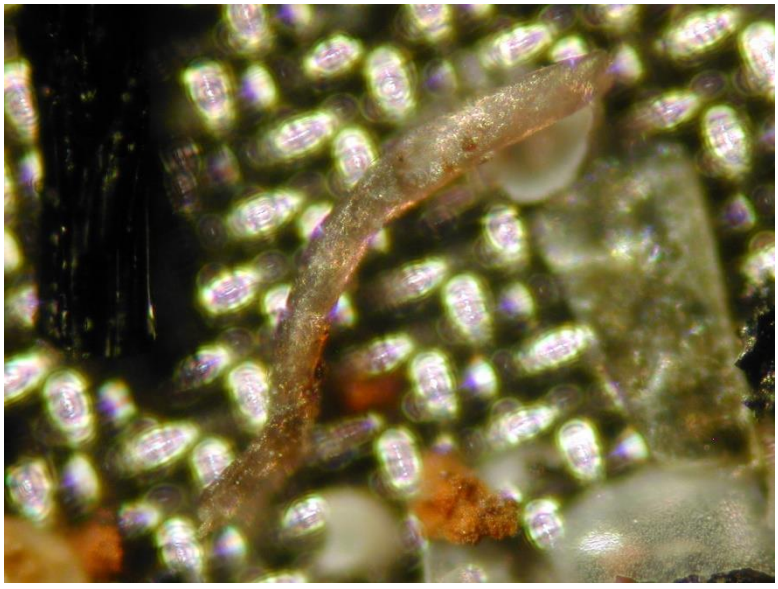

Core depth: 3-4 cm

Shape: fibre

Size: 208 µm (size category B)

Colour: red

FT-IR identification: polypropylene (PP)

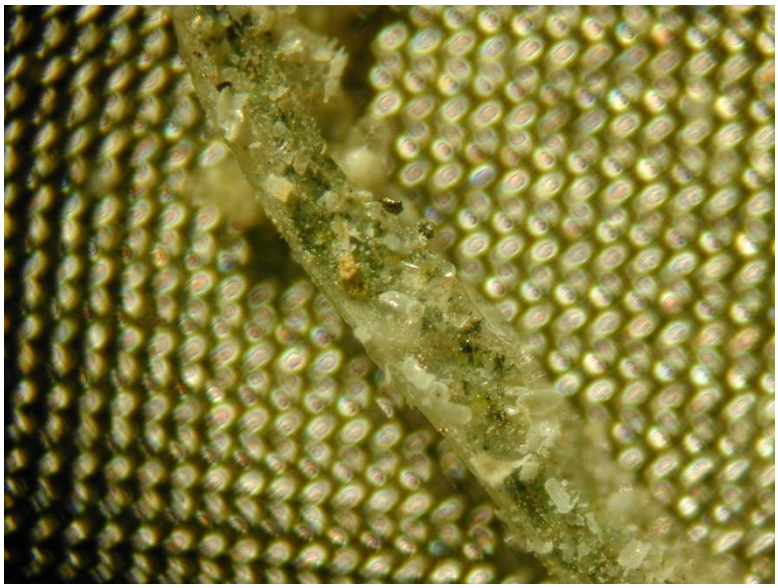

Core depth: 6-7 cm

Shape: fibre

Size: 2.86 mm (size category D)

Colour: green

FT-IR identification: polypropylene (PP)

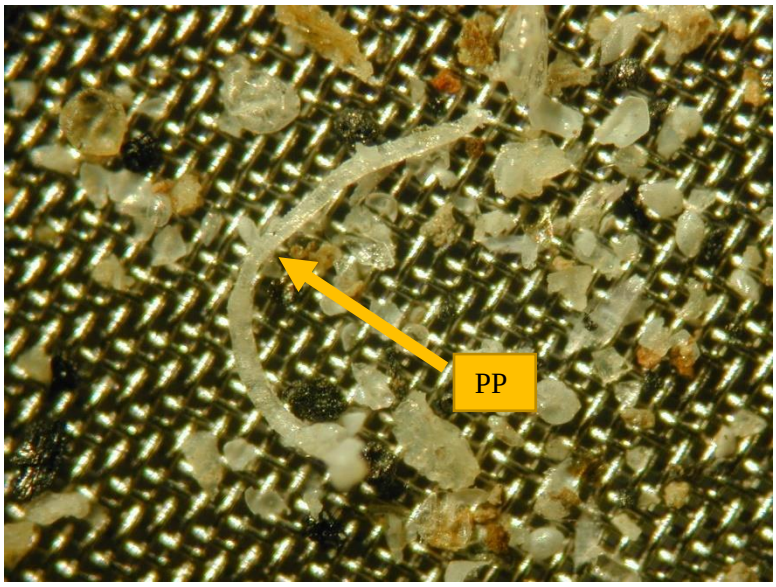

Core depth: 6-7 cm

Shape: fibre

Size: 546 µm (size category C)

Colour: clear/white

FT-IR identification: polypropylene (PP)

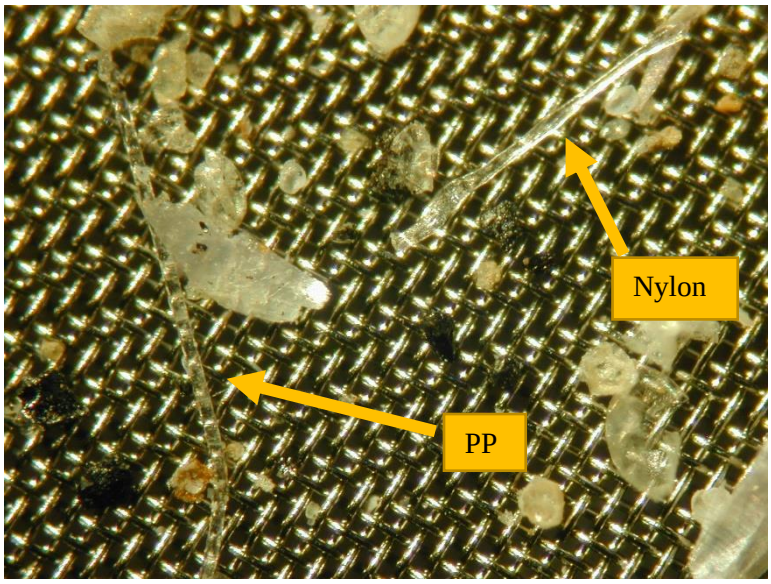

Core depth: 6-7 cm

Shape: fibre

Size: 364 µm (size category C)

Colour: clear

FT-IR identification: nylon

Core depth: 6-7 cm

Shape: fibre

Size: 468 µm (size category C)

Colour: clear

FT-IR identification: polypropylene (PP)

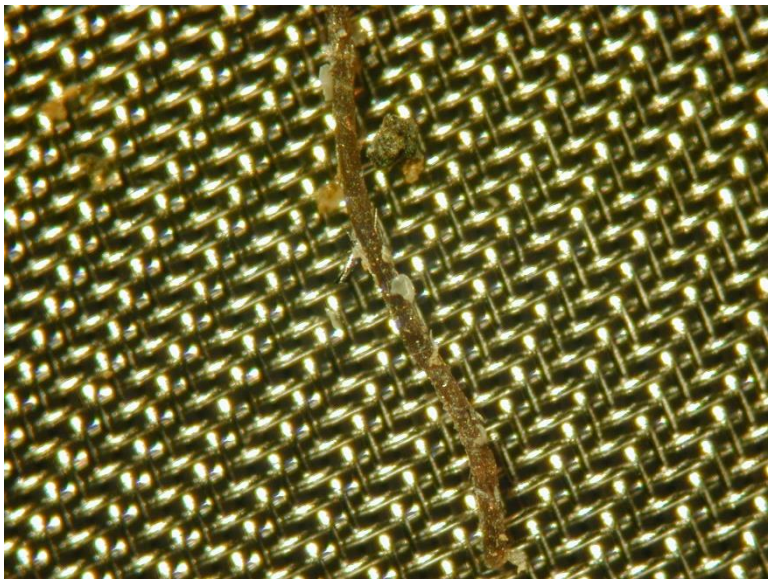

Core depth: 7-8 cm

Shape: fibre

Size: 1.27 mm (size category D)

Colour: dark brown

FT-IR identification: polypropylene (PP)

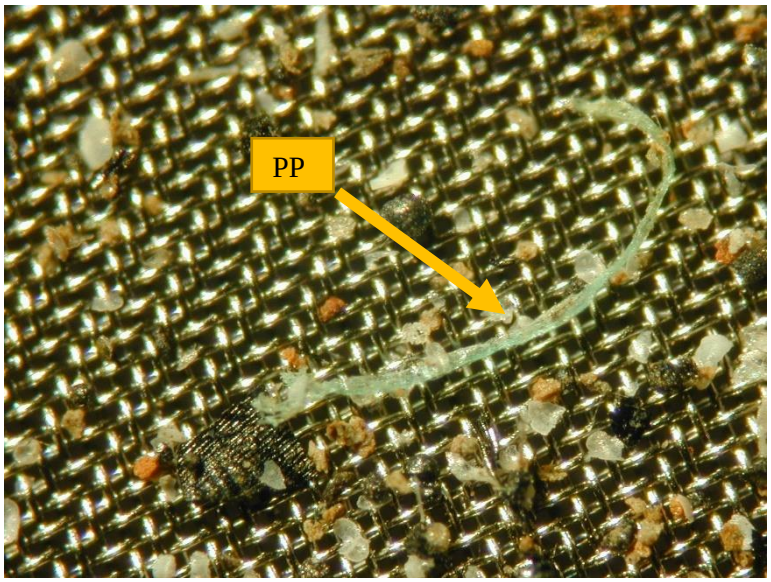

Core depth: 7-8 cm

Shape: fibre

Size: 624 µm (size category C)

Colour: green-blue

FT-IR identification: polypropylene (PP)

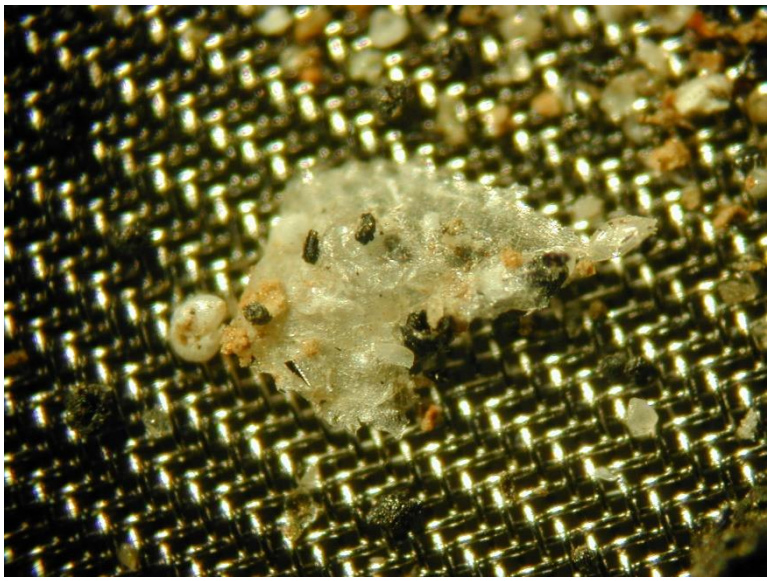

Core depth: 7-8 cm

Shape: film

Size: 416 µm (size category C)

Colour: clear/white

FT-IR identification: polyvinyl chloride (PVC)

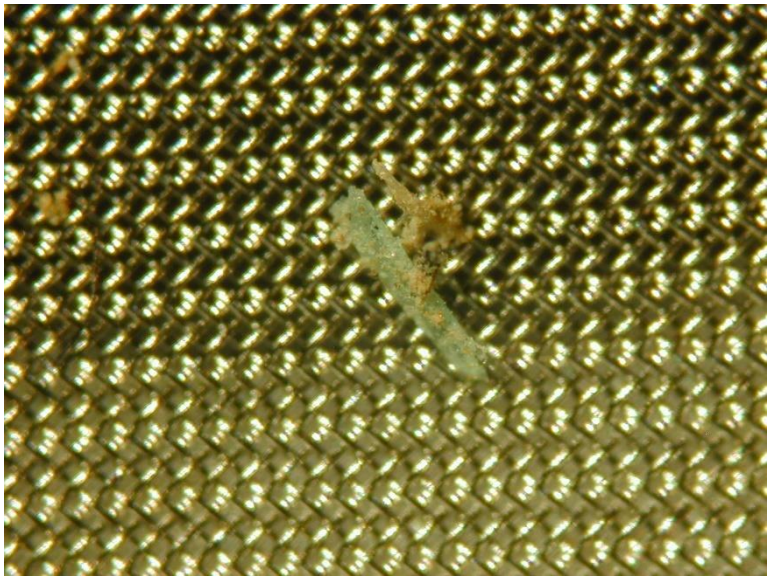

Core depth: 8-9 cm

Shape: elongated granulate

Size: 260 µm (size category B)

Colour: green

FT-IR identification: polypropylene (PP)

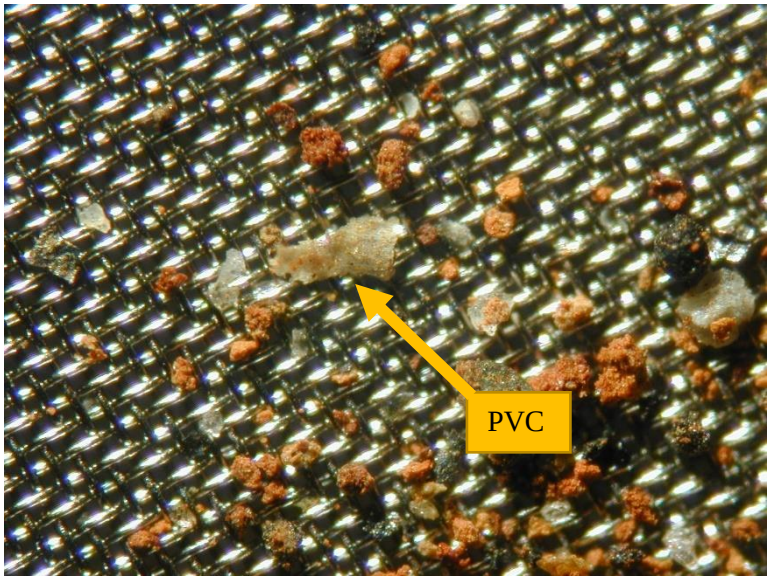

Core depth: 14-15 cm

Shape: film

Size: 156 µm (size category B)

Colour: light brown

FT-IR identification: polyvinyl chloride (PVC)

G.2 – CORE BC-B

Core depth: 8-11 cm

Shape: elongated granulate

Size: 338 µm (size category C)

Colour: green

FT-IR identification: polypropylene (PP)

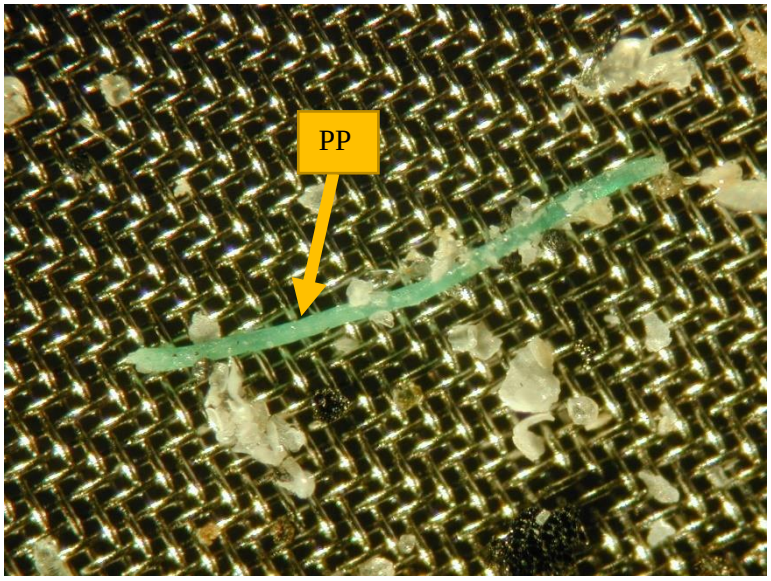

Core depth: 8-11 cm

Shape: fibre

Size: 624 µm (size category C)

Colour: green

FT-IR identification: polypropylene (PP)

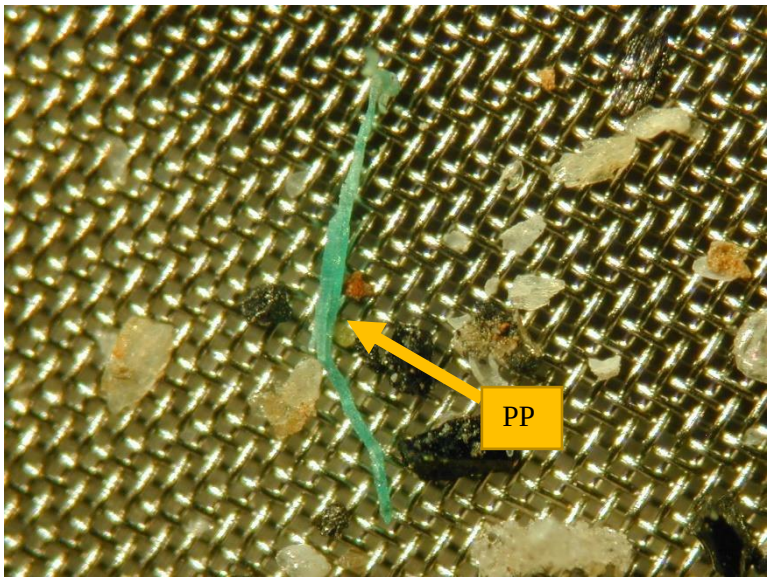

Core depth: 8-11 cm

Shape: fibre

Size: 546 µm (size category C)

Colour: green

FT-IR identification: polypropylene (PP)

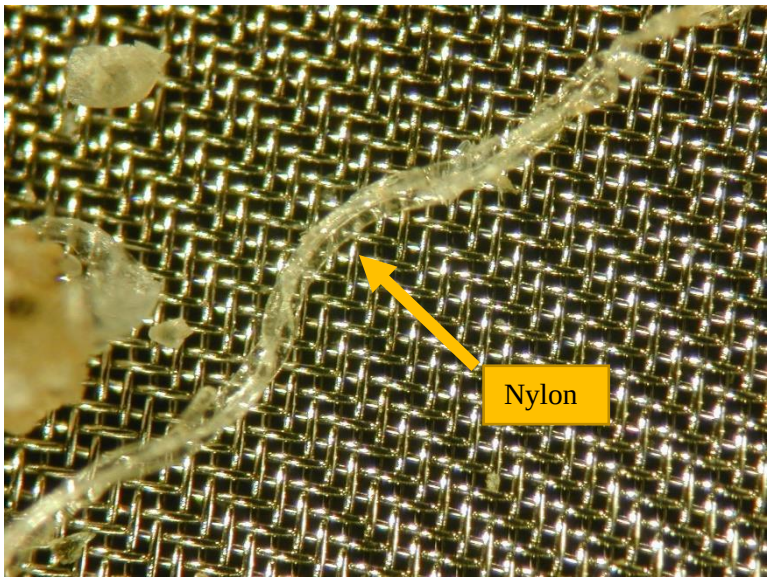

Core depth: 8-11 cm

Shape: fibre

Size: 936 µm (size category C)

Colour: clear

FT-IR identification: nylon

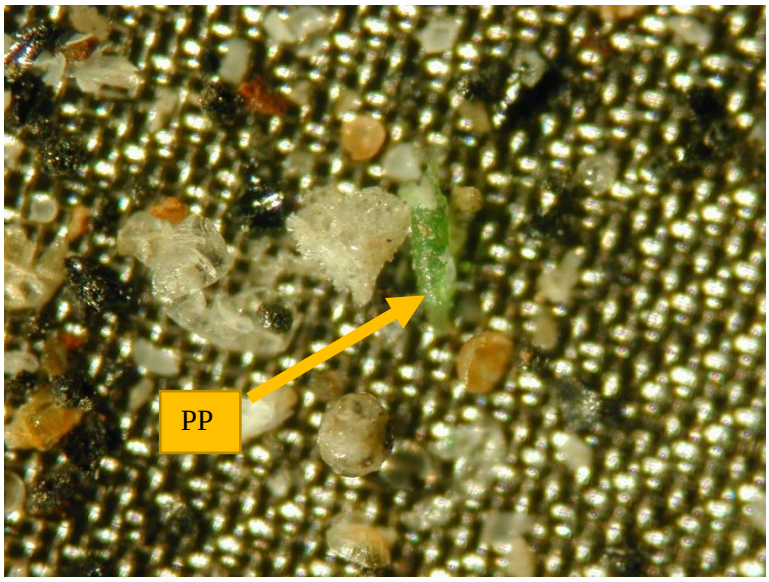

Core depth: 11-15 cm

Shape: short granulate

Size: 208 µm (size category B)

Colour: green

FT-IR identification: polypropylene (PP)

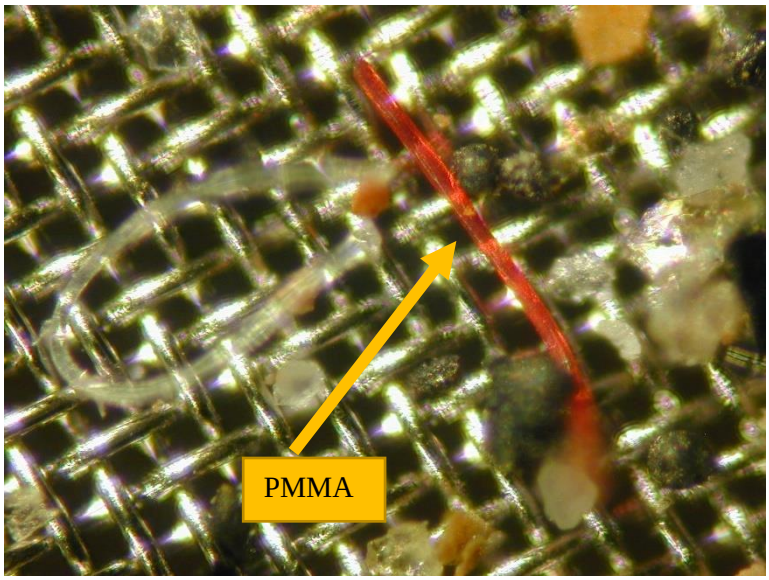

Core depth: 15-18 cm

Shape: fibre

Size: 234 µm (size category B)

Colour: red

FT-IR identification: poly(methyl methacrylate) (PMMA)

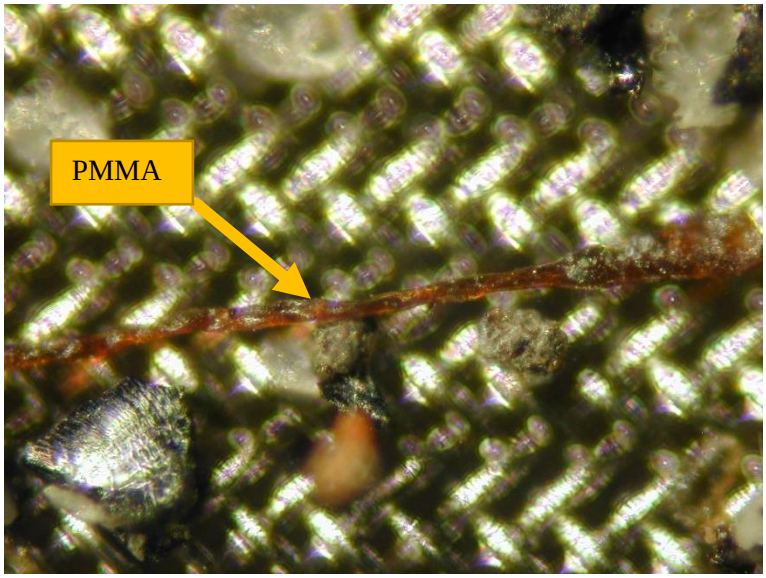

Core depth: 20-22 cm

Shape: fibre

Size: 286 µm (size category B)

Colour: dark brown

FT-IR identification: poly(methyl methacrylate) (PMMA)

G.3 – SURFACE SAMPLES

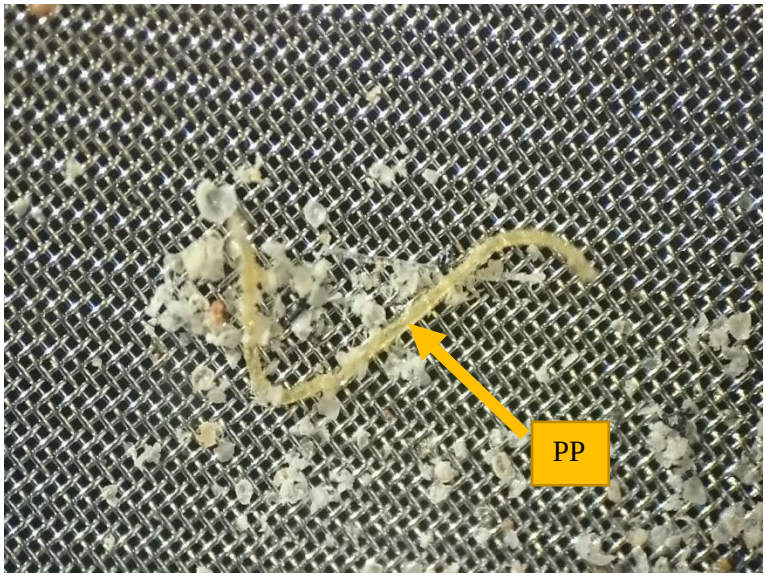

Water depth: 65 m ("BC-65")

Shape: fibre

Size: 988 µm (size category C)

Colour: yellow

FT-IR identification: polypropylene (PP)

APPENDIX H – MICROFT-IR ANALYSIS

H.1 – CORE BC-A

CONCENTRATION IN NUMBER OF PARTICLES/ KG DRY SEDIMENT

Sample ID	Number of particles per kg dry sediment			
	Oxy-resin	Petro-pyro	Plastic	Rubber
BC-A 0-1	3610	19	13087	3610
BC-A 1-2	2475	2475	14245	n.d.
BC-A 2-3	n.d.	1655	2015	n.d.
BC-A 3-4	228	2966	5369	685
BC-A 4-5	446	3565	5514	1337
BC-A 5-6	294	1765	3178	294
BC-A 6-7	300	1501	4919	300
BC-A 7-8	n.d.	2372	30326	1186
BC-A 8-9	772	n.d.	13322	2317
BC-A 9-10	n.d.	n.d.	30129	n.d.
BC-A 10-11	5913	5913	19607	n.d.
BC-A 11-12	1598	17577	9188	n.d.
BC-A 12-13	n.d.	36954	15573	6719
BC-A 13-14	41321	82641	106745	13774
BC-A 14-15	n.d.	85949	82368	114599

CONCENTRATION IN MG/ KG DRY SEDIMENT

Sample ID	mg per kg dry sediment			
	Oxy-resin	Petro-pyro	Plastic	Rubber
BC-A 0-1	2.11	2.50	7.65	2.11
BC-A 1-2	2.41	2.41	14.05	n.d.
BC-A 2-3	n.d.	5.09	3.49	n.d.
BC-A 3-4	0.71	9.26	16.68	2.14
BC-A 4-5	0.70	5.57	8.62	2.09
BC-A 5-6	0.35	2.07	8.43	0.35
BC-A 6-7	0.47	2.35	7.71	0.47
BC-A 7-8	n.d.	2.32	29.68	1.16
BC-A 8-9	0.90	n.d.	15.60	2.71
BC-A 9-10	n.d.	n.d.	22.00	n.d.
BC-A 10-11	5.65	5.65	20.88	n.d.
BC-A 11-12	1.45	15.92	8.32	n.d.
BC-A 12-13	n.d.	65.67	30.27	11.94
BC-A 13-14	96.64	193.29	249.66	32.21
BC-A 14-15	n.d.	273.00	261.62	364.00

MOST FREQUENT PLASTIC

Sample ID	Oxy-resin, plastic, rubber			Most frequent plastic
	Most frequent	Second most frequent	Third most frequent	
BC-A 0-1	Phenoxy resin	Rubber (plasthall)	PE-chlorinated	PE-chlorinated
BC-A 1-2	PP	PE	Tin(oxy-resin)	PP
BC-A 2-3	PP	Others	PE-chlorinated	PP
BC-A 3-4	PP	PE	PVC	PP
BC-A 4-5	PP	Rubber (plasthall)	PVC	PP
BC-A 5-6	PE	PU	PP	PE
BC-A 6-7	PP	PE	PMMA	PP
BC-A 7-8	PP	PE	PVC	PP
BC-A 8-9	PP	PVC	Rubber (resinall)	PP
BC-A 9-10	Others	PP	PVC	Others
BC-A 10-11	PE	Epoxy resin	PVC	PE
BC-A 11-12	PS	Epoxy resin	PE:PP	PS
BC-A 12-13	Others	Rubber (others)	Rubber (resinall)	Others
BC-A 13-14	PE-chlorinated	Phenoxy resin	PE	PE-chlorinated
BC-A 14-15	Rubber (others)	PVC	Rubber (resinall)	PVC

PERCENTAGE OF DIFFERENT PLASTIC TYPES

Sample ID	Percentage of separated sample (%)			
	PE	PE-oxidized	PP	PE:PP
BC-A 0-1	n.d.	n.d.	0.2207	n.d.
BC-A 1-2	0.4011	n.d.	0.6576	n.d.
BC-A 2-3	0.0014	n.d.	0.2311	n.d.
BC-A 3-4	0.7498	n.d.	1.7452	0.1932
BC-A 4-5	0.3987	n.d.	1.2755	n.d.
BC-A 5-6	1.8763	n.d.	0.6393	n.d.
BC-A 6-7	0.6682	0.1510	1.0402	n.d.
BC-A 7-8	1.1637	0.1482	1.2025	n.d.
BC-A 8-9	0.3900	n.d.	1.0399	0.2081
BC-A 9-10	0.2356	n.d.	0.5383	n.d.
BC-A 10-11	0.7278	n.d.	0.2755	n.d.
BC-A 11-12	0.1782	n.d.	n.d.	0.2037
BC-A 12-13	0.1456	0.1456	n.d.	n.d.
BC-A 13-14	0.4011	n.d.	n.d.	0.2140
BC-A 14-15	n.d.	n.d.	n.d.	n.d.

Sample ID	Percentage of separated sample (%)			
	PE-chlorinated	PE-chlorosulfonated	PP-chlorinated	PVC
BC-A 0-1	0.2207	n.d.	n.d.	n.d.
BC-A 1-2	0.0001	n.d.	n.d.	n.d.
BC-A 2-3	0.2108	n.d.	n.d.	0.1845
BC-A 3-4	0.1932	n.d.	n.d.	0.7482
BC-A 4-5	0.2127	n.d.	n.d.	0.3987
BC-A 5-6	0.0001	n.d.	n.d.	0.6066
BC-A 6-7	0.1725	n.d.	n.d.	n.d.
BC-A 7-8	0.1694	n.d.	n.d.	0.4867
BC-A 8-9	n.d.	n.d.	n.d.	0.8060
BC-A 9-10	n.d.	n.d.	n.d.	0.5047
BC-A 10-11	n.d.	n.d.	n.d.	0.5164
BC-A 11-12	0.2037	n.d.	n.d.	n.d.
BC-A 12-13	0.0742	n.d.	n.d.	0.1456
BC-A 13-14	0.8555	n.d.	n.d.	0.1873
BC-A 14-15	0.2465	n.d.	n.d.	0.4621

Sample ID	Percentage of separated sample (%)				
	PS	PET	Nylon	PU	PVF
BC-A 0-1	n.d.	n.d.	n.d.	n.d.	n.d.
BC-A 1-2	0.1873	n.d.	n.d.	n.d.	n.d.
BC-A 2-3	0.1845	n.d.	n.d.	n.d.	n.d.
BC-A 3-4	n.d.	n.d.	0.3380	n.d.	n.d.
BC-A 4-5	0.1861	n.d.	0.1596	n.d.	n.d.
BC-A 5-6	n.d.	n.d.	0.1583	1.0204	0.4220
BC-A 6-7	0.1510	n.d.	0.1498	n.d.	n.d.
BC-A 7-8	n.d.	0.3386	n.d.	n.d.	n.d.
BC-A 8-9	n.d.	n.d.	0.3641	n.d.	0.2081
BC-A 9-10	n.d.	n.d.	n.d.	n.d.	n.d.
BC-A 10-11	0.2410	n.d.	n.d.	n.d.	n.d.
BC-A 11-12	0.3818	0.2037	n.d.	n.d.	n.d.
BC-A 12-13	n.d.	n.d.	n.d.	n.d.	n.d.
BC-A 13-14	n.d.	n.d.	n.d.	n.d.	n.d.
BC-A 14-15	n.d.	n.d.	n.d.	n.d.	n.d.

Sample ID	Percentage of separated sample (%)				
	PMMA	Polyacrylamide	Melamine	EVA	Unresolved
BC-A 0-1	n.d.	n.d.	0.1655	n.d.	n.d.
BC-A 1-2	n.d.	n.d.	n.d.	n.d.	0.4221
BC-A 2-3	n.d.	n.d.	n.d.	n.d.	0.2110
BC-A 3-4	n.d.	n.d.	n.d.	n.d.	0.3622
BC-A 4-5	n.d.	n.d.	n.d.	n.d.	n.d.
BC-A 5-6	n.d.	n.d.	n.d.	n.d.	0.4221
BC-A 6-7	0.3450	n.d.	n.d.	n.d.	0.1512
BC-A 7-8	0.1694	n.d.	n.d.	0.1694	0.4869
BC-A 8-9	n.d.	n.d.	0.3641	n.d.	0.2082
BC-A 9-10	n.d.	n.d.	n.d.	n.d.	0.5385
BC-A 10-11	n.d.	n.d.	n.d.	n.d.	0.2756
BC-A 11-12	n.d.	n.d.	n.d.	n.d.	n.d.
BC-A 12-13	n.d.	n.d.	n.d.	n.d.	0.3328
BC-A 13-14	n.d.	n.d.	n.d.	n.d.	n.d.
BC-A 14-15	n.d.	n.d.	n.d.	n.d.	n.d.

H.2 – CORE BC-B

CONCENTRATION IN NUMBER OF PARTICLES/ KG DRY SEDIMENT

Sample ID	Number of particles per kg dry sediment			
	Oxy-resin	Petro-pyro	Plastic	Rubber
BC-B 0-5	n.d.	3563	33075	n.d.
BC-B 5-8	n.d.	151	2893	n.d.
BC-B 8-11	n.d.	533	5310	n.d.
BC-B 11-15	n.d.	659	2891	94
BC-B 15-18	n.d.	4796	9554	1439
BC-B 18-20	426	2558	4963	426
BC-B 20-22	14	1164	1738	146
BC-B 22-25	15	3891	6736	2162
BC-B 25-27	n.d.	29672	57088	n.d.

CONCENTRATION IN MG/ KG DRY SEDIMENT

Sample ID	mg per kg dry sediment			
	Oxy-resin	Petro-pyro	Plastic	Rubber
BC-B 0-5	n.d.	1.77	25.61	n.d.
BC-B 5-8	n.d.	0.30	7.10	n.d.
BC-B 8-11	n.d.	1.15	28.96	n.d.
BC-B 11-15	n.d.	1.60	7.78	0.23
BC-B 15-18	n.d.	2.49	8.90	0.75
BC-B 18-20	0.53	3.18	6.18	0.53
BC-B 20-22	0.03	4.37	6.42	0.55
BC-B 22-25	0.02	5.05	10.70	2.80
BC-B 25-27	n.d.	54.35	117.17	n.d.

MOST FREQUENT PLASTIC

Sample ID	Oxy-resin, plastic, rubber			Most frequent plastic
	Most frequent	Second most frequent	Third most frequent	
BC-B 0-5	PMMA	PE	Melamine	PMMA
BC-B 5-8	PP	PE	PMMA	PP
BC-B 8-11	PE	PP	PS	PE
BC-B 11-15	PE	PP	PS	PE
BC-B 15-18	PE	PS	PP	PE
BC-B 18-20	PP	PE	Epoxy resin	PP
BC-B 20-22	PVC	Others	PMMA	PVC
BC-B 22-25	PP	Rubber (resinall)	PE	PP
BC-B 25-27	PVC	PE	PU	PVC

PERCENTAGE OF DIFFERENT PLASTIC TYPES

Sample ID	Percentage of separated sample (%)			
	PE	PE-oxidized	PP	PE:PP
BC-B 0-5	2.1268	n.d.	0.6023	n.d.
BC-B 5-8	5.0490	0.6427	5.1301	0.7345
BC-B 8-11	18.8509	n.d.	3.9987	n.d.
BC-B 11-15	7.3643	n.d.	3.0416	n.d.
BC-B 15-18	3.6512	n.d.	1.3739	0.2739
BC-B 18-20	1.0376	n.d.	1.3034	n.d.
BC-B 20-22	0.2028	n.d.	0.0044	0.2318
BC-B 22-25	1.1208	n.d.	1.4711	n.d.
BC-B 25-27	0.5193	n.d.	0.2584	n.d.

Sample ID	Percentage of separated sample (%)			
	PE-chlorinated	PE-chlorosulfonated	PP-chlorinated	PVC
BC-B 0-5	n.d.	n.d.	n.d.	n.d.
BC-B 5-8	n.d.	n.d.	n.d.	1.3771
BC-B 8-11	n.d.	n.d.	n.d.	n.d.
BC-B 11-15	n.d.	n.d.	n.d.	0.3244
BC-B 15-18	0.2739	n.d.	n.d.	1.3345
BC-B 18-20	n.d.	n.d.	n.d.	0.2277
BC-B 20-22	n.d.	n.d.	n.d.	1.1293
BC-B 22-25	0.3009	n.d.	n.d.	0.5424
BC-B 25-27	0.4489	n.d.	n.d.	1.0010

Sample ID	Percentage of separated sample (%)				
	PS	PET	Nylon	PU	PVF
BC-B 0-5	n.d.	n.d.	0.4118	n.d.	n.d.
BC-B 5-8	0.6427	n.d.	1.4197	n.d.	n.d.
BC-B 8-11	0.6223	0.3320	0.2490	0.3320	n.d.
BC-B 11-15	1.6248	n.d.	0.2780	n.d.	n.d.
BC-B 15-18	1.4925	0.2739	n.d.	0.2739	n.d.
BC-B 18-20	n.d.	n.d.	0.2061	n.d.	n.d.
BC-B 20-22	n.d.	0.2318	n.d.	n.d.	n.d.
BC-B 22-25	0.8754	n.d.	0.2244	n.d.	n.d.
BC-B 25-27	0.4844	0.5167	0.1939	0.5167	n.d.

Sample ID	Percentage of separated sample (%)				
	PMMA	Polyacrylamide	Melamine	EVA	Unresolved
BC-B 0-5	3.3535	n.d.	0.9606	n.d.	0.4805
BC-B 5-8	2.2033	n.d.	n.d.	n.d.	n.d.
BC-B 8-11	0.3320	n.d.	n.d.	n.d.	0.2906
BC-B 11-15	n.d.	n.d.	n.d.	n.d.	n.d.
BC-B 15-18	0.8213	n.d.	n.d.	n.d.	n.d.
BC-B 18-20	n.d.	n.d.	n.d.	n.d.	0.2604
BC-B 20-22	0.4634	n.d.	n.d.	n.d.	0.4636
BC-B 22-25	0.2893	n.d.	n.d.	n.d.	0.6950
BC-B 25-27	0.2584	n.d.	n.d.	n.d.	0.2586

H.3 – SURFACE SAMPLES

CONCENTRATION IN NUMBER OF PARTICLES/ KG DRY SEDIMENT

Sample ID	Number of particles per kg dry sediment			
	Oxy-resin	Petro-pyro	Plastic	Rubber
BC-15	n.d.	76415	66890	229244
BC-25	n.d.	38046	n.d.	n.d.
BC-35	n.d.	158700	32728	8578
BC-45	n.d.	7719	30784	7696
BC-65	n.d.	n.d.	13485	n.d.
BC-B	n.d.	n.d.	4030	1105

CONCENTRATION IN MG/ KG DRY SEDIMENT

Sample ID	mg per kg dry sediment			
	Oxy-resin	Petro-pyro	Plastic	Rubber
BC-15	n.d.	29.79	26.64	89.36
BC-25	n.d.	50.99	n.d.	n.d.
BC-35	n.d.	373.56	80.83	20.19
BC-45	n.d.	9.04	36.06	9.02
BC-65	n.d.	n.d.	13.54	n.d.
BC-B	n.d.	n.d.	48.13	5.87

MOST FREQUENT PLASTIC

Sample ID	Percentage of separated sample (%)			
	PE-chlorinated	PE-chlorosulfonated	PP-chlorinated	PVC
BC-15	0.2216	n.d.	n.d.	n.d.
BC-25	n.d.	n.d.	n.d.	n.d.
BC-35	0.6370	n.d.	n.d.	n.d.
BC-45	n.d.	n.d.	n.d.	0.3911
BC-65	n.d.	n.d.	n.d.	0.4121
BC-B	1.9717	n.d.	n.d.	0.3774

Sample ID	Percentage of separated sample (%)				
	PS	PET	Nylon	PU	PVF
BC-15	n.d.	n.d.	n.d.	n.d.	n.d.
BC-25	n.d.	n.d.	n.d.	n.d.	n.d.
BC-35	n.d.	0.2124	n.d.	n.d.	n.d.
BC-45	0.1826	n.d.	0.1565	n.d.	n.d.
BC-65	0.4121	0.2198	0.1863	n.d.	n.d.
BC-B	n.d.	n.d.	0.3235	n.d.	n.d.

Sample ID	Percentage of separated sample (%)				
	PMMA	Polyacrylamide	Melamine	EVA	Unresolved
BC-15	n.d.	n.d.	0.1662	n.d.	n.d.
BC-25	n.d.	n.d.	n.d.	n.d.	n.d.
BC-35	n.d.	n.d.	0.3717	n.d.	0.0811
BC-45	n.d.	n.d.	0.3651	n.d.	0.3913
BC-65	n.d.	n.d.	0.1649	n.d.	0.1925
BC-B	n.d.	n.d.	n.d.	n.d.	n.d.

APPENDIX I – MACROFT-IR ANALYSIS

I.1 – CORE BC-A

Sample ID	Colour	Shape	Length/ width (mm)	Comments	Oxy-resin, Petro-Pyro, Plastic, Rubber	Type
BC-A 0-1						
Administrator 200	White	Film	0.85		Unknown	
Administrator 201	White	Film	1.07		Petro-pyro	
Administrator 202	Light brown	Fibre	1.60		Unknown	
BC-A 1-2						
Administrator 204	Black	Granule	1.85	Brittle	Unknown	
Administrator 205	White	Film	1.61	Brittle	Unknown	
Administrator 206	Clear/white	Fibre	8.14		Unknown	
Administrator 214	White	Fibre	13.84		Plastic	PP
BC-A 2-3						
Administrator 104	Blue	Fibre	4.24		Plastic	PP
Administrator 105	White	Film	2.84	Brittle. Looked like a shell fragment	Mineral	
Administrator 106	Light brown	Film	4.05		Organic	
Administrator 107	White	Film	1.62	Brittle	Unknown	
Administrator 108	Light brown	Fibre	4.77		Organic	
Administrator 109	Grey	Fibre	1.03	Difficult to get the fibre off the tweezer	Plastic	PE
Administrator 110	Clear	Fibre	6.12		Plastic	PP

Administrator 111	Light brown	Film	5.17		Organic	
Administrator 112	Black	Granule	1.10	Difficult to clean the ATR crystal (sticky particle)	Petro-Pyro	
Administrator 113	Blue	Fibre	0.85		Plastic	PP
Administrator 114	Clear	Fibre	5.24		Plastic	PP
BC-A 3-4						
Administrator 115	White	Fibre	3.05		Unknown	
Administrator 116	White	Granule	2.70	Brittle	Unknown	
Administrator 117	Light brown	Film	2.31		Organic	
Administrator 118	White	Fibre	1.58		Plastic	PE
Administrator 119	Brown	Granule	1.79	Brittle	Unknown	
Administrator 120	Black	Film	1.77		Unknown	
Administrator 121	Black	Fibre	2.70		Unknown	
Administrator 123	Clear/white	Film	2.17		Organic	
Administrator 124	White	Film	2.40	Brittle	Unknown	
Administrator 125	Light brown/orange	Granule	0.68		Organic	
Administrator 126	Clear	Fibre	7.20		Plastic	PP
Administrator 127	Blue	Fibre	0.31		Plastic	PP
BC-A 4-5						
-	Clear/white	Fibre	10.00	Lost.	Unknown	
Administrator 194	Black	Fibre	3.22		Unknown	
Administrator 195	Green	Film	0.54		Unknown	
Administrator 196	Light brown	Granule	1.66	Brittle	Unknown	
Administrator 198	Dark brown	Film	3.49		Unknown	

Administrator 199	Black	Granule	1.26		Unknown	
BC-A 5-6						
Administrator 128	Clear/white	Fibre	9.79		Unknown	
Administrator 130	Clear/white	Fibre	6.10		Unknown	
Administrator 131	Clear/white	Fibre	10.22	Very thin	Unknown	
Administrator 132	Clear/white	Fibre	11.38	Very thin	Unknown	
Administrator 171	Clear/white	Fibre	6.84		Unknown	
Administrator 172	Clear/white	Fibre	16.39		Unknown	
Administrator 173	White	Film	3.35		Plastic	PE
Administrator 174	White	Film	3.21		Unknown	
Administrator 175	Clear/white	Fibre	17.26		Unknown	
Administrator 177	Clear/white	Fibre	26.44		Unknown	
Administrator 178	White	Fibre	2.18		Plastic	PE
Administrator 179	Clear/white	Fibre	10.15		Unknown	
Administrator 180	Clear/white	Fibre	10.57		Unknown	
Administrator 181	Clear/white	Fibre	11.02		Unknown	
Administrator 182	Clear/white	Fibre	13.03		Unknown	
Administrator 184	Black/dark brown	Fibre	2.51		Plastic	PP
Administrator 185	Green	Granule	0.31		Unknown	
Administrator 186	White	Film	2.32		Plastic	PU
BC-A 6-7						
Administrator 165	White	Film	4.37		Unknown	
Administrator 166	Dark brown	Granule	2.64		Unknown	
Administrator 167	Clear/white	Fibre	2.45		Plastic	PP
Administrator 168	Clear/white	Fibre	6.70		Plastic	Nylon

Administrator 169	Red	Granule	0.33		Organic	
Administrator 170	Black	Granule	0.90		Unknown	
BC-A 7-8						
Administrator 157	Green	Fibre	1.51		Plastic	PP
Administrator 158	Black/dark brown	Fibre	5.68		Plastic	PP
Administrator 159	Red	Fibre	4.02		Plastic	PP
Administrator 160	Clear/white	Fibre	3.64		Plastic	PP
Administrator 161	Black	Film	5.27		Unknown	
Administrator 162	Dark brown	Granule	3.56		Unknown	
Administrator 163	Green	Fibre	1.39		Plastic	PP
Administrator 164	White	Film	1.48		Organic	
BC-A 8-9						
Administrator 149	Black	Film	2.39	Brittle	Unknown	
Administrator 151	White	Fibre	7.37		Organic	
Administrator 152	Light brown	Film	2.33		Organic	
Administrator 153	White	Fibre	6.17		Organic	
Administrator 154	White	Fibre	3.19		Organic	
Administrator 155	Dark brown	Granule	2.12	Brittle	Unknown	
Administrator 156	White	Fibre	4.82		Organic	
BC-A 9-10						
Administrator 142	White	Fibre	5.90		Organic	
Administrator 143	White	Fibre	1.60		Organic	
Administrator 144	White	Fibre	1.97		Organic	
Administrator 145	White	Fibre	2.61		Organic	
Administrator 146	White	Film	3.74		Organic	

Administrator 147	Beige	Film	3.31		Unknown	
Administrator 148	Black	Granule	0.84		Unknown	
BC-A 10-11						
Administrator 03	Dark brown	Granule	4.09	Very brittle	Unknown	
Administrator 04	Black	Film	5.46	Brittle	Unknown	
Administrator 05	Light brown	Film	7.70		Organic	
Administrator 06	Clear/white	Film	2.10		Organic	
Administrator 07	Green	Film	2.26		Plastic	PE
Administrator 08	Light brown	Fibre	3.23		Organic	
Administrator 09	Light brown	Fibre	4.55		Organic	
Administrator 10	White	Film	2.00	Looked like a shell from a bivalve	Unknown	
Administrator 11	Black/dark brown	Film	2.88	Brittle	Unknown	
Administrator 12	Light brown	Film	3.32		Organic	
Administrator 13	White	Fibre	2.44		Organic	
BC-A 11-12						
Administrator 14	White	Fibre	2.06		Unknown	
Administrator 15	Black	Granule	3.82	Brittle	Unknown	
BC-A 12-13						
Administrator 91	Orange-brown	Granule	5.55		Unknown	
Administrator 92	Dark brown	Granule	3.60		Unknown	
Administrator 93	Light brown	Granule	2.56	Brittle	Unknown	
Administrator 94	White	Fibre	1.50		Unknown	
Administrator 95	Black/grey	Granule	2.38		Unknown	

Administrator 96	Red	Granule	0.68		Plastic	PE-chlorinated
Administrator 97	White	Film	0.94		Plastic	PE-chlorinated
Administrator 98	Orange	Granule	1.39		Unknown	
Administrator 99	Black	Granule	2.13		Unknown	
BC-A 13-14						
Administrator 100	Brown	Granule	2.37	Brittle	Unknown	
Administrator 101	White	Film	1.86		Unknown	
Administrator 102	Black	Granule	1.69		Unknown	
Administrator 103	Black	Granule	1.53		Unknown	
BC-A 14-15						
Administrator 136	Black/dark brown	Granule	2.16	Brittle	Unknown	
Administrator 137	Black/dark brown	Granule	1.65	Brittle	Unknown	
Administrator 138	Black/dark brown	Granule	1.20		Organic	
Administrator 139	Dark brown	Granule	2.56	Brittle	Organic	
Administrator 140	White	Fibre	1.11		Unknown	
Administrator 141	Light brown	Fibre	1.65		Organic	

I.2 – CORE BC-B

Sample ID	Colour	Granule/ film/fibre	Longest length/width (mm)	Comments	Oxy-resin, Petro-Pyro, Plastic, Rubber	Type
BC-B 0-5						
Administrator 16	White	Fibre	9.00		Plastic	PP
Administrator 17	White	Granule	0.97		Plastic	PMMA
BC-B 5-8						
Administrator 18	Green/white	Fibre	0.97		Plastic	PP
Administrator 19	Blue	Fibre	7.50		Plastic	PP
Administrator 20	Light brown	Film	0.91		Plastic	Nylon
Administrator 21	Black	Granule	0.63		Plastic	PP
BC-B 8-11						
Administrator 22	White/light brown	Film	5.77		Plastic	PE
Administrator 23	White/light brown	Film	2.65		Organic	
Administrator 24	White	Fibre	2.66		Plastic	PP
Administrator 25	Green/white	Film	0.98		Plastic	PE
Administrator 26	Black	Film	1.68		Plastic	PE
Administrator 27	White/light brown	Film	1.67		Unknown	
BC-B 11-15						
Administrator 28	Orange	Film	1.53		Plastic	PS
Administrator 29	Orange	Film	1.92		Unknown	
Administrator 30	Clear/white	Fibre	9.78	Very thin	Plastic	PP

Administrator 31	White/light brown	Film	1.41		Organic	
Administrator 32	White	Film	1.66	Same shape as a seed	Unknown	
BC-B 15-18						
Administrator 33	Light brown	Film	3.39		Organic	
Administrator 34	Green	Film	2.39		Plastic	PE
Administrator 35	Green	Fibre	1.26		Plastic	PP
Administrator 36	Green	Film	1.10		Plastic	PE
Administrator 37	White	Fibre	1.64		Plastic	PE
Administrator 38	White	Fibre	2.37		Plastic	PE
Administrator 39	Black	Granule	0.56	Brittle	Unknown	
Administrator 40	White	Granule	1.02	Flattened by the gauge, after the scan	Plastic	PE
Administrator 41	White	Film	1.56		Plastic	PS
BC-B 18-20						
Administrator 42	Red	Fibre	9.20		Plastic	PE
Administrator 43	White/light brown	Film	8.80		Organic	
-	Brown	Fibre	4.00	Lost	Unknown	
Administrator 44	Black	Granule	1.91	Brittle	Unknown	
Administrator 45	Clear/white	Film	3.35		Organic	
Administrator 46	White/light brown	Film	1.94		Unknown	
Administrator 47	Brown	Fibre	2.60		Plastic	Nylon
Administrator 48	Green/white	Fibre	0.91		Plastic	PP

BC-B 20-22						
Administrator 49	Brown	Granule	2.36	Brittle	Unknown	
Administrator 50	White/light brown	Granule	2.04	Flattened by the gauge, after the scan	Organic	
Administrator 51	Black	Granule	1.91	Flattened by the gauge, after the scan	Unknown	
Administrator 52	White/light brown	Fibre	2.13		Organic	
Administrator 53	White/light brown	Film	1.56		Organic	
Administrator 54	Blue/white	Fibre	0.93		Plastic	PP
Administrator 55	Blue	Fibre	1.32		Plastic	PP
Administrator 56	White	Fibre	5.00	Curly. Difficult to measure the length	Oxy-resin	Other
Administrator 57	White/light brown	Fibre	2.64		Organic	
Administrator 58	Light brown	Film	3.06		Organic	
BC-B 22-25						
Administrator 59	White	Fibre	4.25		Plastic	PE-chlorinated
Administrator 60	White	Fibre	10.17	Curly. Difficult to measure the length	Plastic	PP
Administrator 61	White	Fibre	3.37		Oxy-resin	Other

Administrator 62	Clear/white	Film	1.46		Organic	
Administrator 63	Light brown	Fibre	1.97		Organic	
Administrator 64	White	Film	1.68		Plastic	PS
Administrator 65	White/light brown	Film	1.50		Plastic	PS
Administrator 66	Clear/white	Film	1.84		Organic	
Administrator 67	Brown	Fibre	2.26		Plastic	Nylon
Administrator 68	White	Film	0.94		Plastic	Other
BC-B 25-27						
Administrator 69	White	Film	1.90		Plastic	PE
Administrator 70	White	Film	1.48		Plastic	PE-chlorinated
Administrator 71	White/light brown	Fibre	2.19		Plastic	PE
Administrator 72	Black/grey	Film	1.63		Unknown	
-	Brown	Fibre	2.80	Lost	Unknown	

I.3 – SURFACE SAMPLES

Sample ID	Colour	Granule/ film/fibre	Longest length/width (mm)	Comments	Oxy-resin, Petro-Pyro, Plastic, Rubber	Type
BC-15						
Administrator 207	Clear/white	Fibre	5.60	Lump of fibres	Plastic	PE
BC-25						
Administrator 86	White	Fibre	2.03		Organic	
Administrator 87	Black	Film	3.97	Very brittle	Unknown	
Administrator 220	White/light brown	Fibre	2.07		Organic	
Administrator 221	Light brown	Film	2.76		Organic	
BC-35						
Administrator 208	Black	Granule	1.84		Organic	
Administrator 209	White	Film	1.41		Plastic	Other
Administrator 210	White	Granule	2.30		Organic	
BC-45						
Administrator 211	Clear/white	Fibre	6.60		Unknown	
Administrator 212	White	Granule	2.15		Unknown	
Administrator 213	Blue	Fibre	1.51		Petro-Pyro	
BC-65						
Administrator 215	White	Fibre	17.62		Plastic	PP
Administrator 216	Black	Fibre	8.51		Plastic	Nylon
Administrator 217	White	Fibre	7.49		Unknown	
Administrator 218	Black	Granule	0.99		Unknown	

Administrator 219	Green	Granule	0.44		Plastic	PE
BC-B						
-	White	Granule	2.00	Lost	Unknown	
-	White	Film	3.40		Organic	
-	White	Fibre	4.60		Organic	
-	Black	Granule	1.00		Unknown	
-	White	Granule	2.00		Plastic	PE-chlorinated
Administrator 01	White	Film	3.40		Organic	
Administrator 02	White	Fibre	4.60		Organic	
Administrator 03	Black	Granule	1.00		Unknown	
Administrator 04	White	Granule	2.00		Unknown	